
***National Nanotechnology Coordinated
Infrastructure (NNCI)***

Research and Education Highlights

Year 3 (October 2017 – September 2018)



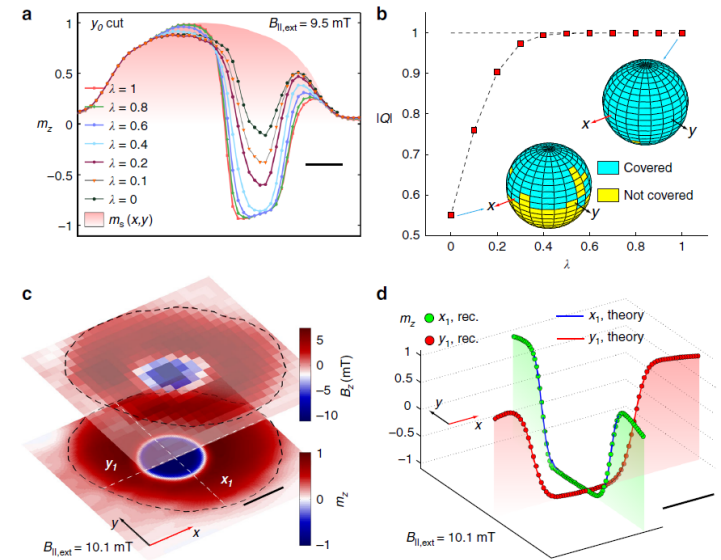
Table of Contents

Center for Nanoscale Systems (CNS)	3
Cornell Nanoscale Science and Engineering Facility (CNF)	12
Kentucky Multi-Scale Manufacturing and Nano Integration Node (KY MMNIN)	25
Mid-Atlantic Nanotechnology Hub (MANTH)	42
Midwest Nanotechnology Infrastructure Corridor (MINIC)	51
Montana Nanotechnology Facility (MONT)	60
Nanotechnology Collaborative Infrastructure Southwest (NCI-SW)	71
Nebraska Nanoscale Facility (NNF)	82
NNCI Site @ Stanford (nano@stanford)	91
Northwest Nanotechnology Infrastructure (NNI)	97
Research Triangle Nanotechnology Network (RTNN)	108
San Diego Nanotechnology Infrastructure (SDNI)	117
Soft and Hybrid Nanotechnology Experimental (SHyNE) Resource	128
Southeastern Nanotechnology Infrastructure Corridor (SENIC)	138
Texas Nanofabrication Facility (TNF)	150
Virginia Tech National Center for Earth and Environmental Nanotechnology Infrastructure (NanoEarth)	161
Education and Outreach	167

Center for Nanoscale Systems (CNS)

Magnetostatic twists in room-temperature skyrmions explored by nitrogen-vacancy center spin texture reconstruction

Magnetic skyrmions are two-dimensional non-collinear spin textures characterized by an integer topological number. Room temperature skyrmions were recently found in magnetic multilayer stacks, where their stability was largely attributed to the interfacial Dzyaloshinskii–Moriya interaction. The strength of this interaction and its role in stabilizing the skyrmions is not yet well understood, and imaging of the full spin structure is needed to address this question. Here, we use a nitrogen-vacancy centre in diamond to measure a map of magnetic fields produced by a skyrmion in a magnetic multilayer under ambient conditions. We compute the manifold of candidate spin structures and select the physically meaningful solution. We find a Néel-type skyrmion whose chirality is not left-handed, contrary to preceding reports. We propose skyrmion tube-like structures whose chirality rotates through the film thickness. We show that NV magnetometry, combined with our analysis method, provides a unique tool to investigate this previously inaccessible phenomenon.



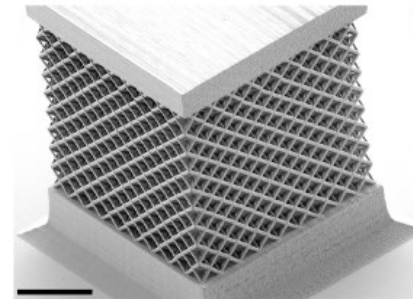
Showing topology nature of skyrmion

Y. Dovzhenko, F. Casola, T. X. Zhou, R. L. Walsworth & A. Yacoby; Department of Physics, Harvard University, F. Casola, Harvard-Smithsonian Center for Astrophysics, S. Schlotter & T. X. Zhou, John A. Paulson School of Engineering and Applied Sciences, Harvard University, F. Buttner & G. S. D. Beach, Department of Materials Science and Engineering, Massachusetts Institute of Technology. Work partially performed at Center for Nanoscale Systems, Harvard University

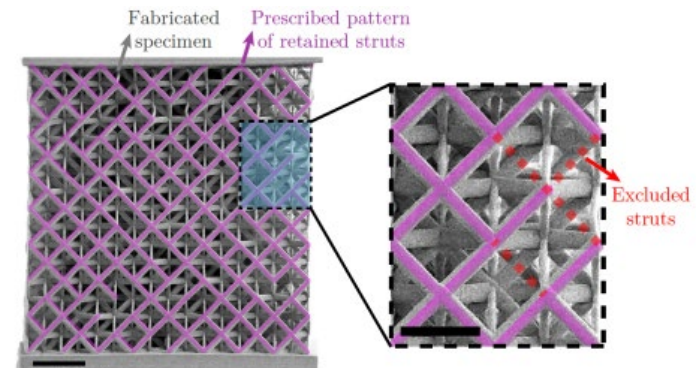
Funding: DOE, ARO, NSF, and Moore Foundation
Nature Communications **volume 9**, 2712 (2018)

Correlation between topology and elastic properties of imperfect truss-lattice materials

Recent advances in additive manufacturing at small scales has revealed the exceptional mechanical properties that can be achieved by truss-lattice materials. This study investigates the response of four topologically distinct truss-lattice architectures to the inclusion of defects in order to elucidate how defects influence the elastic properties of these materials. Numerical results from finite element models of periodic beam networks with missing building blocks are compared to both analytical continuum models with a micromechanical basis and to experiments with characteristic feature sizes on the nano and micro scales. Notably, this comparison reveals that the elastic properties of highly connected lattice-truss materials respond to defects in the same manner as homogeneous materials, no matter if the defects are organized as voids or randomly dispersed.



Perspective view of a pristine octet truss-lattice specimen. 20 μm scale bar.



Front view of an imperfect octet truss-lattice with 15% of struts randomly excluded. 10 μm scale bar in main image, 5 μm scale bar in inset.

A. Gross, P. Pantidis, K. Bertoldi, and S. Gerasimidis, Harvard University and University of Massachusetts Amherst

Funding from the Charles Stark Draper Laboratory, NNCI #1541959
Journal of the Mechanics and Physics of Solids (2019)

Low-Temperature Copper Bonding Strategy with Graphene Interlayer

The reliability of lead-free Cu bonding technology is often limited by high bonding temperature and perpetual growth of intermetallic compounds between Sn solder and Cu substrate. Here, we report a low-bonding-temperature and highly-reliable Cu bonding strategy with the use of graphene as an interlayer. By integrating nanoscale graphene/Cu composite on the Cu substrate prior to thermocompression bonding, we observe a macro-scale phenomenon where reliable Sn-Cu joints can be fabricated at a bonding temperature as low as 150 °C. During the bonding process, nanoscale features are replicated in the Sn solder by the Cu nanocone array morphology. Compared to microscale Sn, nanoscale Sn is mechanically weaker and thus can distribute on the Cu substrate at a much lower temperature. Furthermore, insertion of a graphene interlayer, which is of one-atomic-thick, can successfully retard the intermetallic compounds growth and preserve high bonding yield, following a 96h of aging, as confirmed through SEM and shear strength analyses. Our graphene-based Cu bonding strategy demonstrated in this work is highly reliable, cost-effective, environmentally friendly, representing a much closer step towards industrial applications.

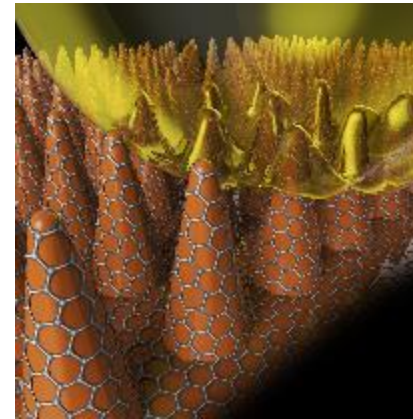


Figure 1: A schematic of bonding interface

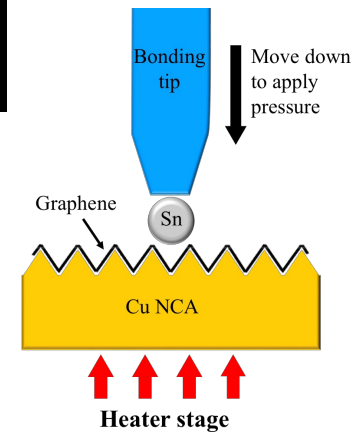


Figure 2: Demonstration of bonding process

H. Wang , W. S. Leong , F. Hu , L. Ju , C. Su , Y. Guo , J. Li , M. Li , A. Hu, J. Kong, Massachusetts Institute of Technology, Shanghai Jiao, Tong University.

Funding: NSF DMR/ECSS – 1509197, AFOSR FATA MURI #FA9550-15-1-0514, and NNSFC grant 61376107,
Publication: ACS Nano (2018)

Nano-optic endoscope for high-resolution optical coherence tomography in vivo

Acquisition of high-resolution images from within internal organs using endoscopic optical imaging has numerous clinical applications. However, difficulties associated with optical aberrations and the trade-off between transverse resolution and depth of focus significantly limit the scope of applications. Here, we integrate a metalens, with the ability to modify the phase of incident light at subwavelength level, into the design of an endoscopic optical coherence tomography catheter (termed nanooptics endoscope) to achieve near diffraction-limited imaging through negating non-chromatic aberrations. Remarkably, the tailored chromatic dispersion of the metalens in the context of spectral interferometry is utilized to maintain high-resolution imaging beyond the input field Rayleigh range, easing the trade-off between transverse resolution and depth of focus. We demonstrate endoscopic imaging in resected human lung specimens and in sheep airways in vivo. The combination of the superior resolution and higher imaging depth of focus of the nano-optic endoscope is likely to increase the clinical utility of endoscopic optical imaging.

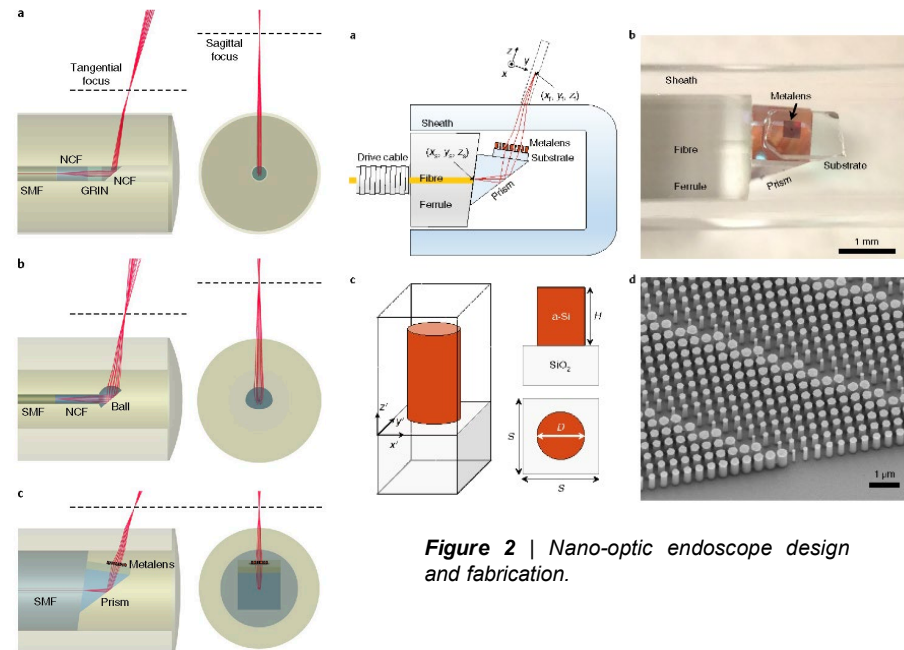


Figure 1 | Endoscopic OCT catheter designs

Figure 2 | Nano-optic endoscope design and fabrication.

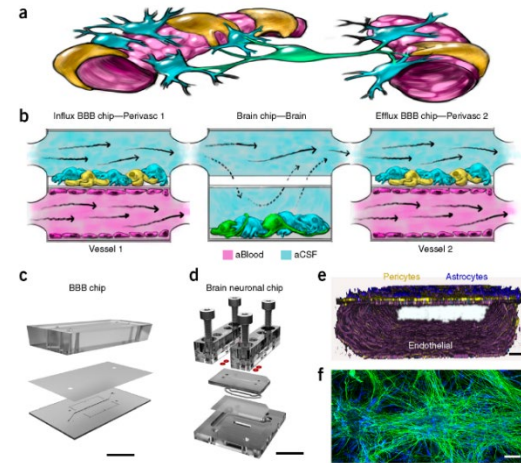
H. Pahlevaninezhad, M. Khorasaninejad, Y.-W. Huang, Z. Shi, L. Hariri, D. Adams, V. Ding, A. Zhu, C.-W. Qiu, F. Capasso and M. Suter; Department of Medicine, Pulmonary and Critical Care Division, Massachusetts General Hospital and Harvard Medical School, Harvard John A. Paulson School of Engineering and Applied Sciences, Harvard University, Department of Electrical and Computer Engineering, National University of Singapore, Department of Physics, Harvard University, University of Waterloo.

This project was supported by funding from NIH (R01CA167827, R01HL133664 a MURI: FA9550-14-1-0389, FA9550-16-1-0156, and the LUNGeVity Foundation/Upstage Lung Cancer.

Nature Photonics, volume 12, pages 540–547 (2018).

A linked organ-on-chip model of the human neurovascular unit reveals the metabolic coupling of endothelial and neuronal cells

The neurovascular unit (NVU) regulates metabolic homeostasis as well as drug pharmacokinetics and pharmacodynamics in the central nervous system. Metabolic fluxes and conversions over the NVU rely on interactions between brain microvascular endothelium, perivascular pericytes, astrocytes and neurons, making it difficult to identify the contributions of each cell type. Here we model the human NVU using microfluidic organ chips, allowing analysis of the roles of individual cell types in NVU functions. Three coupled chips model influx across the blood brain barrier (BBB), the brain parenchymal compartment and efflux across the BBB. We used this linked system to mimic the effect of intravascular administration of the psychoactive drug methamphetamine and to identify previously unknown metabolic coupling between the BBB and neurons. Thus, the NVU system offers an in vitro approach for probing transport, efficacy, mechanism of action and toxicity of neuroactive drugs.



B. Maoz, A. Herland, E. FitzGerald, T. Grevesse, C. Vidoudez, A. Pacheco, S. Sheehy, T.-E. Park, S. Dauth, R. Mannix, N. Budnik, K. Shores, A. Cho, J. Nawroth, D. Segrè, B. Budnik, D. Ingber and K. Parker; Harvard John A. Paulson School of Engineering and Applied Sciences, Harvard University, Wyss Institute for Biologically Inspired Engineering at Harvard University, Department of Biomedical Engineering, Tel Aviv University, Sagol School of Neuroscience, Tel Aviv University, The Center for Nanoscience and Nanotechnology, Tel Aviv University, Department of Micro and Nanosystems, KTH Royal Institute of Technology, Swedish Medical Nanoscience Center, Department of Neuroscience, Karolinska Institute, Small Molecule Mass Spectrometry Facility, Harvard University, Graduate Program in Bioinformatics and Biological Design Center, Boston University, Vascular Biology Program and Department of Surgery, Boston Children's Hospital and Harvard Medical School, Department of Biology, Department of Biomedical Engineering, Department of Physics, Boston University, Mass Spectrometry and Proteomics Resource Laboratory, Harvard University, Harvard John A. Paulson School of Engineering and Applied Sciences, Harvard University.

This research was supported by the Wyss Institute for Biologically Inspired Engineering at Harvard University, Defense Advanced Research Projects Agency (DARPA) under Cooperative Agreement Number W911NF-12-2-0036, and Sverige Amerika Stiftelsen, Carl Trygger Stiftelse, Erik och Edith Fernstrom's stiftelse

Nature Biotechnology VOLUME 36 NUMBER 9 SEPTEMBER 2018

Photon-mediated interactions between quantum emitters in a diamond nanocavity

Photon-mediated interactions between quantum systems are essential for realizing quantum networks and scalable quantum information processing. We demonstrate such interactions between pairs of silicon-vacancy (SiV) color centers coupled to a diamond nanophotonic cavity. When the optical transitions of the two color centers are tuned into resonance, the coupling to the common cavity mode results in a coherent interaction between them, leading to spectrally resolved superradiant and subradiant states. We use the electronic spin degrees of freedom of the SiV centers to control these optically mediated interactions. Such controlled interactions will be crucial in developing cavity-mediated quantum gates between spin qubits and for realizing scalable quantum network nodes.

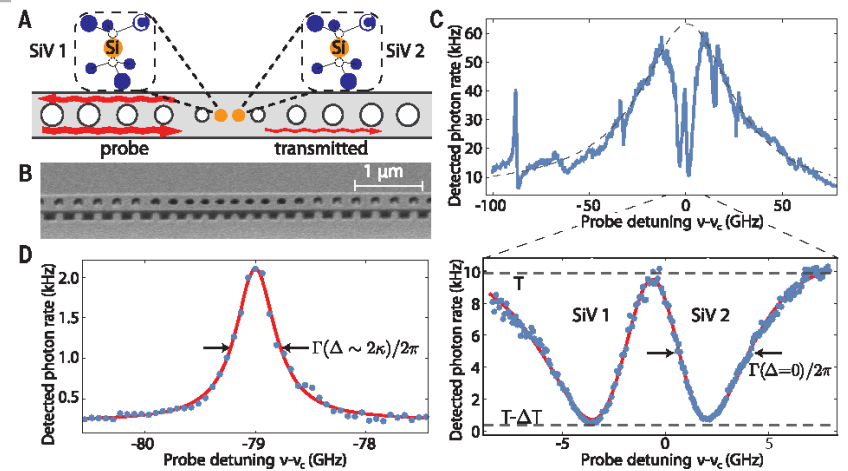


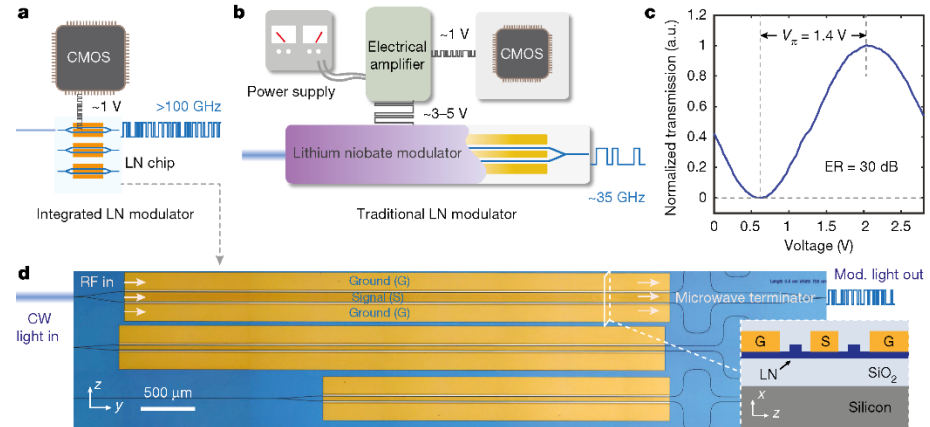
Figure | High cooperativity SiV-photon interface. (A) Schematic of a diamond nanocavity containing two SiV centers. (B) Scanning electron micrograph of a nanocavity. (C) Transmission spectrum of the coupled SiV-cavity system (blue). The broad Lorentzian response of an empty cavity (dashed) is modulated by cavity-coupled SiVs. Near the cavity resonance (lower panel), two SiVs each result in greater than 95% extinction in transmission and are broadened by the Purcell effect [$G(D=0) = 2p \text{ \AA} \sim 4.6 \text{ GHz}$]. (D) In the dispersive regime ($D = 2p \text{ \AA} \sim 79 \text{ GHz} \sim 2k$), SiVs appear as narrow peaks in transmission [$G(D = 2p \text{ \AA} \sim 0.5 \text{ GHz})$]. The solid lines in (D) and the lower panel of (C) are fits to a model.

R. E. Evans, M. K. Bhaskar, D. D. Sukachev, C. T. Nguyen, A. Sipahigil, M. J. Burek, B. Machielse, G. H. Zhang, A. S. Zibrov, E. Bielejec, H. Park, M. Lončar, M. D. Lukin; Department of Physics, Harvard University, Institute for Quantum Information and Matter and Thomas J. Watson, Sr., Laboratory of Applied Physics, California Institute of Technology, John A. Paulson School of Engineering and Applied Sciences, Harvard University, Sandia National Laboratories, Department of Chemistry and Chemical Biology

This work was supported by the NSF, CUA, DoD/ARO DURIP, AFOSR MURI, ONR MURI, ARL, Vannevar Bush Faculty Fellowship, DoD NDSEG, and NSF GRFP. NSF Award # ECCS-123456. Science **362**, 662–665 (2018).

Integrated lithium niobate electro-optic modulators operating at CMOS-compatible voltages

Electro-optic modulators translate high-speed electronic signals into the optical domain and are critical components in modern telecommunication networks and microwave-photonic systems. They are also expected to be building blocks for emerging applications such as quantum photonics and non-reciprocal optics. All of these applications require chip-scale electro-optic modulators that operate at voltages compatible with complementary metal-oxide-semiconductor (CMOS) technology, have ultrahigh electro-optic bandwidths and feature very low optical losses. Integrated modulator platforms based on materials such as silicon, indium phosphide or polymers have not yet been able to meet these requirements simultaneously because of the intrinsic limitations of the materials used. On the other hand, lithium niobate electrooptic modulators, the workhorse of the optoelectronic industry for decades, have been challenging to integrate on-chip because of difficulties in microstructuring lithium niobate. Here we demonstrate the first monolithically integrated lithium niobate electro-optic modulators that feature a CMOS-compatible drive voltage, support data rates up to 210 gigabits per second and show an on-chip optical loss of less than 0.5 decibels. Engineered to achieve high electro-optical efficiencies, ultra-low optical losses and group velocity matching simultaneously our scalable modulator devices provide a cost-effective, low-power and ultra-high-speed solutions for next-generation optical communication networks and microwave photonic systems, enabling a wide range of quantum and classical applications including feed-forward photonic quantum computation.



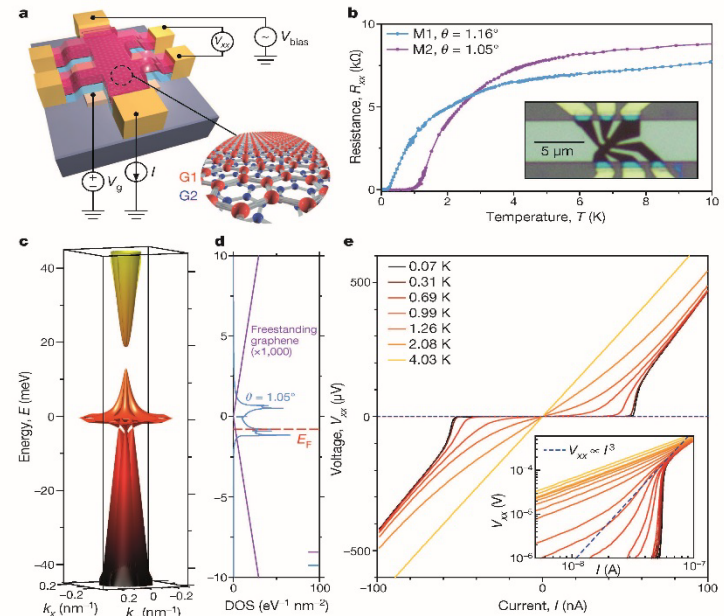
C. Wang, M. Zhang, X. Chen, M. Bertrand, A. Shams-Ansari, S. Chandrasekhar, P. Winzer & M. Lončar; John A. Paulson School of Engineering and Applied Sciences, Harvard University, Department of Electronic Engineering, City University of Hong Kong, Nokia Bell Labs, LP2N, Institut d'Optique Graduate School, CNRS, University of Bordeaux, Department of Electrical Engineering and Computer Science, Howard University.

This work was supported in part by the NSF (ECCS1609549, ECCS-1740296 E2CDA and DMR-1231319), The CNS Scholars Program (NNCI 1541959), and by Harvard University Office of Technology Development.

Nature volume 562, pages101–104 (2018)

Unconventional superconductivity in magic-angle graphene superlattices

The behavior of strongly correlated materials, and in particular unconventional superconductors, has been studied extensively for decades, but is still not well understood. This lack of theoretical understanding has motivated the development of experimental techniques for studying such behaviour, such as using ultracold atom lattices to simulate quantum materials. Here we report the realization of intrinsic unconventional superconductivity—which cannot be explained by weak electron–phonon interactions—in a two-dimensional superlattice created by stacking two sheets of graphene that are twisted relative to each other by a small angle. For twist angles of about 1.1° —the first ‘magic’ angle—the electronic band structure of this ‘twisted bilayer graphene’ exhibits flat bands near zero Fermi energy, resulting in correlated insulating states at half-filling. Upon electrostatic doping of the material away from these correlated insulating states, we observe tunable zero-resistance states with a critical temperature of up to 1.7 kelvin. The temperature–carrier-density phase diagram of twisted bilayer graphene is similar to that of copper oxides (or cuprates), and includes dome-shaped regions that correspond to superconductivity. Moreover, quantum oscillations in the longitudinal resistance of the material indicate the presence of small Fermi surfaces near the correlated insulating states, in analogy with underdoped cuprates. The relatively high superconducting critical temperature of twisted bilayer graphene, given such a small Fermi surface (which corresponds to a carrier density of about 10^{11} per square centimetre), puts it among the superconductors with the strongest pairing strength between electrons. Twisted bilayer graphene is a precisely tunable, purely carbon-based, two-dimensional superconductor. It is therefore an ideal material for investigations of strongly correlated phenomena, which could lead to insights into the physics of high-critical-temperature superconductors and quantum spin liquids.



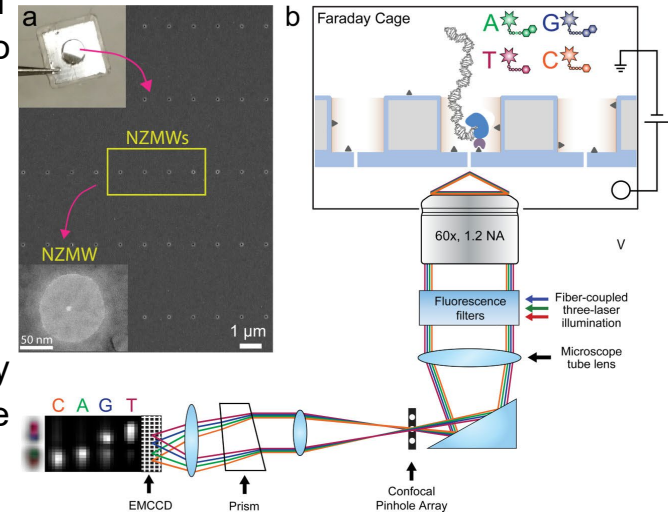
Y. Cao, V. Fatemi, S. Fang, K. Watanabe, T. Taniguchi, E. Kaxiras and P. Jarillo-Herrero; Department of Physics, Massachusetts Institute of Technology, Department of Physics, Harvard University, National Institute for Materials Science, Japan, John A. Paulson School of Engineering and Applied Sciences, Harvard University.

This work was primarily supported by the Gordon and Betty Moore Foundation EPIQS Initiative through grant GBMF4541 and the STC Center for Integrated Quantum Materials (NSF grant number DMR-1231319) *Nature* volume 556, pages 43–50 (05 April 2018)

Cornell Nanoscale Science and Engineering Facility (CNF)

Length-independent DNA packing into nanopore zero-mode

In *Nature Nanotechnology*, Wanunu and his group (Northeastern) and scientists from Pacific BioSciences use the Cornell Nanoscale Facility to show that the efficiency of voltage-induced DNA loading into waveguides equipped with nanopores at their floors is five orders of magnitude greater than existing methods. Compared to conventional methods, single molecule, real-time (SMRT) DNA sequencing exhibits longer read lengths than conventional methods, less GC per cent bias, and the ability to read DNA base modifications. However, reading DNA sequence from sub-ng quantities is impractical due to inefficient delivery of DNA molecules into the confines of zero-mode waveguides, zeptolitre optical cavities in which DNA sequencing proceeds. In addition, they find that DNA loading is nearly length-independent, unlike diffusive loading, which is biased towards shorter fragments. The authors demonstrate here loading and proof-of-principle four-colour sequence readout of a polymerase-bound 20,000 bp long DNA template within seconds from a sub-ng input quantity, a step towards low-input DNA sequencing and mammalian epigenomic mapping of native DNA samples. Pacific Biosciences was a CNF startup that is now a \$500,000,000 company.

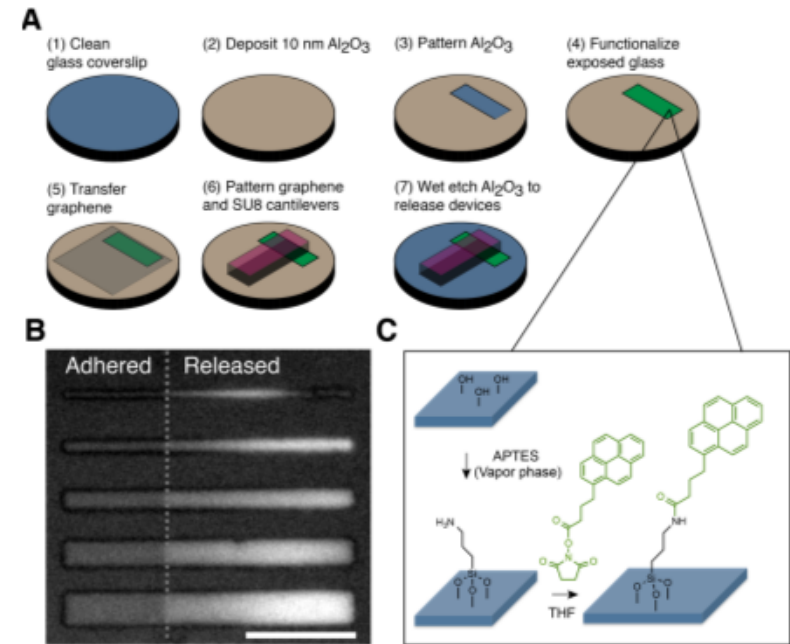


M. Wanunu and coworkers, Northeastern University. Work performed at the Cornell Nanoscale Facility.

This work was supported by NSF Award #ECCS-1542081, NIH (HG006873 and HG009186).
Nat Nanotechnol. 2017 12(12): 1169–1175.

Measuring and Manipulating the Adhesion of Graphene

In **Nanoletters**, McEuen and colleagues at Cornell and Northwestern used the Cornell Nanoscale Facility to characterize the delamination of single-layer graphene from monolayers of pyrene tethered to glass in water and maximize the work of separation between these surfaces by varying the density of pyrene groups in the monolayer. They present a technique to precisely measure the surface energies between two-dimensional materials and substrates that is simple to implement and allows exploration of spatial and chemical control of adhesion at the nanoscale. Control of this energy scale enables high-fidelity graphene-transfer protocols that can resist failure under sonication. hysteresis, differing by a factor of 100. This work establishes a rational means to control the adhesion of 2D materials and enables a systematic approach to engineer stimuli-responsive adhesives and mechanical technologies at the nanoscale.

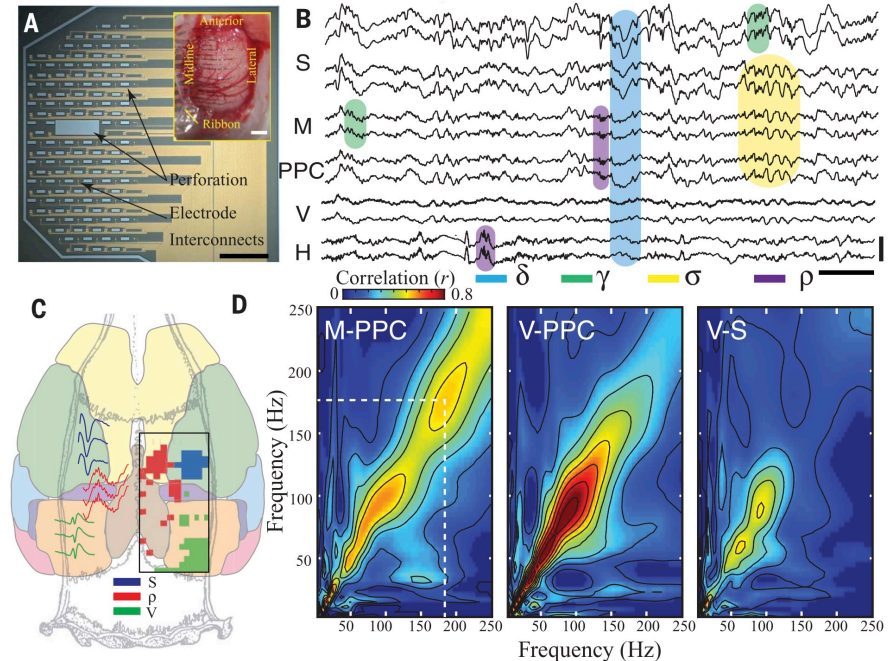


I. Cohen, P. McEuen (Cornell University), W. Dichtel (Northwestern University) and coworkers. Work performed at the Cornell Nanoscale Facility.

This work was supported by NSF Award #ECCS-1542081; CCMR NSF DMR-1719875 and the Kavli Institute at Cornell. *Nano Lett.* 2018, 18, 449–454

Learning-enhanced coupling between ripple oscillations in the brain

In **Science**, Khodagholy et al. (NYU) and colleagues at Columbia used the Cornell Nanoscale Facility to produce a conducting polymer-based conformable microelectrode array (NeuroGrid) and used it to record local field potentials and neural spiking across the dorsal cortical surface of the rat brain, and combined with silicon probe recordings in the hippocampus, to identify candidate physiological patterns. Consolidation of declarative memories requires hippocampal-neocortical communication. Although experimental evidence supports the role of sharp-wave ripples in transferring hippocampal information to the neocortex, the exact cortical destinations and the physiological mechanisms of such transfer are not known. Parietal, midline, and prefrontal, but not primary cortical areas, displayed localized ripple (100 to 150 hertz) oscillations during sleep, concurrent with hippocampal ripples. Coupling between hippocampal and neocortical ripples was strengthened during sleep following learning.

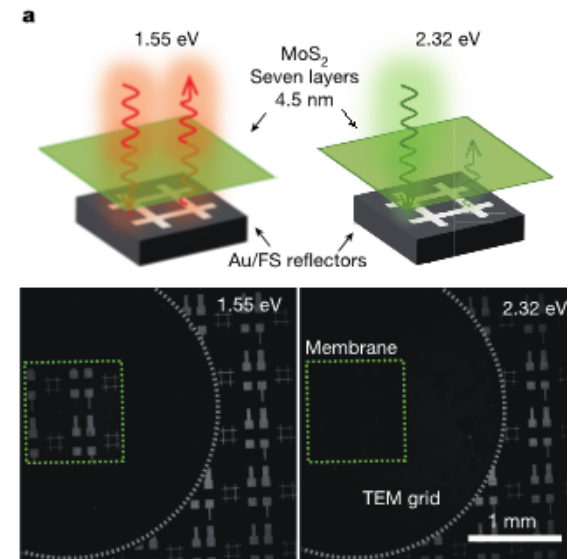


Khodagholy (New York University) and colleagues at Columbia University School of Medicine. Work performed at the Cornell Nanoscale Facility.

This work was supported by NSF Award #ECCS-1542081; NIH grants UO1NS099705, U01NS090583, and MH107396 and DARPA N66001-17-C-4002. *Science* 358, 369–372 (2017).

Assembly of two-dimensional materials into wafer-scale heterostructures

In *Nature*, Park et al. (Chicago) use the Cornell Nanoscale Facility to assemble multilayer stacks of graphene and transition-metal dichalcogenides—which represent one- and three-atom-thick two-dimensional building blocks, respectively—and to realize previously inaccessible heterostructures with interesting physical properties. Here they report the generation of wafer-scale semiconductor films with a very high level of spatial uniformity and pristine interfaces. They fabricate several large-scale, high-quality heterostructure films and devices, including superlattice films with vertical compositions designed layer-by-layer, batch-fabricated tunnel device arrays with resistances that can be tuned over four orders of magnitude, band-engineered heterostructure tunnel diodes, and millimetre-scale ultrathin membranes and windows. The stacked films are detachable, suspendable and compatible with water or plastic surfaces, which will enable their integration with advanced optical and mechanical systems.



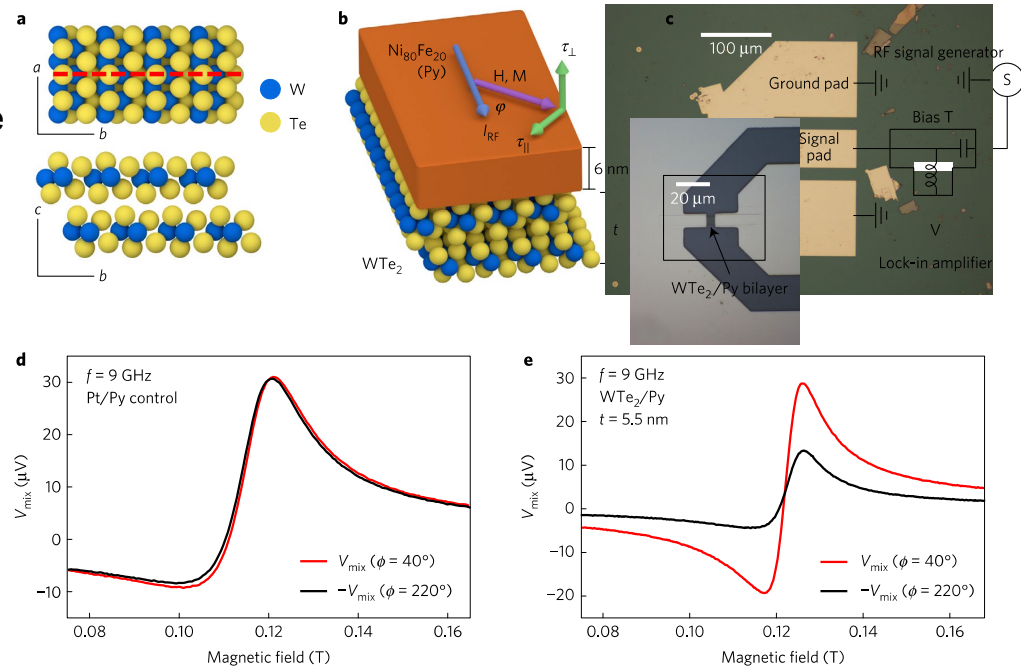
J. Park (University of Chicago), D. Mueller (Cornell University) and coworkers. Work performed at the Cornell Nanoscale Facility.

This work was supported by NSF Award #ECCS-1542081; AFOSR (FA9550-16-1-0031, FA2386-13-1-4118); PARADIM DMR-1539918; CCMR NSF DMR-1120296; NSF DMR-1420709.

Nature 550, 229–233 (12 October 2017)

Control of spin-orbit torques in WTe₂/ferromagnet bilayers

In *Nature Physics*, the Park (U Chicago) and Ralph (Cornell) groups used the Cornell Nanoscale Facility to show that one can change the allowed symmetries of spin-orbit torques in spin-source/ferromagnet bilayer devices by using a spin-source material with low crystalline symmetry. Recent discoveries regarding current-induced spin-orbit torques produced by heavy-metal/ferromagnet and topological insulator/ferromagnet bilayers provide the potential for dramatically improved efficiency in the manipulation of magnetic devices. In this work the authors show experimentally that this state of affairs is not fundamental but can be selected.



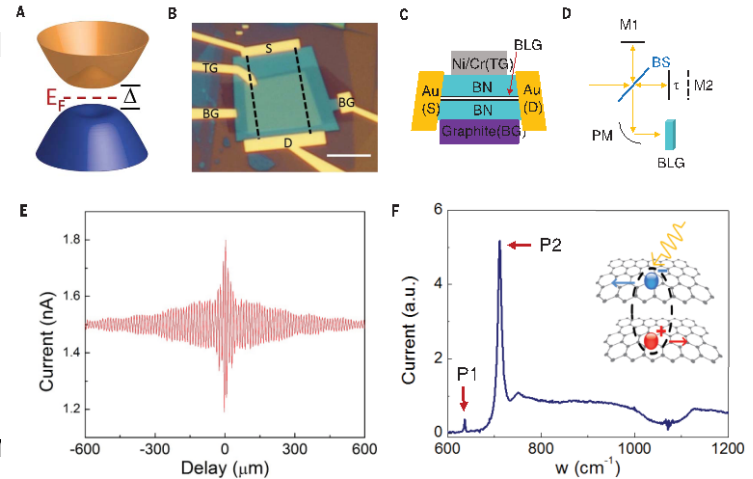
D. Ralph, R. Buhrman (Cornell University). J. Park (University of Chicago) and coworkers. Work performed at the Cornell Nanoscale Facility.

This work was supported by NSF Award #ECCS-1542081; DMR-1406333; ARO (W911NF-15-1-0447); NSF DGE-1144153; PARADIM (DMR-1539918; NNCI grant ECCS-1542081).

Nature Physics, 2017, 13, 301

Tunable excitons in bilayer graphene

In *Science*, McEuen et al. (Cornell) use the Cornell Nanoscale Facility to show that excitons, the bound states of an electron and a hole in a solid material, play a key role in the optical properties of insulators and semiconductors. They report the observation of excitons in bilayer graphene (BLG) using photocurrent spectroscopy of high-quality BLG encapsulated in hexagonal boron nitride. They observed two prominent excitonic resonances with narrow line widths that are tunable from the mid-infrared to the terahertz range. These excitons obey optical selection rules distinct from those in conventional semiconductors and feature an electron pseudospin winding number of 2. An external magnetic field induces a large splitting of the valley excitons, corresponding to a g-factor of about 20. These findings open up opportunities to explore exciton physics with pseudospin texture in electrically tunable graphene systems.



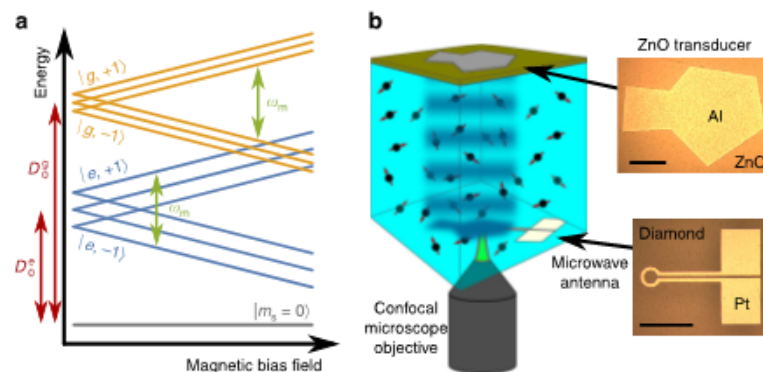
P. McEuen, F. Rana, J. Park (Cornell University), K. Watanabe (NIMS Japan) and coworkers. Work performed at the Cornell Nanoscale Facility.

This work was supported by NSF Award # ECCS-1542081; CCMR (DMR-1120296); AFOSR (MURI: FA9550-16-1-0031); ONR N00014-12-1-0072.

Ju et al., *Science* 358, 907–910 (2017)

Cooling a mechanical resonator with nitrogen-vacancy centres

In *Nature Communications*, Fuchs (Cornell) and colleagues at Argonne National Labs used the Cornell Nanoscale Facility to experimentally demonstrate that the spin–strain coupling in the excited state is 13.5 ± 0.5 times stronger than the ground state spin–strain coupling. Cooling a mechanical resonator mode to a sub-thermal state has been a long-standing challenge in physics. This pursuit has recently found traction in the field of optomechanics in which a mechanical mode is coupled to an optical cavity. By dissipatively cooling a room temperature mechanical resonator using a nitrogen-vacancy centre ensemble, the spin ensemble is coupled to the resonator through its orbitally-averaged excited state, which has a spin–strain interaction that has not been previously studied.

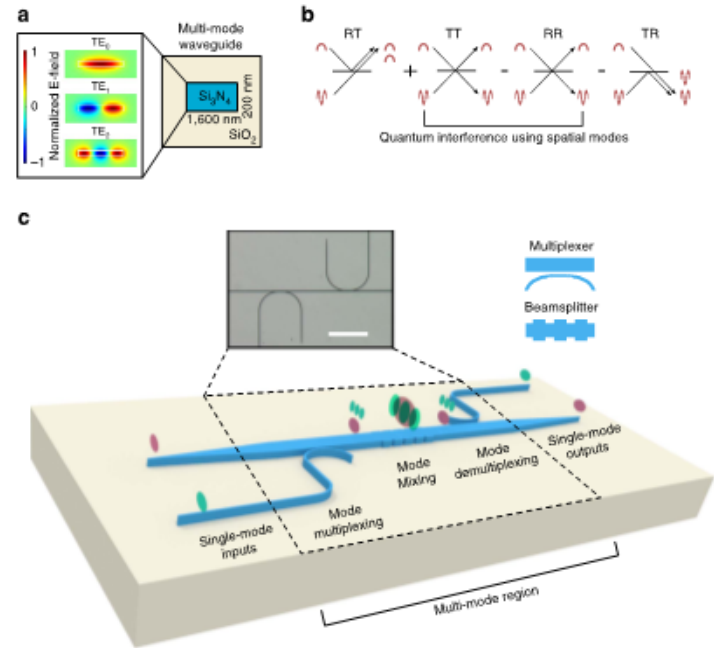


E.R. McQuarrie, M. Otten, G. Fuchs (Cornell University), S. G. Gray (Argonne National Laboratory). Work performed at the Cornell Nanoscale Facility.

This work was supported by NSF Award #ECCS-15420819, ONR (Grant N000141410812).
Nature Communications 8, 14358 (2017)

Quantum interference between transverse spatial waveguide modes

In **Nature Communications**, Lipson et al. (Columbia) used the Cornell Nanoscale Facility to quantum interference between the transverse spatial modes within a single multi-mode waveguide using quantum circuit-building blocks. Integrated quantum optics has the potential to markedly reduce the footprint and resource requirements of quantum information processing systems, but its practical implementation demands broader utilization of the available degrees of freedom within the optical field. This work shows that spatial modes can be controlled to an unprecedented level and have the potential to enable practical and robust quantum information processing.

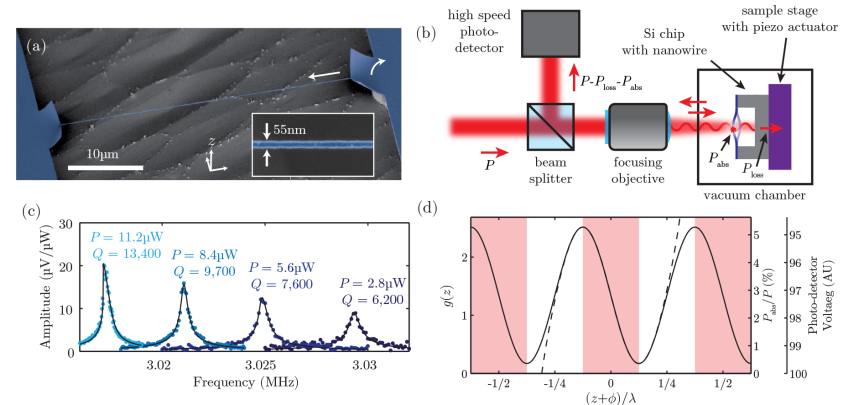


M. Lipson (Columbia University), M. Zhiang (Harvard University), S. Ramelow (Cornell University) and coworkers. Work performed at the Cornell Nanoscale Facility.

This work was supported by NSF Award # ECCS-1542081; NSF ERC (EEC-0812072).
Nature Communications **8**, 14010 (2017)

Low-Power Photothermal Self Oscillation of Bimetallic Nanowires

In **Nanoletters**, Parpia and colleagues at Cornell used the Cornell Nanoscale Facility to investigate the nonlinear mechanics of a bimetallic, optically absorbing SiN–Nb nanowire in the presence of incident laser light and a reflecting Si mirror. Situated in a standing wave of optical intensity and subject to photothermal forces, the nanowire undergoes self-induced oscillations at low incident light thresholds of $<1 \mu\text{W}$ due to engineered strong temperature-position (T - z) coupling. Along with inducing self-oscillation, laser light causes large changes to the mechanical resonant frequency ω_0 and equilibrium position z_0 . They study the linearized equations of motion to show that the optimal thermal time constant τ for photothermal feedback is $\tau \rightarrow \infty$ rather than the previously reported $\tau = 1$. Lastly, they demonstrate photothermal quality factor (Q) enhancement of driven motion as a means to counteract air damping.



J. Parpia, H. Craighead, R. Rand and coworkers at Cornell University. Work performed at the Cornell Nanoscale Facility.

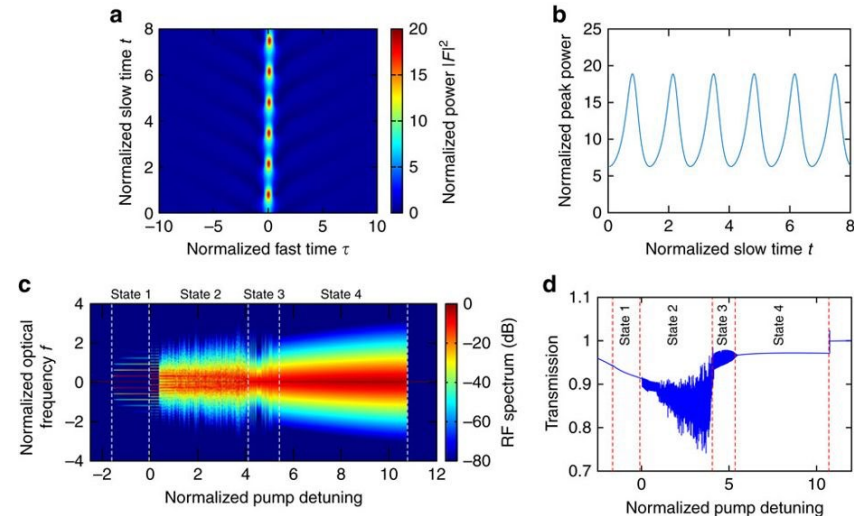
This work was supported by NSF Award # ECCS-1542081; NSF CCMR DMR-1120296; NSF DMR-1202991.
Nano Lett. 2017, 17, 3995–4002

Breather soliton dynamics in microresonators

In **Nature Communications**, Gaeta et al. (Columbia) use the Cornell Nanoscale Facility to demonstrate the excitation of breather solitons in two different microresonator platforms based on silicon nitride and on silicon. The generation of temporal cavity solitons in microresonators results in coherent low-noise optical frequency combs that are critical for applications in spectroscopy, astronomy, navigation or telecommunications. Breather solitons also form an important part of many different classes of nonlinear wave systems, manifesting themselves as a localized temporal structure that exhibits oscillatory behaviour. To date, the dynamics of breather solitons in microresonators remains largely unexplored, and its experimental characterization is challenging. We investigate the dependence of the breathing frequency on pump detuning and observe the transition from period-1 to period-2 oscillation. Our study constitutes a significant contribution to understanding the soliton dynamics within the larger context of nonlinear science.

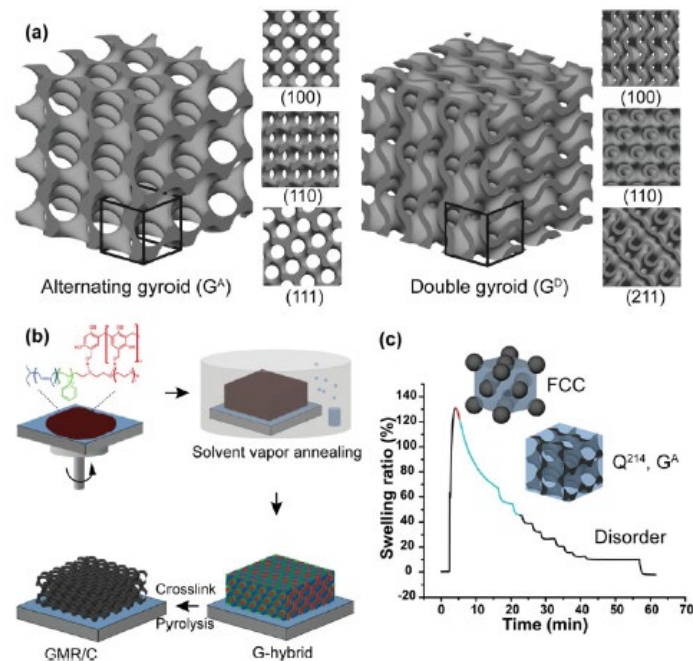
A. Gaeta, M. Lipson (Columbia University), A. Griffin, K. Luke (Cornell University), and coworkers. Work performed at the Cornell Nanoscale Facility.

This work was supported by NSF Award # ECCS-1542081; DARPA W31P4Q-15-1-0015, AFOSR (FA9550-15-1-0303), NSF (ECS-0335765, ECCS-1306035). *Nature Communications*, **8**, 14569 (2017).



Mesoporous Resin/Carbon Thin Films with Alternating Gyroid Morphology

In *ACS Nano*, Wiesner et al. (Cornell) and Nealey et al. (Chicago) have used the Cornell Nanoscale Facility to create single (alternating) gyroidal and double gyroidal mesoporous thin-film structures via solvent vapor annealing assisted co-assembly of poly(isoprene-block-styrene-block-ethylene oxide) (PI-b-PS-b-PEO, ISO) and resorcinol/phenol formaldehyde resols. Three-dimensional (3D) mesoporous thin films with sub-100 nm periodic lattices are of increasing interest as templates for a number of nanotechnology applications, yet are hard to achieve with conventional top-down fabrication methods. Block copolymer self-assembly derived mesoscale structures provide a toolbox for such 3D template formation. In particular, the alternating gyroid thin-film morphology is highly desirable for potential template backfilling processes as a result of the large pore volume fraction. In situ grazing-incidence small-angle X-ray scattering during solvent annealing is employed as a tool to elucidate and navigate the pathway complexity of the structure formation processes. The thin films have tunable hydrophilicity from pyrolysis at different temperatures, while pore sizes can be tailored by varying ISO molar mass. Increased conductivity after pyrolysis at high temperatures demonstrates that these gyroidal mesoporous resin/carbon thin films have potential as functional 3D templates for a number of nanomaterials applications.

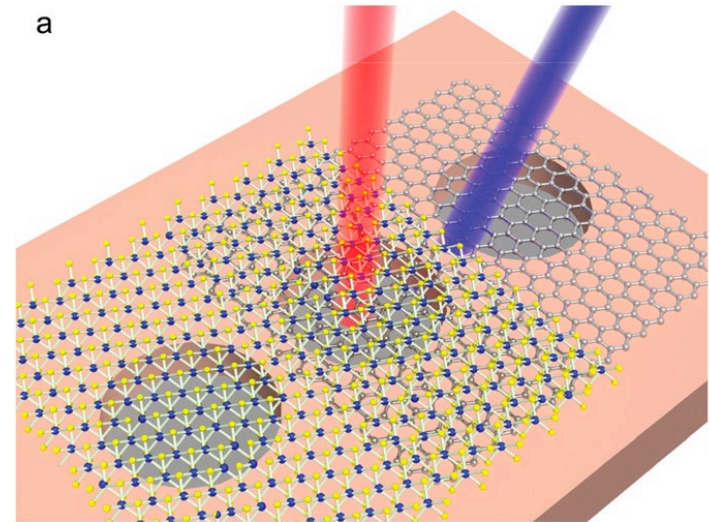


U. Wiesner (Cornell University), D. Smilgies (CHESS), P. Nealey (University of Chicago) and coworkers. Work performed at the Cornell Nanoscale Facility.

This work was supported by NSF Award # ECCS-154208, NSF DMR-1707836; CCMR DMR-1719875. *ACS Nano* 2018, 12, 347–358.

Atomic layer MoS₂-graphene van der Waals nanomechanical resonators

In *Nanoscale*, Feng and coworkers (Case Western) used the Cornell Nanoscale Facility to create the first experimental demonstration of freestanding van der Waals heterostructures and their functional nanomechanical devices. Heterostructures play significant roles in modern semiconductor devices and micro/nanosystems in a plethora of applications in electronics, optoelectronics, and transducers. While state-of-the-art heterostructures often involve stacks of crystalline epi-layers, each down to a few nanometers thick, the intriguing limit would be hetero-atomic-layer structures. By stacking single-layer (1L) MoS₂ on top of suspended single-, bi-, tri- and four-layer (1L to 4L) graphene sheets, we realize an array of MoS₂-graphene heterostructures with varying thickness and size. These heterostructures all exhibit robust nanomechanical resonances in the very high frequency (VHF) band (up to ~100 MHz). We observe that fundamental-mode resonance frequencies of the heterostructure devices fall between the values of graphene and MoS₂ devices. Quality (Q) factors of heterostructure resonators are lower than those of graphene but comparable to those of MoS₂ devices, suggesting interface damping related to interlayer interactions in the van der Waals heterostructures. This study validates suspended atomic layer heterostructures as an effective device platform and provides opportunities for exploiting mechanically coupled effects and interlayer interactions in such devices.



P. X.-L. Feng (Case Western) and coworkers. Work performed at the Cornell Nanoscale Facility.

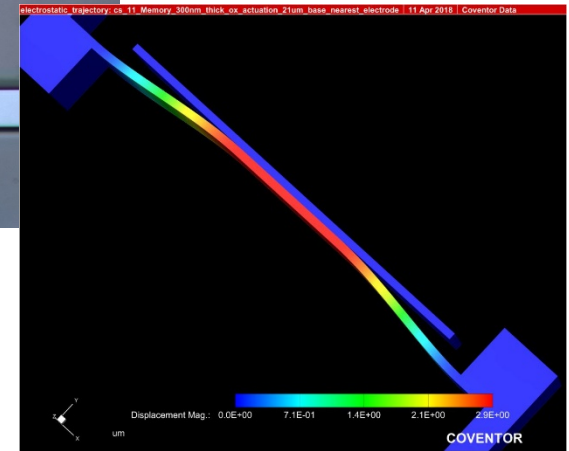
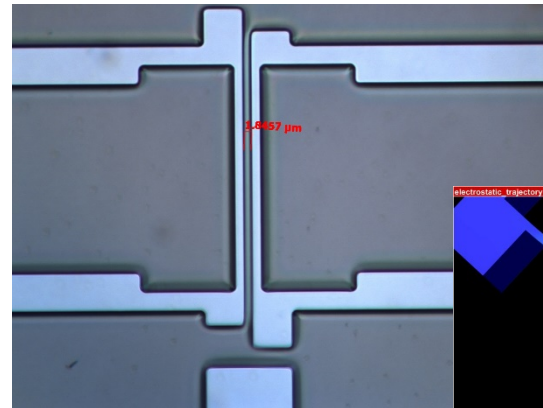
This work was supported by NSF Award #ECCS-1542081; NSF CAREER (ECCS-1454570); NSF CCSS (Grant ECCS-1509721).

Nanoscale, 2017, 9, 18208–18215

Kentucky Multi-Scale Manufacturing and Nano Integration Node (KY MMNIN)

Bi-Stable MEMS Structures

Bi-stable mechanical structures may be used for many applications, including relays, switches (incl. electrical, pneumatic, optical), shutters, positioning systems, energy harvesters, memory, and for latches for zero-power sensors. The PI's are investigating the effects of radiation, such as x-rays and protons, on the performance and stability of the bi-stable structures. In this work, a composite beam consisting of silicon and SiO₂ is being investigated. The silicon provides structural integrity, while the SiO₂ provides a compressive layer. A feature of this system is that it is easily fabricated using SOI wafers commonly used for many MEMS devices.



Top: Optical image of silicon beam. When released, the silicon beam buckles laterally.

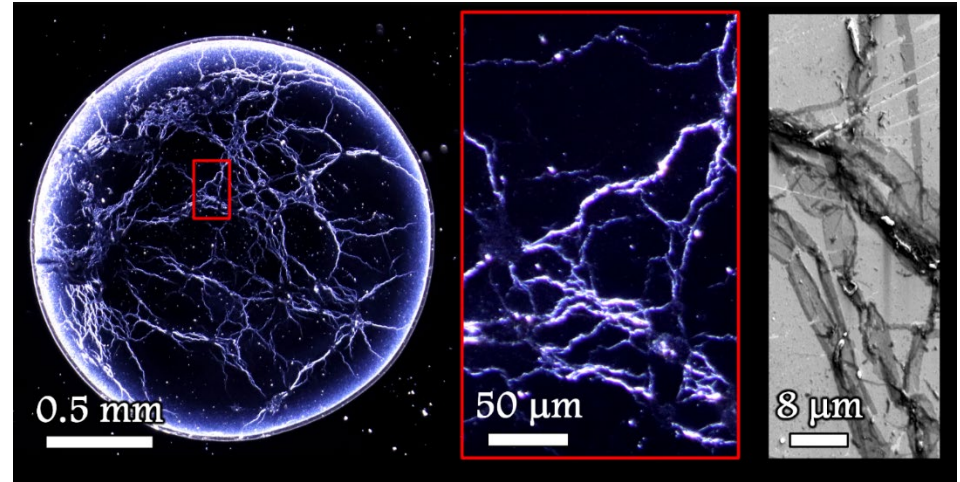
Bottom: Simulation showing the buckled state.

Bruce Alphenaar, Shamus McNamara, Kevin Walsh, Electrical and Computer Engineering, University of Louisville
Work partially performed at the University of Louisville Micro/Nano Technology Center.
The work was supported by DTRA through grant no. HDTRA1-15-0027.

Analysis of Web-like Nanostructures of Evaporated Drops of Bourbon Whiskey

This work focuses on the analysis of self-assembled web-like structures that form when a drop of diluted bourbon whiskey is evaporated. These structures form when lipid-derived monolayers are at the liquid-air interface and are subsequently distorted and assembled via evaporation fluid dynamics.

We have found that through our fixed evaporation conditions (1.0 μL drop, 25% ABV) these patterns form only for new charred barrel products ($n = 65$) and not for other whiskeys ($n = 12$) nor distillates ($n = 5$). Further, patterns are repeatable and are distinctly unique between different brands of bourbon. Findings are used for simplistic analysis of intrinsic properties as well as counterfeit identification.



Microscopic (via light scattering) and SEM images of web-like structures resulting from an evaporated diluted (25% ABV) drop of Jack Daniel's Barrel Strength bourbon whiskey (unpublished).

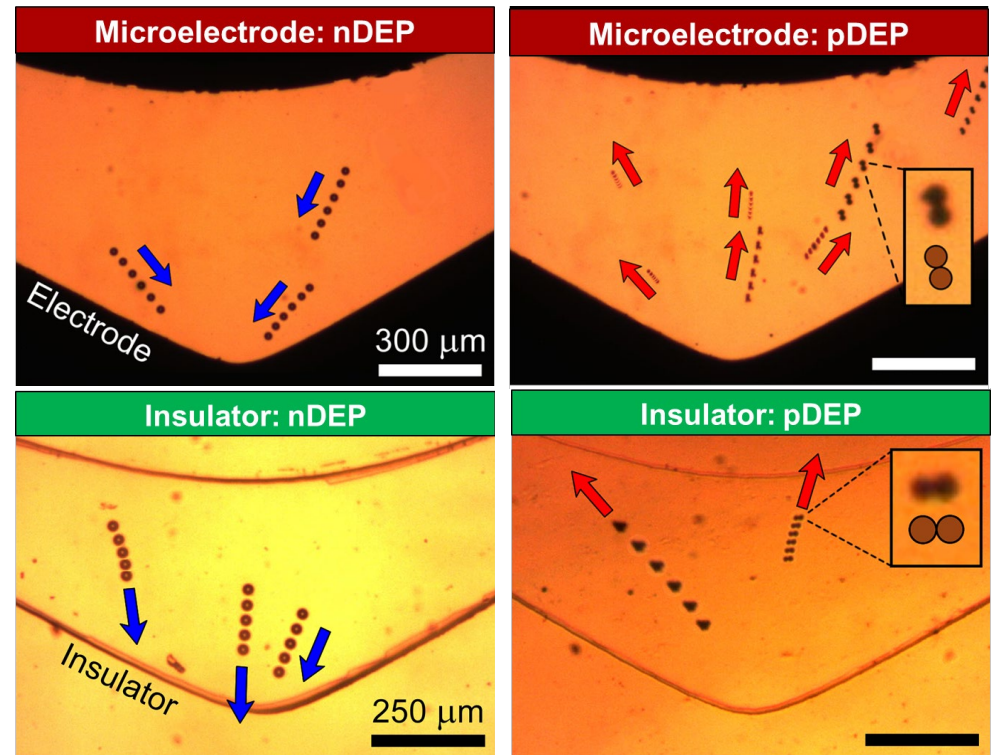
Stuart J. Williams, University of Louisville

Work performed at University of Louisville's Micro/Nano Technology Center

Isomotive Dielectrophoresis (isoDEP) for Dielectric Characterization of Particles

This work focuses on the design of an isomotive dielectrophoresis (isoDEP) platform that provides a uniform DEP force throughout the microchannel. Particle translation is a function of the applied AC signal (voltage, frequency) and gives insight into the dielectric properties of the suspended particles.

Two platforms have been fabricated and tested. First, the field is applied across the microchannel sidewalls as the walls themselves serve as electrodes. The walls were patterned via DRIE of doped silicon. Second, an insulator version is created with PDMS via standard soft lithography; the field is applied through the length of the microchannel. Interestingly, both configurations yield an isomotive solution.



Two microfluidic isoDEP platforms (microelectrode, insulator) demonstrating both positive and negative dielectrophoresis. Figure modified from *Electrophoresis* **38**, 1441-1449 (2017).

Stuart J. Williams, Mechanical Engineering, University of Louisville
Work performed at University of Louisville's Micro/Nano Technology Center

Characterization of Pig Digestive Development from Late Gestation through 25 kg Body Weight

This project will generate information that will expand our knowledge of the growth and development of the gastrointestinal tract (GIT) and highlight key changes that occur in the development of the GIT over critical times of the pig's life (e.g., immediately following birth and immediately following weaning). By focusing on the changes of the intestinal villi and microvilli in the gut that are responsible for nutrient absorption, and therefore overall growth of the pig, a clear visual aid will be developed to show how the surface of the villi and microvilli change with age and different physiological states of life. Obtaining micrographs of the changes in the villi and microvilli including shape, relative size, and density in the small intestine at specific locations over a period time will allow determination of the time points that are most crucial in the development of the small intestine. The overall enhanced knowledge and understanding that will result from this project will provide descriptive detail of the morphological changes that occur in the natural growth and development of the gut and allow for targeting of specific times and locations in the small intestine to improve overall nutrient utilization and gut health of the pig.



SEM image of pig intestinal villi

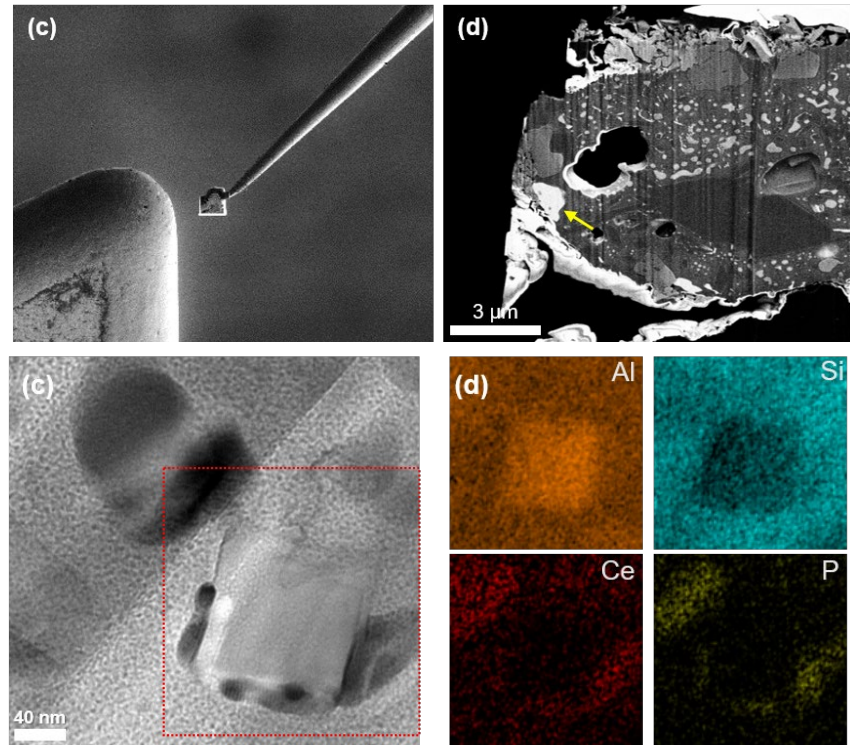
S. K. Elefson, J. C. Matthews, M. D. Lindemann, Animal and Food Sciences, University of Kentucky

Work performed at the University of Kentucky Electron Microscopy Center

This work is supported by the National Institute of Food and Agriculture, U.S. Department of Agriculture, Hatch-Multistate Program (Project 2350937000) under Accession number 1002298.

Rare Earth Element Associations in the KY State University Stoker Ash

The Kentucky State University heating plant stoker ash, with over 1000 $\mu\text{g/g}$ Rare earth elements + yttrium (REY), was previously shown to be more resistant to acid-extraction than pulverized-coal fly ashes of similar bulk composition. In this study, the petrology and mineralogy of this stoker ash was examined in greater detail as a means to better understand why the REY were relatively inert towards acid extraction. The results showed that this stoker ash is dominated by mullite and quartz/cristobalite with lesser amounts of hematite and magnetite compared to the glass-dominated assemblages of pulverized-coal-combustion fly ashes with similar chemical compositions. On the nanometer to micron scale, La-Ce-Nd-bearing monazite and Ce phosphates are seen to be part of the mineral assemblage. Overall, the results demonstrate that despite the presence of discrete REY-bearing minerals in the sample, their encapsulation within other phases may explain their low extractability.



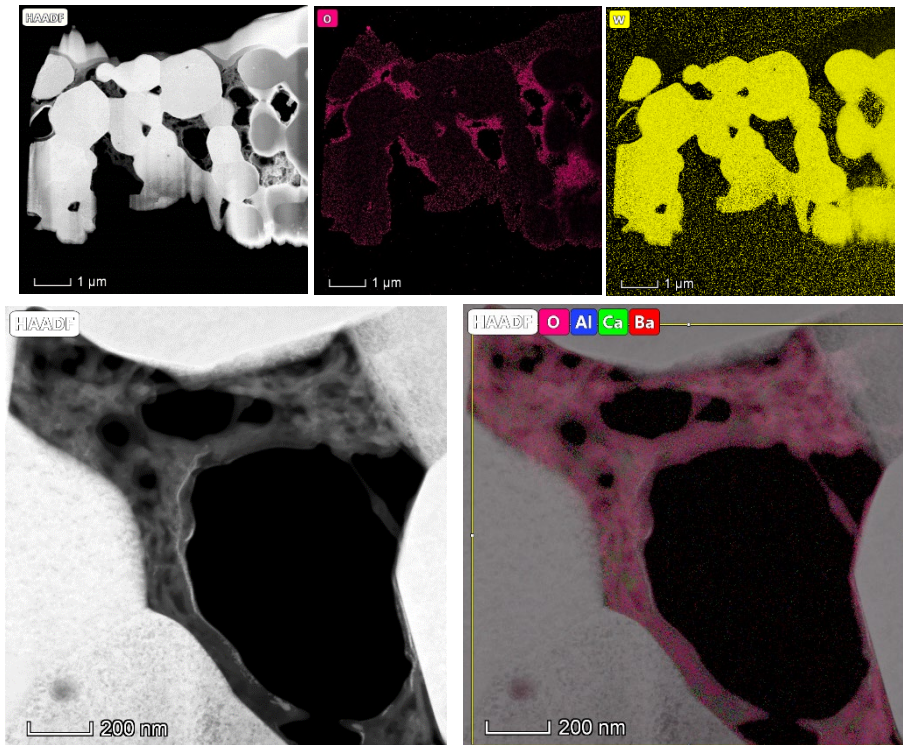
TEM lamella fabrication (lift out) and TEM characterization (imaging and EDS)

James Hower, Center for Applied Energy Research, University of Kentucky. Work performed at the University of Kentucky Electron Microscopy Center.

This research was supported by NSF CBET-1510965 and CBET-1510861.
International Journal of Coal Geology, Volume 189, 2018, Pages 75-82

Characterization of Impregnated Tungsten Pellet for Thermoionic Scandate Cathode

Scandate cathodes are next-generation devices that hold promise for significant improvements in thermionic electron emission, with anticipated impact in telecommunications and radar applications. However, the role of scandium (Sc) in these cathodes is not yet understood, which hampers the development of reliable methods for manufacturing them. The sample characterized here, part of ongoing thermionic scandate cathode research, is an impregnated pellet (a porous tungsten pellet impregnated with BaO-CaO-Al₂O₃ mixed oxide) that represents an intermediate stage of cathode processing. EDS mapping of elemental distribution in the sample was performed within the newly installed FEI Talos F200X transmission electron microscope. A liftout cross-section lamella was made with the FIB-SEM (Nanolab 660). A high angle annular dark field (HAADF) image along with elemental maps of a typical area of the cathode lamella are shown in the figure at right. The elemental signals for Ba, Ca, Al and O indicate that the oxide impregnant fills the tungsten pores and likely forms a single phase.



HAADF image and EDS maps of a TEM lamella extracted from a W cathode

Xiaotao Liu, Chemical and Materials Engineering, University of Kentucky

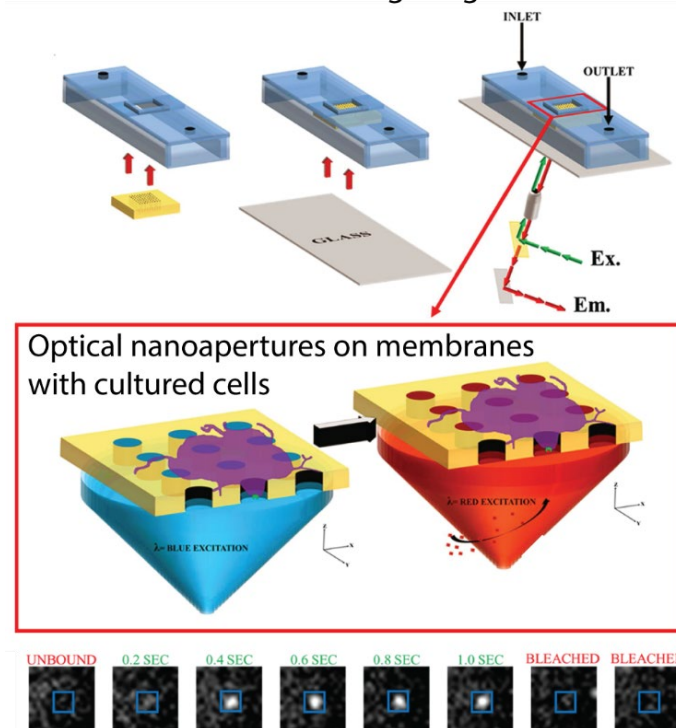
Work performed at the University of Kentucky Electron Microscopy Center.

This research was supported by the Defense Advanced Research Projects Agency (DARPA, grant no. N66001-16-1-4041).

Detecting Single Molecule Interactions with Cells

Measuring molecular binding to cell-surface receptors is important for understanding a variety of biological signaling processes. However, measuring single binding events, rather than taking ensemble measurements, remains quite challenging. U.K. Professors Christine Trinkle and Christopher Richards recently developed nanoaperture optical sensors for detecting single ligand binding on cell surfaces. The sensors consist of gold nanoapertures on a silicon nitride membrane incorporated into a glass and PDMS flow cell. Mouse neuroblastoma cells were cultured on the arrays and single molecules of labeled epidermal growth factor were detected. Such sensors will enable the study of receptor-ligand binding on the surface of live cells while maintaining the cells in a more natural environment.

Microfluidic Chip for Fluorescence Detection of Single Ligands

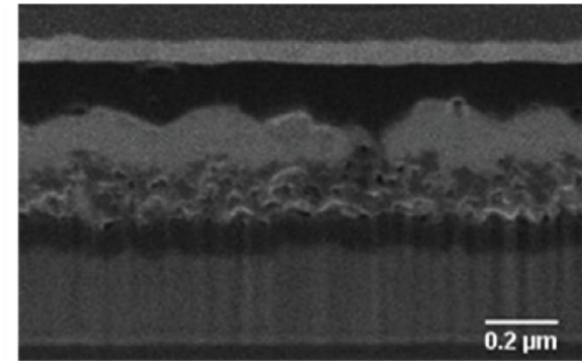


Christine Trinkle, Mechanical Engineering, and Christopher Richards, Chemistry, University of Kentucky
Work partially performed at the UK Center for Nanoscale Science and Engineering

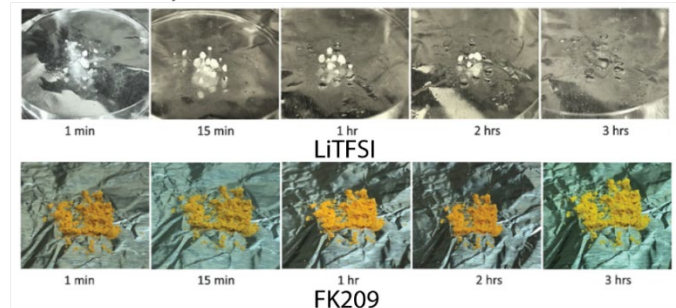
This research was supported by the Human Frontiers Science Program (RGY0081/2014) and the NIH DA038817.
ACS Omega 2.7 (2017): 3858-3867

Fabrication of Perovskite Solar Cells under Ambient Conditions

Perovskite solar cells have remarkable potential in terms of performance and cost. However, the materials for these cells are often sensitive to manufacturing conditions, particularly moisture, and require highly controlled fabrication environments. This level of control adversely affects manufacturing costs. Professors Chen and Singh at the University of Kentucky have recently demonstrated that an alternative, LiTFSI free, hole transport material enables the fabrication of solar cells with power conversion efficiencies of 13% *entirely* under ambient conditions with humidity above 36%. This includes preparation and storage of all solutions. Moreover, they discovered that exposure of samples to both air and light are important for maximizing current density and fill factor.



Cross-section of perovskite solar cell fabricated entirely under ambient conditions.



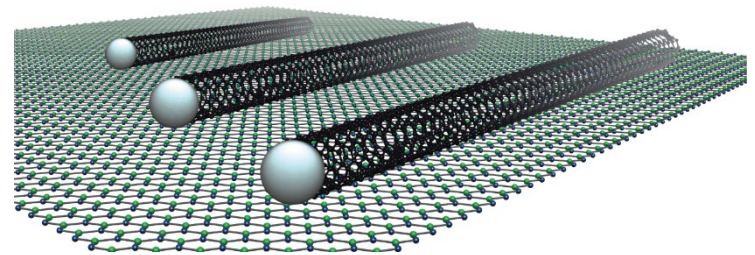
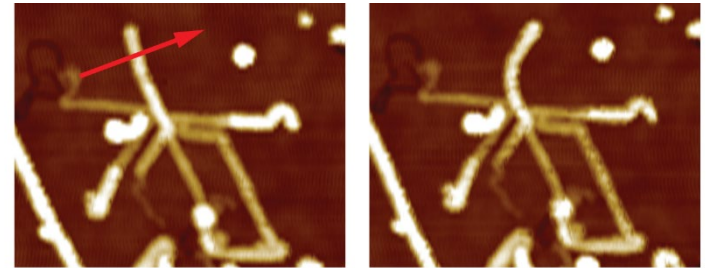
Comparison of moisture sensitivity of hole transport materials.

Zhi Chen and Vijay Singh, Electrical Engineering, University of Kentucky.
Work partially performed at the UK Center for Nanoscale Science and Engineering and Electron Microscopy Center.
Supported in part by Advanced Semiconductor Processing Technology LLC,
China Scholarship Council, and National Natural Science Foundation of China under Grants 61421002, 61574029,
and 61371046.

IEEE Journal of Photovoltaics 8.4 (2018): 1051-1057

Growing Carbon Nanotubes Aligned to Hexagonal Boron Nitride

One and two dimensional materials show exceptional promise for a variety of electronic, photonic, and mechanical applications. Recently, Professor Strachan's group at U.K. combined materials, carbon nanotubes and hexagonal boron nitride (hBN), with dissimilar properties and dimensions having nearly the same lattice spacing to form ordered interfaces along specific crystal directions. The nanotubes show clear preference to align to specific crystal directions of the hBN substrate during growth processing. The direct integrated growth of components consisting of contrasting material properties and dimensionalities provides an important step to developing high-performance nanoscale electrical circuits on these ideal insulating substrates.



Top: Crystallographically-aligned nanotubes shown that were grown on a boron nitride (hBN) surface. There are three clear preferred growth directions along the hBN lattice. The nanotubes can be pushed along the surface of the hBN, as they are van der Waals coupled to it.

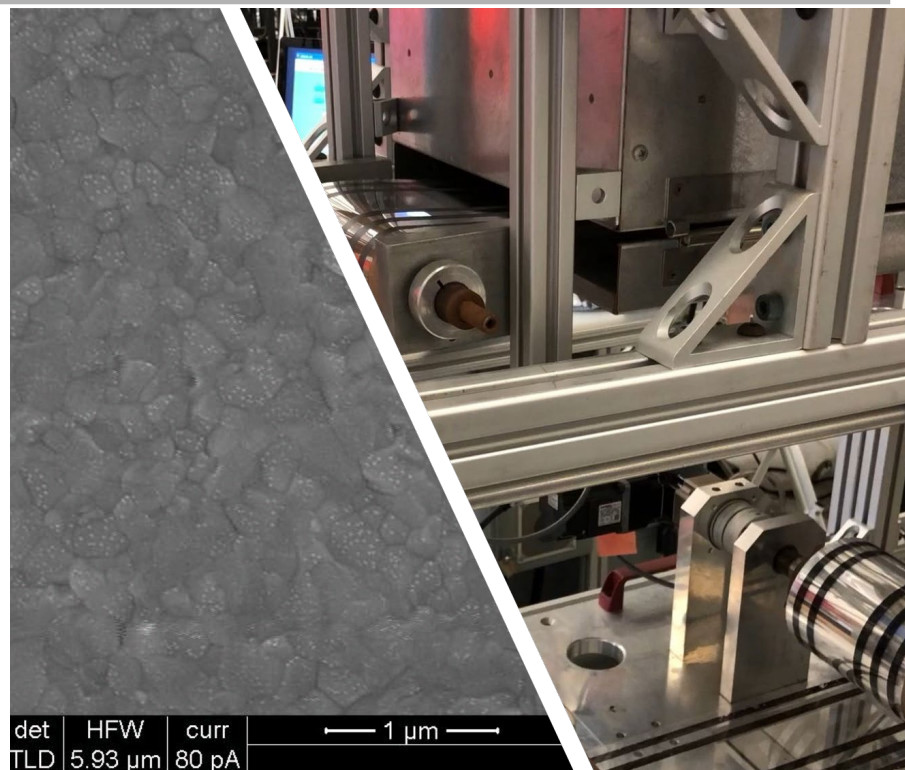
Bottom: Illustration of one-dimensional carbon nanotubes aligned on a two-dimensional hBN substrate.

Douglas Strachan, Physics, University of Kentucky. Work partially performed at the University of Kentucky Center for Nanoscale Science and Engineering

The work was supported by DOE No. 0000223282 and the Kentucky EPSCoR Program.
Advanced Materials Interfaces (2018): 1800793

Roll-to-roll Production of Flexible Perovskite Solar Cells

This work involves scaling the production of the deposition of an alkyl ammonium metal halide over a large area using roll-to-roll techniques. The deposition of the perovskite material was accomplished using a slot die system and was deposited at 300 nm thickness. The material was then annealed using photonic sources; infrared to evolve the solvents and intense pulsed light to both unlock precursors and crystallize the films. The full process was accomplished at 1 m/min and is capable of much higher speeds. These techniques have been used to produce devices with very high currents and is currently being optimized for the flexible substrates.

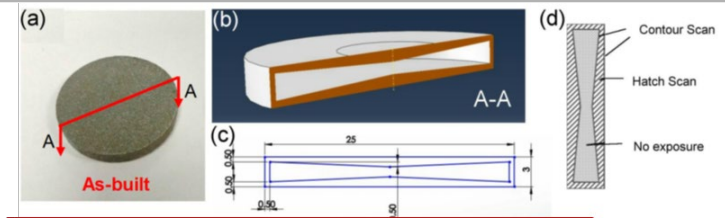


Crystal structure of the perovskite material (left) and the roll-to-roll deposition (right).

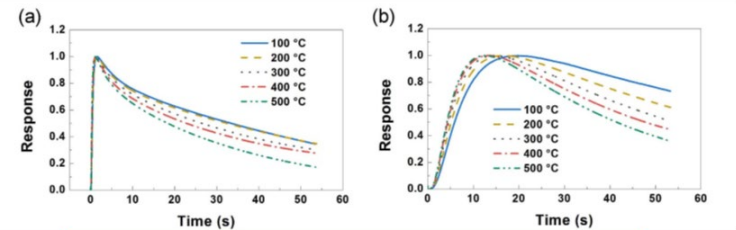
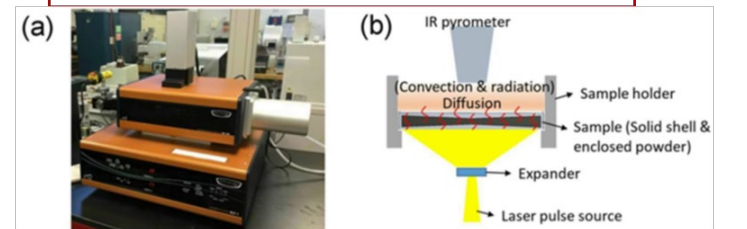
Thad Druffel, Conn Center for Renewable Energy Research, University of Louisville
Work performed at the University of Louisville Conn Center for Renewable Energy Research

Metal Powder Thermal Conductivity in Laser Powder Bed Fusion Additive Manufacturing

This study investigated the thermal conductivity of nickel and titanium alloy powders used in laser powder-bed fusion (LPBF) additive manufacturing. A hollow test specimen enclosed the unmelted powder, matching powder bed conditions. Specimens were analyzed in a laser flash system to measure their transient temperature response. A model and a multi-point optimization algorithm were applied to inversely extract the thermal diffusivity and conductivity of the powder. The results indicate that the thermal conductivity of IN625 powder ranges from 0.65 W/(m·K) to 1.02 W/(m·K) at 100 °C and 500 °C, respectively. Ti64 powder has a thermal conductivity 35 % to 40 % smaller. However, the thermal conductivity ratio of the powder to the respective solid counterpart is not much different between the two materials, about 4 % to 7 % and is largely temperature independent.



Fabricated sample encloses powder for laser flash thermal diffusivity measurement



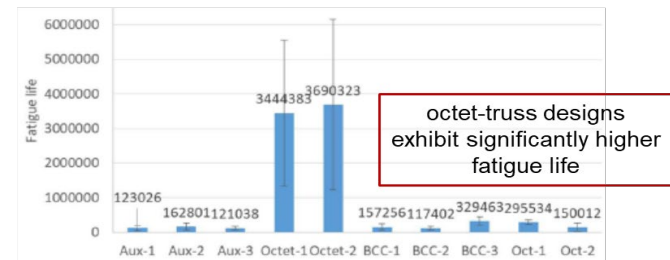
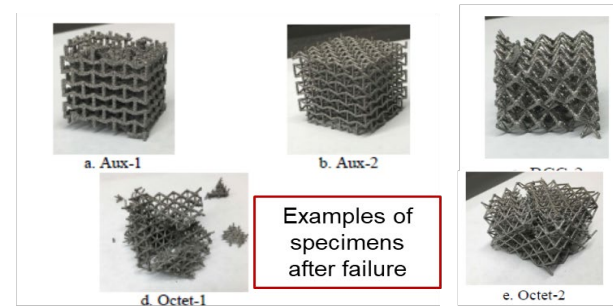
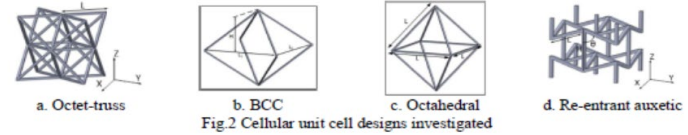
Thermal properties are determined inversely by matching model to experiment.

Shanshan Zhang and Kevin Chou, Industrial Engineering, University of Louisville
Work performed in the UofL Rapid Prototyping Center

Support from National Institute of Standards and Technology.
Proceedings of the 29th Annual International Solid Freeform Fabrication Symposium (2018).

Fatigue of Cellular Structures Fabricated by E-Beam Additive Manufacturing

In this study multiple cellular structures, including the re-entrant auxetic, the octet-truss, and the BCC lattice, were evaluated for their relative fatigue strength under compression-compression cyclic loading. Various design variations with different dimensions were fabricated via electron beam powder bed fusion (EB-PBF) additive manufacturing (AM) process. Initial S-N based fatigue strength characterization with the BCC lattice shows significantly decreased fatigue strength of the cellular parts compared to the solid samples. Cross-design comparison were consequently carried out using constant maximum stress ratio level. The results indicate that the fatigue characteristics of the EB-PBF cellular structures are not only dependent on their topology types but also their geometry.

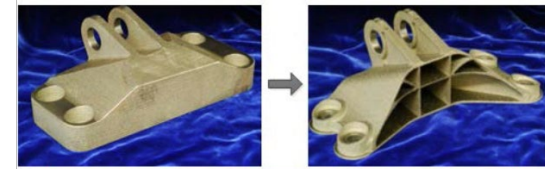


Abigail Orange, Yan Wu and Li Yang, University of Louisville
This work was performed in the UofL Rapid Prototyping Center.

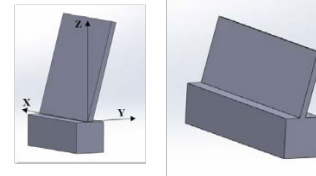
Research supported by the Office of Naval Research (grant #N00014-16-1-2394)
Proceedings of the 29th Annual International Solid Freeform Fabrication Symposium (2018)

Characterization of Thin Wall Structures using LPBF Additive Manufacturing

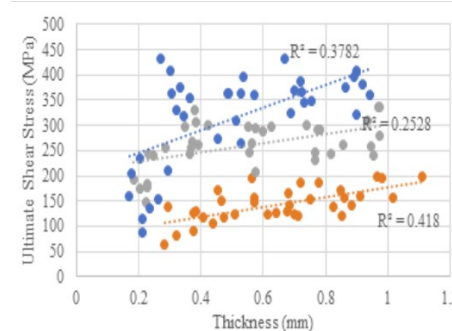
Geometry-process-material characteristics of the Ti6Al4V thin wall features fabricated by the EOS M270 laser melting powder bed fusion (LM-PBF) additive manufacturing (AM) was investigated. Samples with varying wall thickness, orientation, scanning speeds and laser power were fabricated and analyzed. The dimensional accuracies, microstructural characteristics and mechanical properties of the samples were evaluated experimentally. The results clearly indicate significant coupling between the geometry of these thin wall features and their material properties. Understanding this coupling is critical to the design and manufacturing of many AM lightweight structures. By identifying significant design and process parameters for the thin wall structures, this study will enable further investigations of the integrated design theories for the AM lightweight structures.



Optimized designs often use thin featured to reduce weight



Test specimens with range of process parameters and feature geometry



Test results provide design allowables for thin features

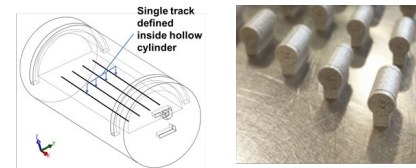
Sean Dobson, Yan Wu and Li Yang, University of Louisville. This work was performed in the UofL Rapid Prototyping Center.

Research supported by NASA (grant #NNM17AA10A)

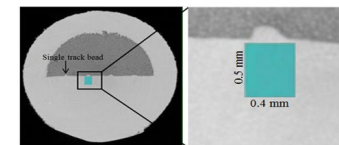
Proceedings of the 29th Annual International Solid Freeform Fabrication Symposium (2018)

Micro-CT analysis of Pore Generation in Laser Powder Bed Fusion Additive Manufacturing

Residual porosity affects the performance of metal parts fabricated using laser powder bed fusion (LPBF) additive manufacturing (AM). Subsurface pores are formed when laser energy is too high. A test specimen was designed for creating single scan tracks with a range of laser powers and scan velocities. Micro-CT scanning was used to visualize and measure “keyhole” porosity. Results show that keyhole behavior is affected more by laser power than scan speed. At same energy density (power/speed) lower power would produce balling behavior. Pore volume is maximum at around 140 W laser power. Future work will include study of the effect of hatch spacing and multiple layers.

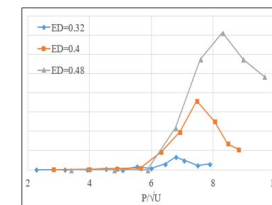


Titanium specimens fabricated using range of laser powers and scan speeds



Pore size and shape analysis

Pore volume relates to $\frac{power}{\sqrt{speed}}$

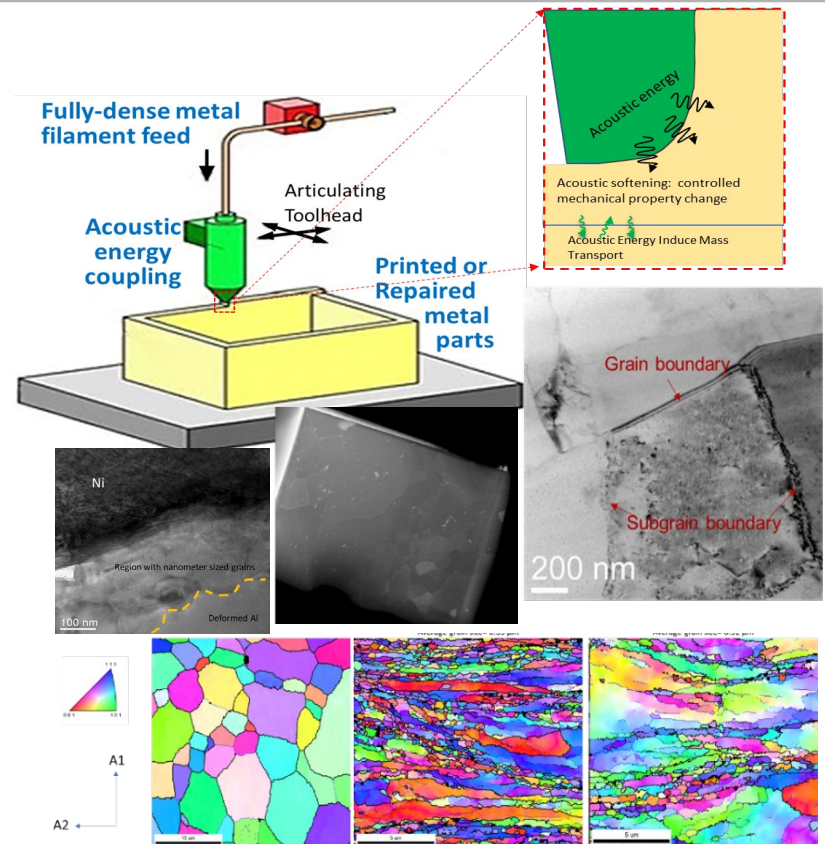


Subin Shrestha, Thomas Starr and Kevin Chou, University of Louisville.
This work was performed at the University of Louisville Rapid Prototyping Center.

Research support from NSF Grant 1662662
Annual International Solid Freeform Fabrication Symposium in Austin TX on August 12-14, 2018.

Uncovering Physics of Ultrasound-Induced Transport & Metallurgical Transformations

A knowledge gap exists in observation of ultrasonic vibration induced metal crystalline defect kinetics and its utilization for advanced manufacturing of metals. UofL Professor Keng Hsu is working on developing comprehensive models of the kinetics of 1D, 2D, and 3D lattice defect interactions with oscillatory strains induced by ultrasonic vibrations to understand the physics of his recently demonstrated Directed Acoustic Energy Deposition (DAED) metal additive manufacturing technique. Newly observed ultrasound-induced Continuous Dynamic Recovery (CDR) and Continuous Dynamic Recrystallization (CDRX) were observed and explained in FCC metals with different stacking fault energy processed using DAED. Knowledge produced from these studies will enable the creation of techniques to initiate, control, and reverse the effects of those interactions for new “athermal” metal processing and manufacturing techniques.



Keng Hsu, Mechanical Engineering, University of Louisville. This work was partially performed at the University of Louisville Rapid Prototyping Center and the University of Kentucky Center for Nanoscale Science and Engineering.

This research was supported by the Ivaldi Group

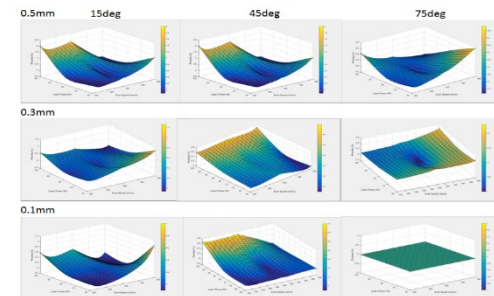
Investigation of Additive Manufacturing Lightweight Structure Design

The design of additive manufacturing (AM) lightweight structures such as cellular structures and topology optimized structures involve the integrated design of both the geometries and the processes (materials). Various factors, such as the intrinsic process variability, the heterogeneous material properties, and the geometry boundary effects, contribute to the performance deviation of AM lightweight structures from idealized structures.

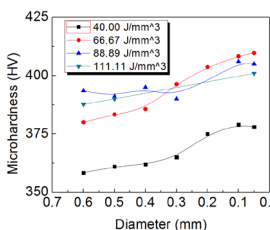
Experimental study results identified that the various material properties of AM lightweight features (thin strut/wall) are dependent on the coupled effects of geometry (thickness, orientation) and process setting (e.g. beam energy, scan speed). Analytical and numerical modeling based study results showed that the properties of these structures are also dominated by their boundary conditions (e.g. boundary constraints, free surfaces).



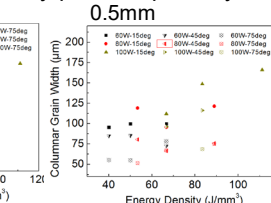
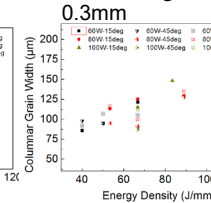
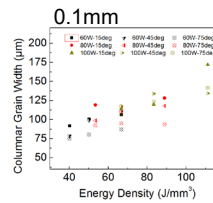
Experimental samples



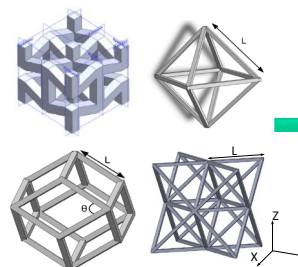
Thin strut geometry-process-porosity



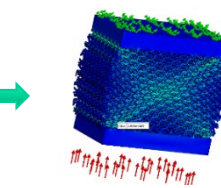
Thin strut hardness



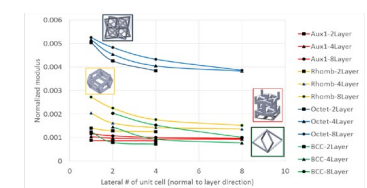
Thin strut grain size



Cellular unit cell designs



Nonhomogeneous stress condition due to boundary constraints and pattern design



Size effects due to boundary constraints

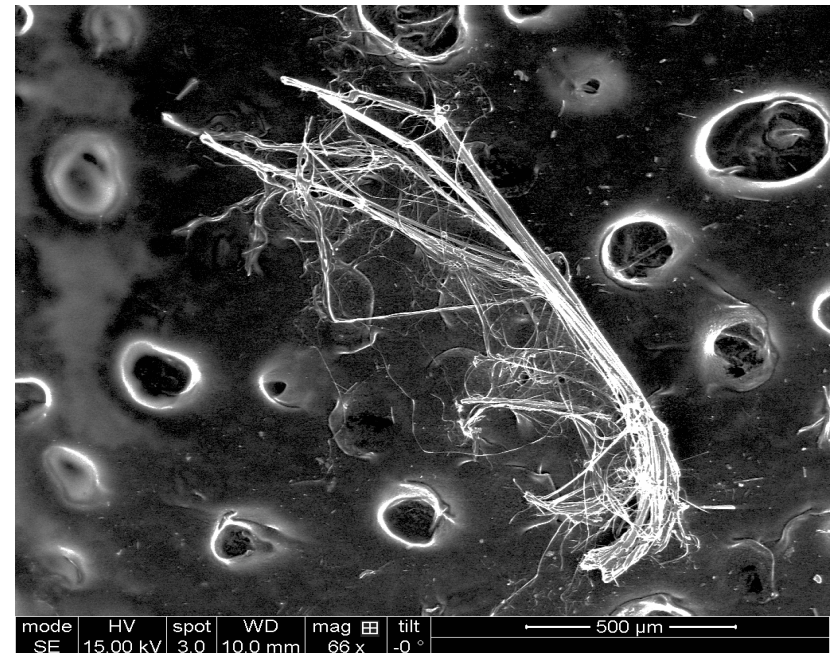
Shanshan Zhang, Yan Wu, Li Yang, University of Louisville. This work was performed at the University of Louisville Rapid Prototyping Center.

Support from ONR #N00014-16-1-2394 and NASA CAN #NNM17AA10A.

Mid-Atlantic Nanotechnology Hub (MANTH)

Geosciences Research at MANTH

The study of the transformation of minerals down to the nano- and near-atomic scale allows for exploration of their geological history and the effects of environmental exposure (e.g., weathering). Analogously, transformations occurring at this scale can be used to improve our knowledge of the mechanisms and lead to understanding mineral-related health effects and comprehend how to “disarm” these minerals through bioremediation strategies. The combination of ESEM and advanced TEM techniques give a complete picture of the state of minerals starting from their crystallo-chemical identity and morphology down to the oxidation state and binding of its atoms.

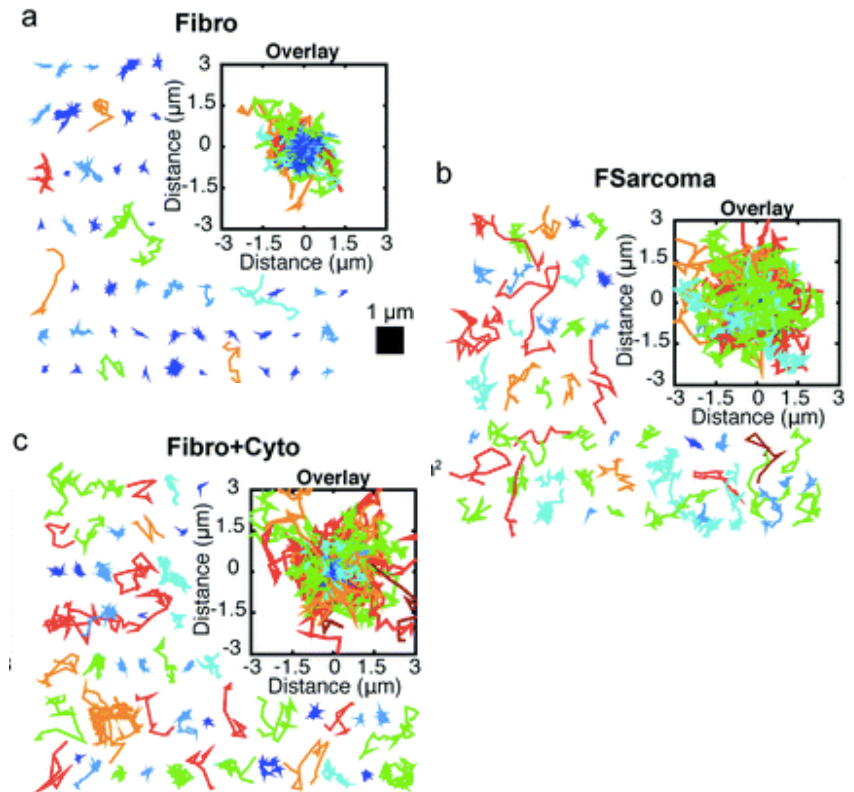


Ruggero Vigliaturo's group, Earth and Environmental Sciences, University of Pennsylvania

Gualtieri et al., *Toxicology Letters*, 2017, **24**, p20-30.

Life Sciences and Engineering Collaborative Research at MANTH

Researchers from the Penn schools of Medicine and Materials Science and Engineering studied the diffusion of quantum dots (QDs) within cells to gain a better understanding of drug delivery mechanism. The QDs were injected into individual cells with a nano-pipette and then tracked via fluorescence microscopy at the MANTH scanning probe facility. Particle tracking, illustrated in the figure, revealed significant enhancement in the mobility of biocompatible quantum dots within fibrosarcoma cells versus their healthy counterparts, fibroblasts, as well as in actin destabilized fibroblasts versus untreated fibroblasts, demonstrating that intracellular diffusion of non-specific nanoparticles is enhanced by disrupting the actin network, which has implications for drug delivery efficacy.

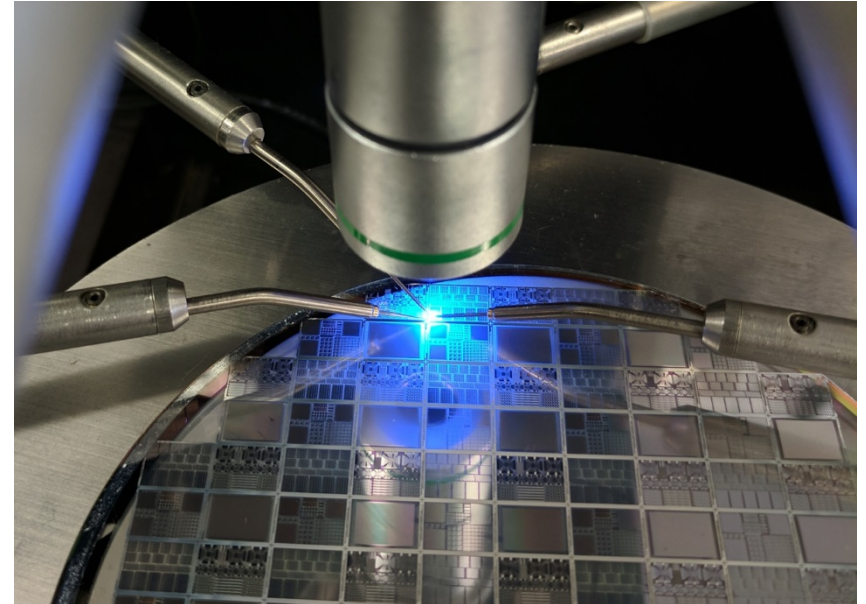


R. Composto group, Materials Science and Engineering, University of Pennsylvania

Martha E. Grady et al., *Soft Matter*, 2017, 13, 1873-1880.

MANTH Industry User: Lumiode Light Engines

Lumiode is a semiconductor startup working on next generation microdisplays for augmented reality. Their core-technology is the integration of LEDs with silicon thin-film transistors to address the need for high-brightness and high-efficiency displays. Much of our development work relies on flexible R&D facilities to perform fast iterations on semiconductor process development and process optimization. Within MANTH Lumiode engineers use a wide variety of equipment in the nanofabrication facility including photolithography, deposition, etch, and metrology. Ultimately, Lumiode's aim is to perform process optimization develop a scalable semiconductor process and work towards commercialization of these microdisplays.

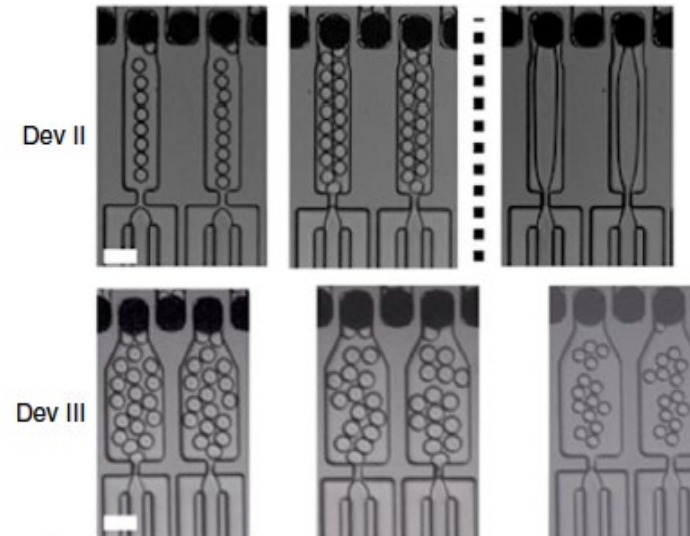


Lumiode Light Engines is a New York City based semiconductor technology startup, founded by Vincent Lee. This work was partially performed at the MANTH Quattrone Nanofabrication Lab.

Academic and Industry Collaboration at MANTH: Microfluidics Devices for Pharmaceuticals

Pharmaceuticals owe their effects not only to their chemical composition, but also to their packaging of these drugs into specific physical formulations. Many drugs are encapsulated in solid microparticles, whose size and shape determine the timing of the drug's release. Consistency is a key parameter and standard manufacturing techniques may produce uneven results.

Microfluidics provides a potential solution to these problems. However, there are intrinsic limitations to how fast these microscale devices can work. A team at Penn, in collaboration with researchers at the pharmaceutical company GlaxoSmithKline, has created a new architecture that can manufacture these drug particles a thousand times faster than ever before. These systems, built in MANTH's microfluidics lab, contain more than 10,000 of devices running in parallel, all on a silicon-and-glass chip.



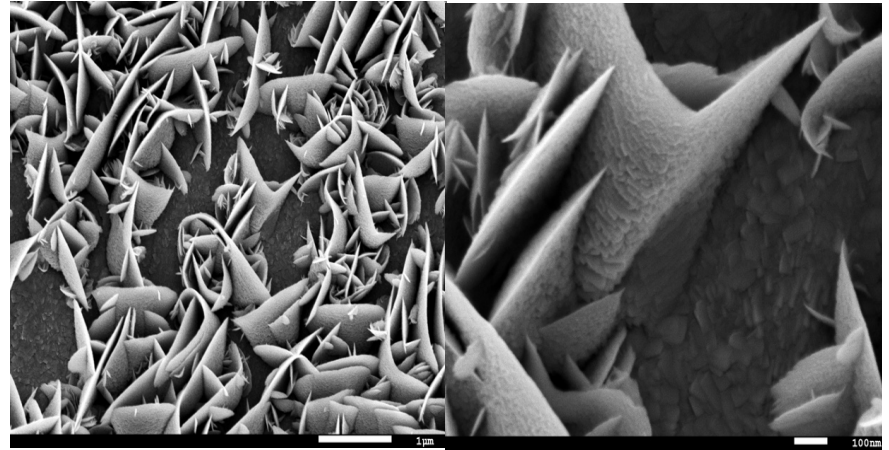
Droplet formation in action for 2 different devices and 3 different flow conditions.

David Issadore, Department of Bioengineering, University of Pennsylvania.

This work has been described in an upcoming article in the journal *Nature Communications*.

Outside Academic Research Use at MANTH: Electrode Coatings for Neurostimulation

The exchange of charge (and information) between biological systems (ion-containing solutions) and implantable electrodes (conduction electrons) can be facilitated using large surface area or reactive coatings. Iridium oxide (IrO_2) coatings have been investigated for this purpose. These have been synthesized using reactive sputter deposition and characterized at MANTH. Under some deposition conditions, including increased deposition pressure, oxygen partial pressure, or temperature, a striking microstructure is observed. The coatings with varying microstructure perform differently when tested electrochemically in phosphate buffered saline solution using cyclic voltammetry measurements. The coatings enhance charge exchange by factors of up to 51 times the exchange found on a bare electrode.

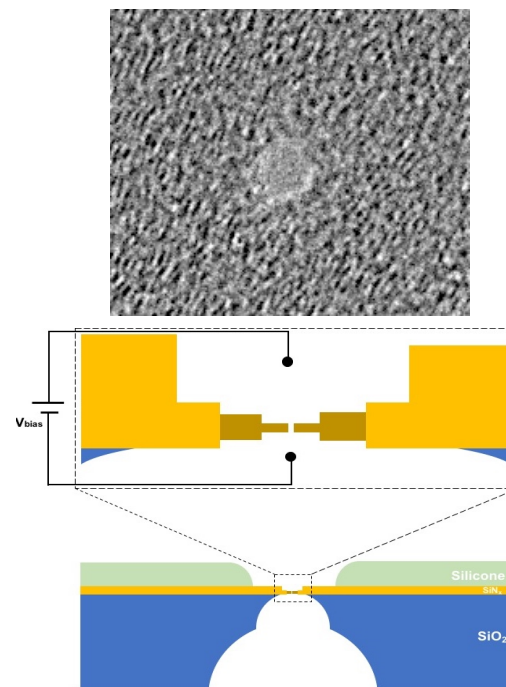


Secondary electron images of the microstructures observed on the surfaces of IrO_2 coatings at two magnifications.

Jeffrey Hettinger's group, Department of Physics and Astronomy, Rowan University

Academic Research to Startup: Nanoscale Pores for DNA Sequencing at MANTH

Precision drilling of nanopores in silicon suspended on glass chips for DNA sequencing has been carried out with MANTH Transmission Electron Microscopes. The nanopore diameter is in the range of 1-2 nm (for comparison, a single stranded DNA molecule is 1.1 nm in diameter) and the measurement error of +/- 0.1 nm. The membrane thickness is about 3 to 5 nm, monitored by the electron energy loss signal at the MANTH. Goeppert, a startup company and user of MANTH, with their nanopore-based DNA sequencing methods based on the technology described above, are able to sequence large continuous DNA strands -- a feature highly desired by the DNA sequencing market. As a MANTH user, Goeppert was able to deliver the first generation of their nanopores to beta customers and researchers worldwide.

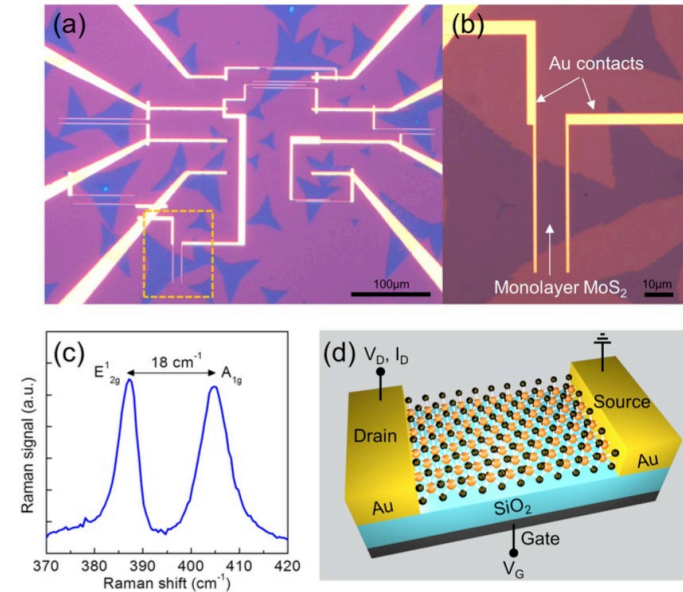


The top image shows an electron microscope view of a pore. The lower figure shows a schematic drawing of the nanopore device.

Marija Drndic, Physics, University of Pennsylvania

2D Materials Characterization and Device Fabrication at MANTH

Monolayer materials are sensitive to their environment because all of the atoms are on their surface. A group at Penn is investigating how exposure to the environment affects the electrical properties of CVD-grown monolayers of MoS₂ by monitoring electrical parameters of MoS₂ transistors as their environment is changed from atmosphere to high vacuum. The mobility increases, and contact resistance decreases simultaneously as either the pressure is reduced, or the sample is annealed in vacuum. A previously unobserved, non-monotonic change in threshold voltage with decreasing pressure was discovered. This result could be explained by charge transfer on the MoS₂ channel and Schottky contact formation due to adsorbates at the interface between the gold contacts and MoS₂.



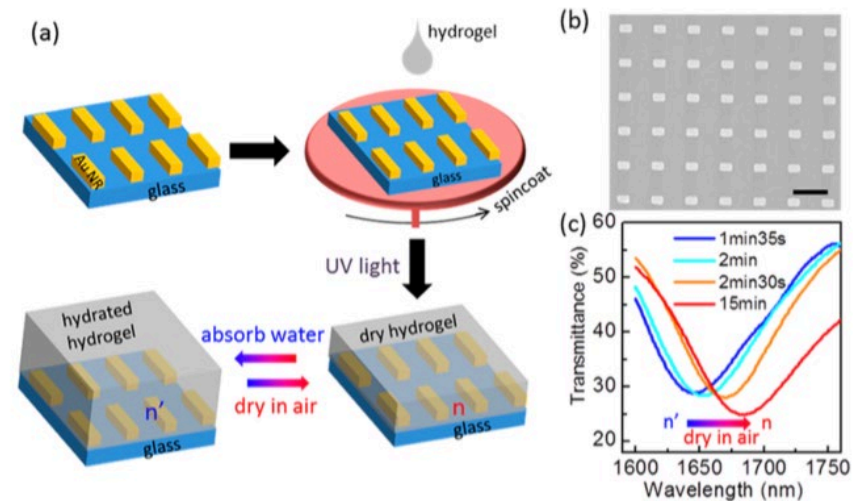
a) a top-down view of MoS₂ devices, b) a close-up of one device. c) the Raman spectra and shift as atmospheric pressure is applied. d) a schematic of the device.

A. T. Charles Johnson, Department of Physics, University of Pennsylvania

JH Ahn, et al., *Scientific Reports*, v 7, iss 1, p 4075, 2017.

Devices for Smart Soil Moisture Monitoring at MANTH

Plasmonic nanostructures provide excellent platforms for colorimetric sensors in chemical, biological, and environmental applications. In contrast to the existing library of plasmonic sensors, an angle-independent optical sensor is designed to monitor soil moisture and operate on rough surfaces. The optical moisture sensor is constructed by coating hydrogel on top of an ultrathin, plasmonic Au nanorod lattice array, built at MANTH's nanofabrication facility. The refractive index changes of the hydrogel upon exposure to moisture are transduced into spectral shifts of the resonances of the array. Robust, eco-friendly optical moisture sensors with angle-independent resonances provide a promising sensing platform for smart soil moisture monitoring important to tackle the challenge of water scarcity in agriculture.



a) the moisture sensor fabrication process. b) a scanning electron microscope view of the Au nanorod array. c) visible light transmission spectra changes with moisture exposure.

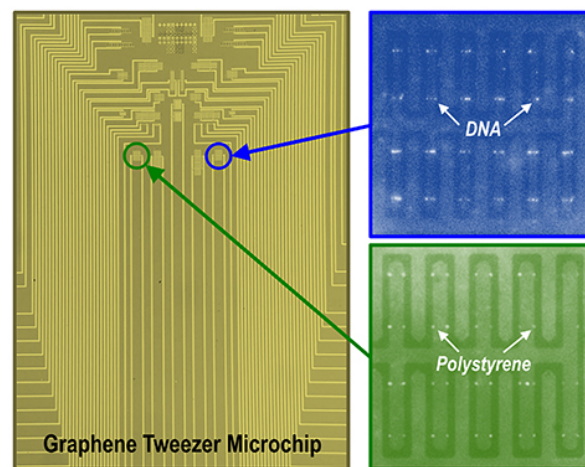
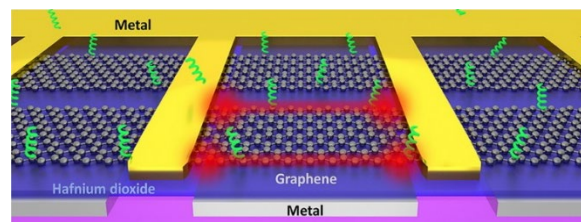
Cherie Kagan, Electrical and Systems Engineering Department, University of Pennsylvania

Midwest Nanotechnology Infrastructure Corridor (MINIC)



Graphene Nanotweezers for DNA Trapping

This work demonstrates the fabrication of the worlds sharpest molecular “tweezers.” These tweezers are made possible by the atomically sharp edges of monolayer graphene which can generate singular electrical field gradients for trapping biomolecules via dielectrophoresis (DEP). In this work, locally backgated structures where graphene (grown in the MINIC CVD graphene furnace) is separated from a buried gate electrode by a high-K HfO₂ dielectric layer. This structure generates 10× higher DEP trapping forces compared to devices using metal-only electrodes. Trapping of nanobeads at voltages of < 0.5 V has been demonstrated. Furthermore, trapping of DNA strands as short as 500 base pairs is also demonstrated. In the future, the inherent electrical readout capability of graphene could lead to a revolutionary handheld disease diagnostic system that can be run on a smart phone.



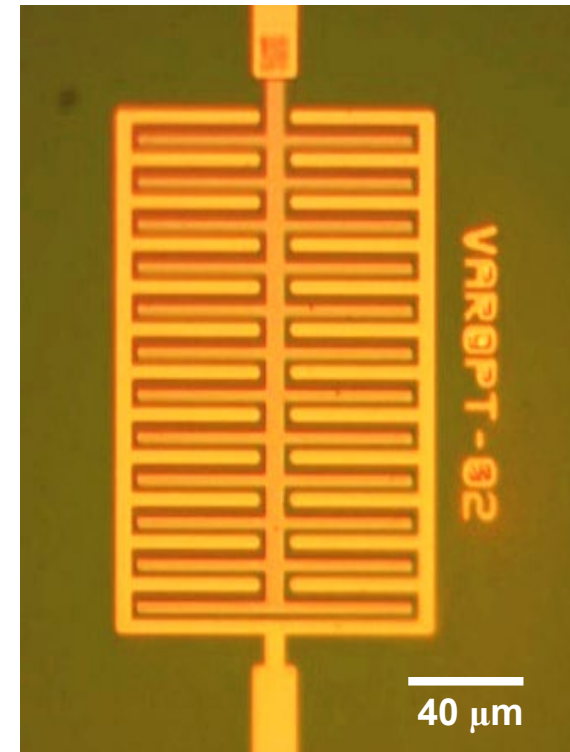
Top: Cartoon showing DNA trapping in graphene tweezers
Bottom: Micrographs of graphene chip (left) and fluorescence images of DNA and polystyrene bead trapping (right).

Sang-Hyun Oh and Steven Koester, ECE, Univ. of Minnesota. Work performed at the Midwest Nano Infrastructure Corridor (MINIC).

This work was supported by the Minnesota Partnership for Biotechnology and Medical Genomics.
A. Barik, et al., *Nat. Commun.* **8**, 1867 (2017).

Wireless VOC Sensors using Graphene Varactors

This work aims at developing a wireless sensor system that can simultaneously detect multiple species of volatile organic compounds (VOCs). The sensor utilizes graphene variable capacitors or “varactors”, which operate based on the quantum capacitance effect. When integrated with an inductor, the sensor forms a resonator structure that can be read out wirelessly. The varactors are fabricated using a high-yield, wafer-level process that starts by patterning a multi-finger local backgate, followed by a high-K dielectric layer, transferred graphene (grown in the MINIC CVD graphene furnace) and a metal counter electrode. The resonator has a frequency shift that changes in response to a mixed gas environment consisting of alcohols and ketones, the concentrations of which can be determined by comparing the response of sensors with and without surface functionalization. The wireless sensing platform has significant potential to create a multi-gas monitoring system for eventual use in early disease diagnostics.



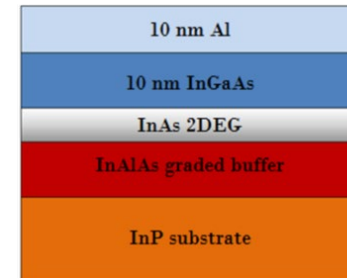
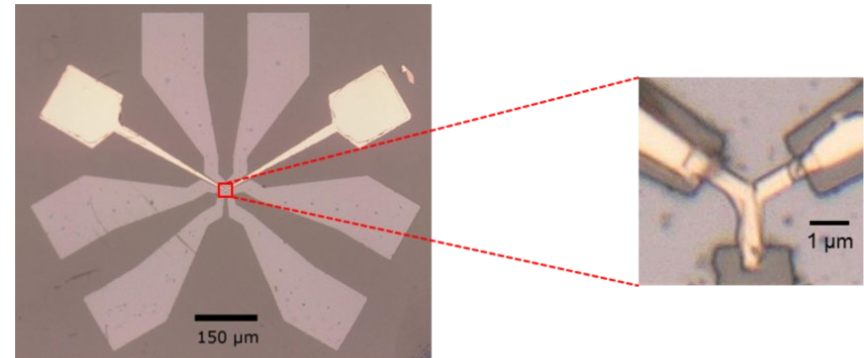
Top: Optical micrograph of a multi-finger graphene variable capacitor (varactor) used to create a VOC wireless sensor.

Steven Koester, ECE, University of Minnesota. Work performed at the Midwest Nano Infrastructure Corridor (MINIC).

This work was supported by Boston Scientific Corporation.

Developing topologically-protected quantum devices based on Josephson junctions

Josephson junctions with three or more superconducting leads are predicted to exhibit a topological Andreev state spectrum in the presence of few conducting modes within the interstitial normal material. Such topological behavior is expected to quantized transport properties between the different terminals, as the device undergoes topological phase transitions as a function of phase and voltage bias. This work investigates the superconducting and resistive properties of top-gated multi-terminal Josephson devices, based on an InAs two-dimensional electron gases (2DEGs) in quantum well heterostructures that become superconducting at low temperatures through proximity with an epitaxial aluminum capping layer.



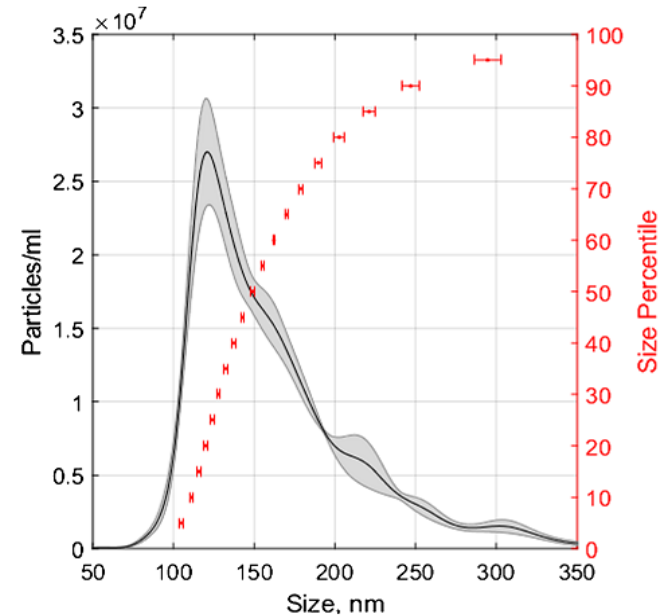
Optical microscope image of a three-terminal Josephson junction fabricated from an InAs quantum well heterostructure with an epitaxial Al superconducting capping layer.

¹Gino Graziano, ²Joon Sue Lee, ²Mihir Pendharkar, ²Chris Palmstrøm and ¹Vlad Pribiag. 1. School of Physics and Astronomy, University of Minnesota. 2. Materials Department, UC Santa Barbara. Work was performed at MINIC.

This work was supported by NSF Award # DMR-1554609.

Sizing Lipid Droplets From Liver Tissue via Nanoparticle Tracking Analysis

The significance of lipid droplets in lipid metabolism, cell signaling, and regulating longevity is increasingly recognized, yet lipid droplets are difficult to size and study using conventional methods. This work demonstrated the capabilities of MINIC's nanoparticle tracking analysis (NTA) tool for sizing of lipid droplets. NTA was found to be able to assess lipid droplet stability over time, indicating that lipid droplet preparations are stable for up to 24 hours. NTA also had the ability to compare the size distributions of lipid droplets from adult and geriatric mouse liver tissue, suggesting an age-related decrease in lipid droplet size. This is the first report on the use of NTA to size intracellular organelles.



Lipid droplet size distribution determined with MINIC's particle analysis tool

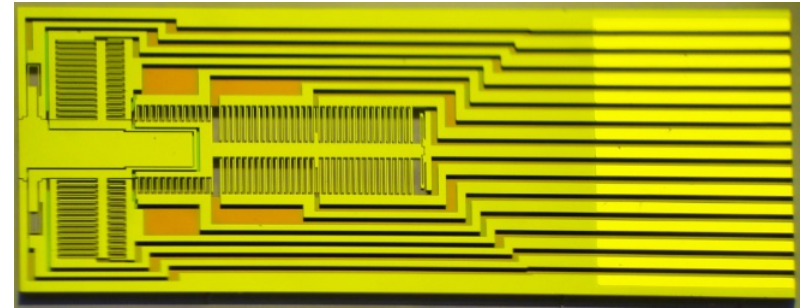
K. A. Muratore, C. P. Najt, D. G. Mashek, Dept. of Biochemistry, Molecular Biology, and Biophysics, N. M. Livezey, E. A. Arriaga, Department of Chemistry, and Jim Marti, Minnesota Nano Center. Work partially performed at MINIC.

This work was supported by NIH Grant #AG020866.

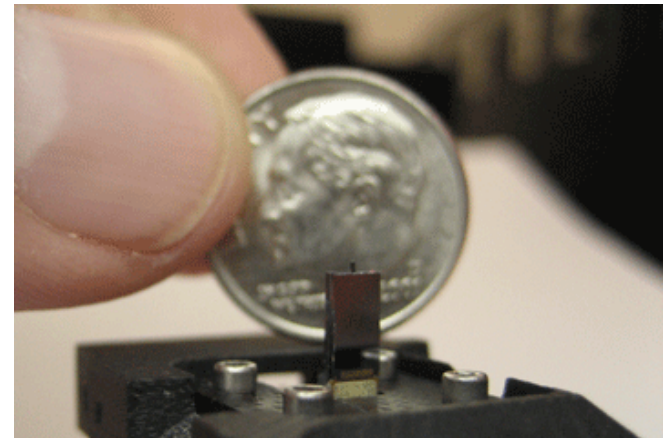
K. A. Muratore, et al, *Analytical and Bioanalytical Chemistry* (2018) 410:3629–3638.

MEMS Based Tribometer

A MEMS based transducer for tribology testing was developed in part at the MINIC node of NNCI. The device is now available commercially to perform simultaneous imaging and mechanical measurements *in-situ* in TEMs and SEMs, providing new insights into material defect formation processes. The MEMS transducer consists of two actuators, two displacement sensors and four springs. The four springs support the movable part of the 2D MEMS transducer. The actuators and the sensors consist of comb drive capacitors. The MEMS transducer has electrostatic actuators and differential capacitive displacement sensors to the normal direction and also to the lateral direction. The measured resonance frequencies are much higher than other commercial tribometers which commonly have resonance frequencies lower than 1 kHz. These high resonance frequencies are achieved by using the lower mass (less than 1 mg) for the normal translation mode and the lower moment-of-inertia for the lateral rotational mode while having comparable stiffness. This high resonance frequency or high transducer bandwidth contributes to faster settling and better controllability. Having higher bandwidth and better control is important in this operation to reduce the measurement error by reducing the control tracking error.



MEMS based transducer designed for tribology test

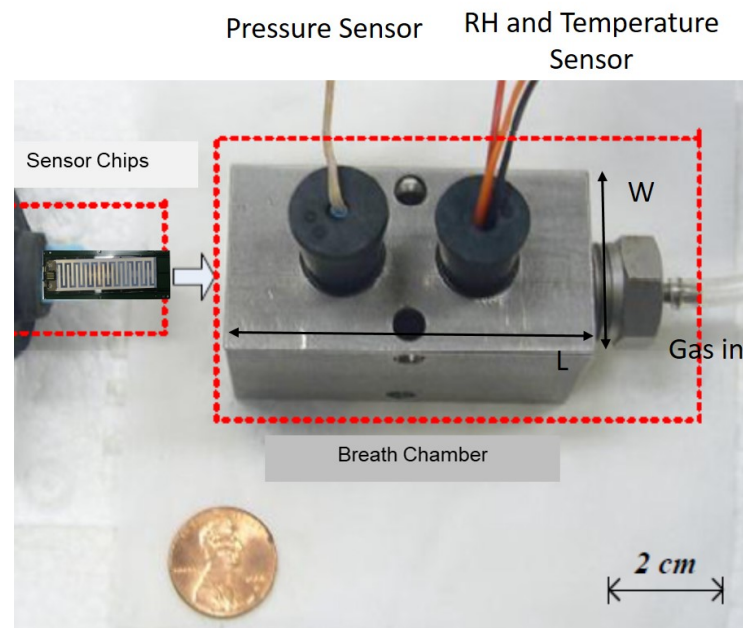


Packaged MEMS tribometer

The work was performed and funded by Hysitron-Bruker. Work performed at MINIC.

Low cost diabetes breath sensor based on nanostructured $K_2W_7O_{22}$

Acetone is an effective biomarker for the identification of type 1 diabetes. Compared to other methods of diagnosis, breath analysis through the detection of acetone in breath has many merits including being non-invasive, accurate, convenient and inexpensive. A chemiresistive sensor based on the novel nanostructured $K_2W_7O_{22}$ has been developed which can effectively detect the acetone gas at room temperature. Preliminary results show that $K_2W_7O_{22}$ can effectively detect a trace amount of acetone at room temperature. A detection limit of ~ 0.1 ppm (much less than 0.8 ppm threshold of pre-diabetic screening) has been achieved with a fast response time within a minute through optimizing electronic circuits of sensor and $K_2W_7O_{22}$ material properties and crystalline structures. A portable sensor device has been designed and ready for practical application.



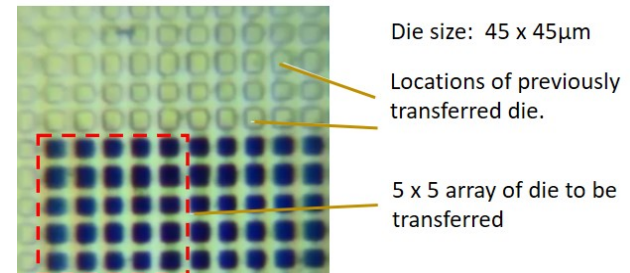
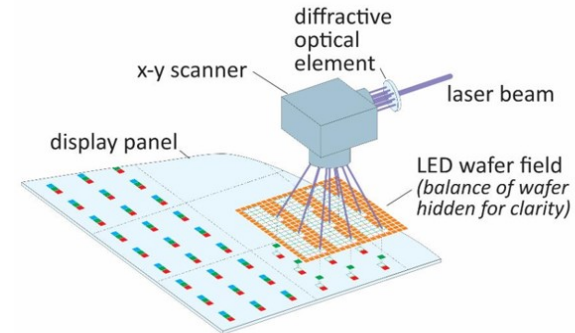
Prototype diabetes breath sensor

Danling Wang, Qifeng Zhang, MD Razuan Hossain, Michael Johnson, Department of Electrical and Computer Engineering, North Dakota State University

Support for this project was provided by the Sanford Health – North Dakota State University Collaborative Research Seed Grant program, NDSU Centennial Endowment award, NDSU NASA EPSCoR Grant, and ND EPSCoR research grant.

Laser-Enabled Massively Parallel Die Transfer

Uniqarta Inc. is developing innovative new manufacturing assembly methods for placement of small, ultra-thin die onto substrates. One application focus area for the technology is placement of mini-LED (100-200 μm /side, 100 μm thick) and micro-LED (40-60 μm /side, 6 μm thick) die. The company is developing a method of ultra-high speed parallel transfer of die using a single laser pulse diffracted into multiple beams. Uniqarta has demonstrated a placement rate of more than 12 million units per hour, about 1,000 times faster than the conventional pick-and-place equipment. The research involves unique wafer preparation processes and laser technology the company is developing. Elements of the research rely heavily on capabilities in the MINIC lab at NDSU.



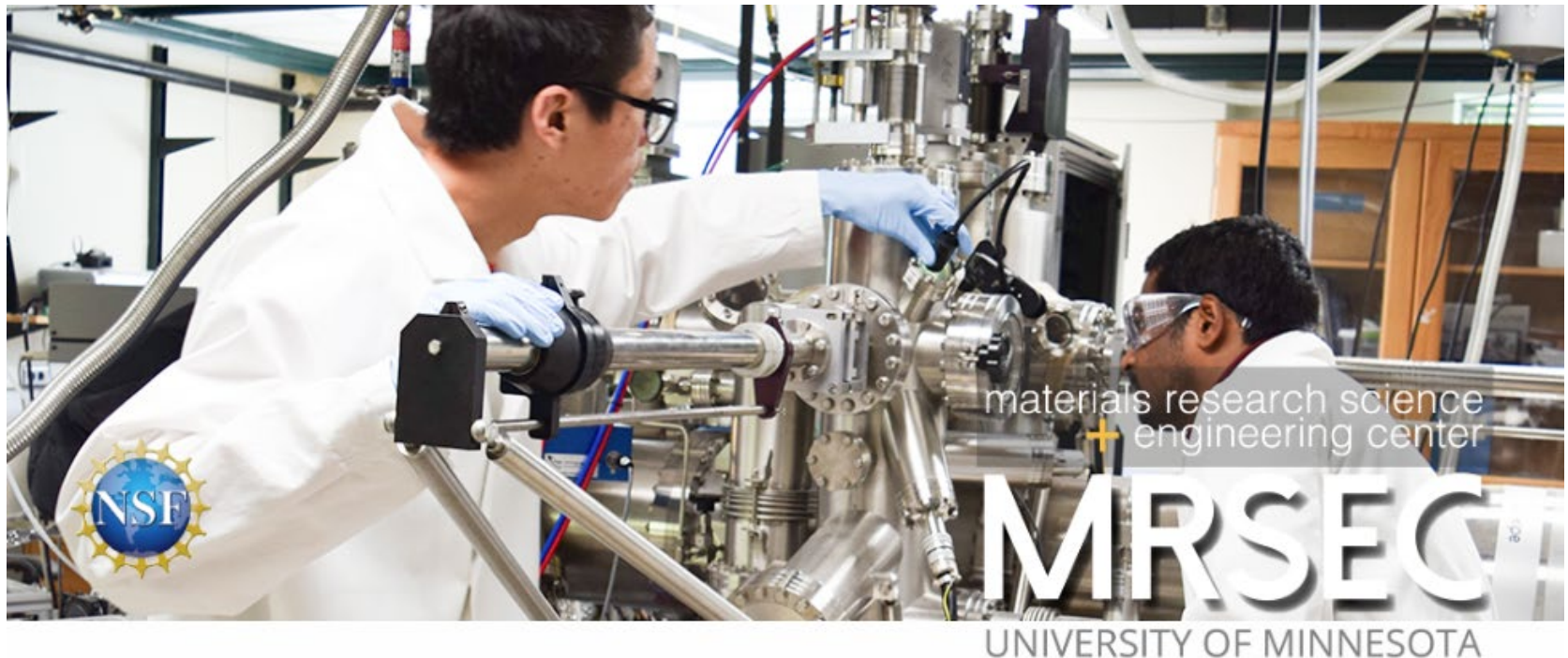
Uniqarta Technology for Laser Based Die Transfer

Work was performed by staff at Uniqarta Inc. using the NDSU facilities of MINIC.

Support for this project provided by NSF SBIR Phase I Grant # 1745903.

Minnesota MRSEC Projects

The University of Minnesota hosts the longest running and one of the largest Materials Research Science and Engineering Centers (MRSEC) of the program. It's programs impact fields from biomedicine, separations, and plastic electronics to security, renewable energy, and information technology. About 20% of the MRSEC researchers use the MINIC facility



NSF supports the Minnesota MRSEC through award #DMR-1420013

Montana Nanotechnology Facility (MONT)

Advanced Neurofluidic Devices for Neurodegenerative Disease Studies

Neuronal cell growth in the brain follows distinct but complex guidance cues. Replicating this complex growth behavior in the Petri dish is essential to better understand the progression of neurodegenerative diseases. However, controlling and guiding neuronal cell growth remains a challenge. Kendra Hergett is an undergraduate student working in the Kunze Neuroengineering lab on new designs for neurofluidic devices. A neurofluidic device comprises microfluidic channels specifically designed to compartmentalize different cell body parts of neurons. Microchannels in PDMS are fabricated from a molding master. We use standard silicon wafers and a two-step photolithography with KMPR 1005 and 1050 to achieve channel depths of 7 μm and 70 μm , respectively. This project tests multi-distance in contrast to equidistance growth and transport behavior of degenerative signals in primary cortical neurons.

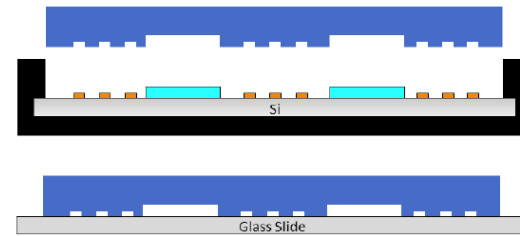


Figure 1: Two-step photolithography to fabricate microchannels in polydimethylsiloxane (PDMS) for axon/dendrite compartmentalization and directed growth in brain cell cultures.



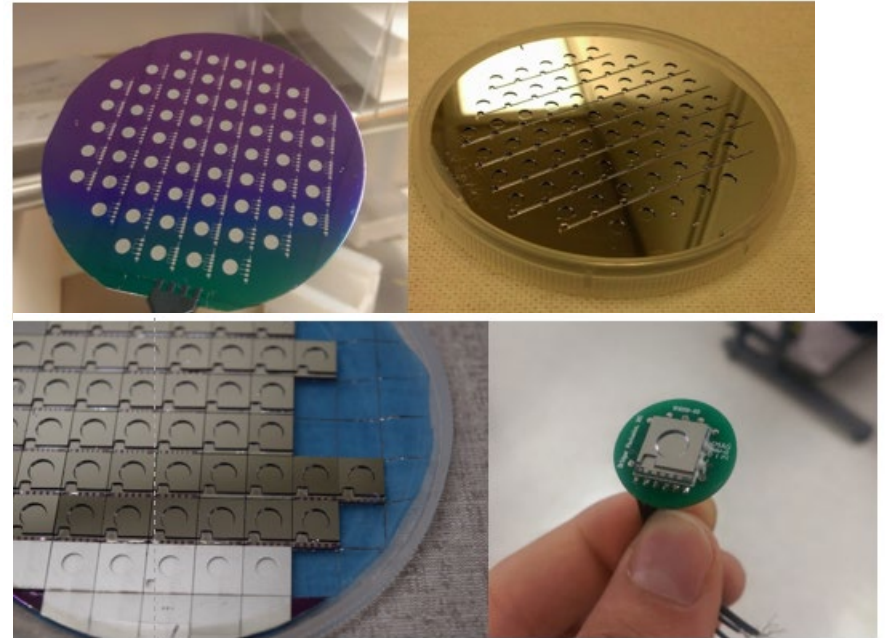
Figure 2: Phase contrast microscope image shows the microfabricated channels after casting into PDMS. Shallow channels reflect upright light more than deeper channels.

Kendra Hergett, Anja Kunze, Montana State University
Work performed at Montana State University, MONT facility MMF

Supported by Montana State University

MEMS Adjustable Focus Mirrors

Revibro Optics is working to commercialize the MEMS deformable mirror technology developed at MSU. Our current work is aimed at developing new optical coatings for our mirrors, and refining the design and fabrication process to increase mirror yield. Our mirrors consist of a metal coated flexible membrane situated above a series of electrodes. Electrostatic actuation produces a curvature change in the surface, and allows for very high-speed focus adjustments – more than 1000 adjustments per second. Our work is enabled by the existence of this MONT facility, and we make extensive use of the MMF as a commercial user.



MEMS deformable mirrors manufactured at MMF.

REVIBRO
OPTICS

Chris Arrasmith, Revibro Optics LLC
Work performed at Montana State University, MONT facility MMF and ICAL

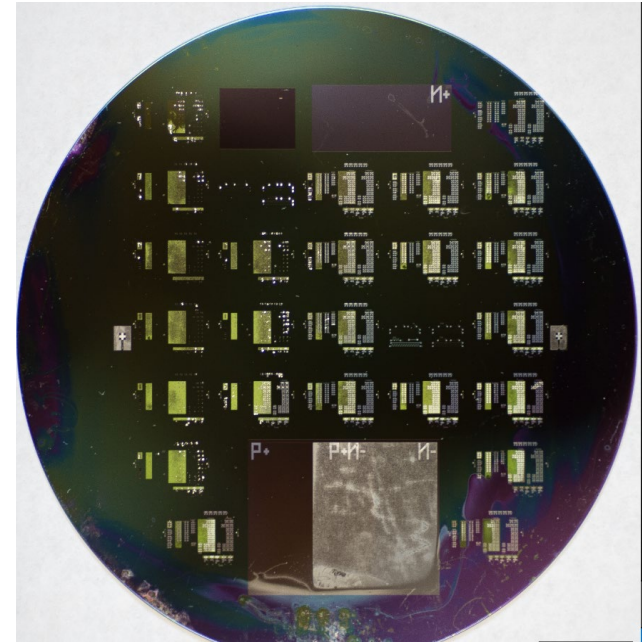
Work funded by NSF SBIR 1648359

Transistor Process Optimization for Micro-Fabrication Courses

CMOS transistors are made in the Montana State micro-fabrication course. Currently the produced wafers have NMOS and PMOS transistors that are not functioning properly.

Doping concentration and dopant profiles after drive in are important variables that are likely limiting transistor function. Measurements of previously made wafers and new wafers made with modified parameters were used to help with the optimization of the process.

The new wafer sample for the N+ region had a depth profile that was still significantly too deep, but the end of the diffused phosphorus was found. This suggests that there are issues related to the phosphorus diffusion sources and lower temperatures and shorter diffusion times need to be tested.



Picture of Transistor Wafer for Micro-Fabrication Course

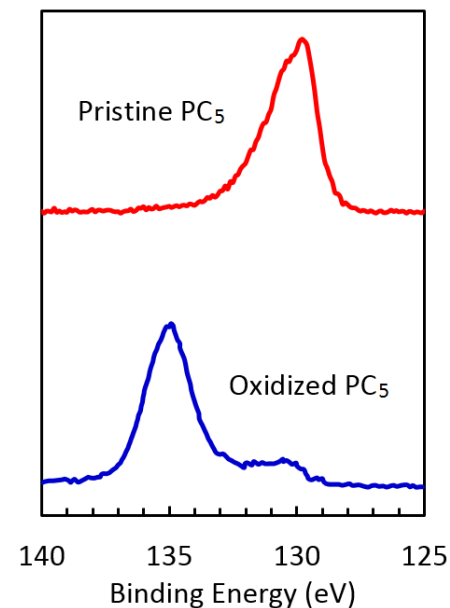
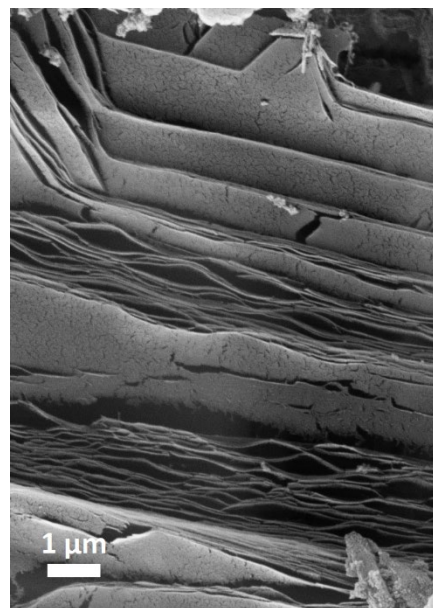
Calvin M. Jones, Tristan Cunderla, University of Colorado at Colorado Springs, Montana State University
Work performed at Montana State University, MONT facilities MMF, ICAL

Work funded by Montana State University.

Heteroatom-Doped Graphitic Carbon

Energy storage materials, whether in the form of ion-storing battery electrodes or gas-storing porous scaffolds, are dominated by the element carbon, specifically its graphitic-amorphous sp^2 hybridization state. We seek to tune both the electronic and physical properties of graphitic carbon materials via controlled, substitutional replacement of the carbon atoms by heteroatom dopants.

We routinely investigate materials containing a wide range of compositions of BC_x , NC_x , and PC_x , where x is above 3. The facilities at ICAL crucially assist in both chemical and structural characterization: compositional analysis (also in profile), impurity analysis (oxygen/halide content), surface/bulk morphology, and chemical environment (chemical bonding analysis).



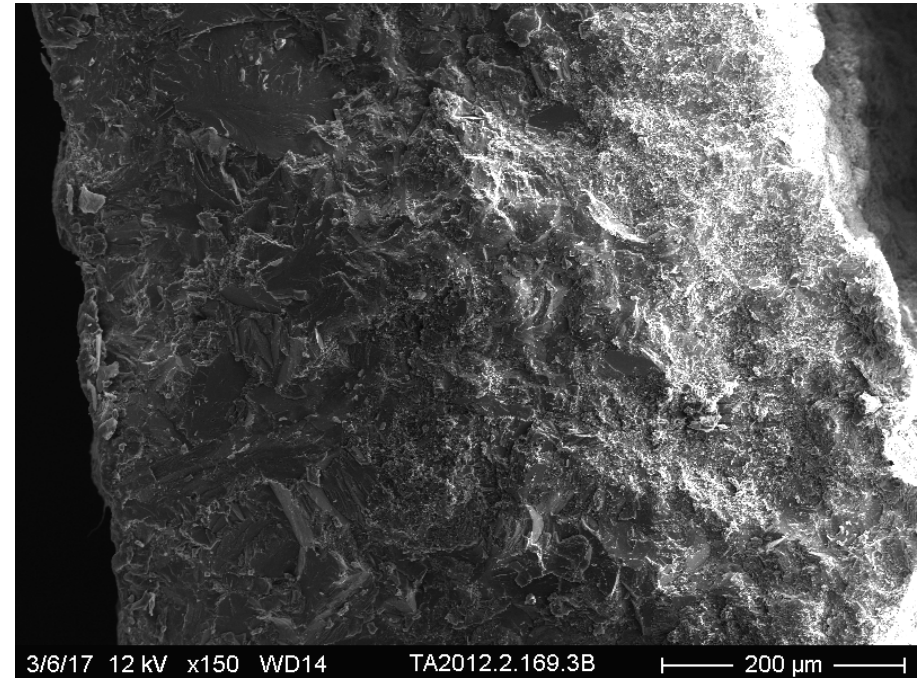
Left: Scanning electron micrograph of a crystalline region of high-boron content graphitic carbon ($\sim BC_3$). Right: X-ray photoelectron spectra of $\sim PC_5$ showing very low oxygen impurities and confirming the presence of P-C bonding.

Devin McGlamery, Julie Muretta, and Nicholas P. Stadie, Montana State University
Work performed at MSU ICAL

Funding from Petroleum Research Fund ACS 59381-DNI10 and MSU.
E. Billeter, et al., *Chem. Mater.*, 30 (2018)

Diversity of Fossil Eggshell from the Late Cretaceous of Montana

A team of students at Montana State University have been investigating a number of eggshell samples from the Upper Cretaceous Two Medicine Formation of Montana using SEM. They have revealed eggshell from theropod dinosaurs and birds as well as possible crocodylians and lizards. These specimens represent otherwise hidden vertebrate diversity, new egg forms, and highlight the variety of nesters at localities like Egg Mountain.



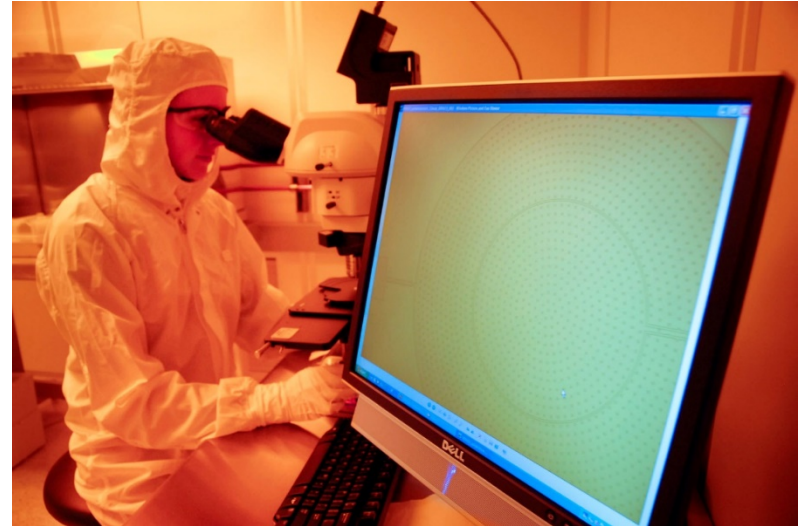
SEM micrograph of the cross-section of a new variety of dinosaur eggshell.

David Varricchio, Jacob Burgo, Eric Przybyszewski, and Paul Germano, Montana State University
Work performed at ICAL, Montana State University

Funding from Montana State University.

Agile Focus Designs brings fast focus and zoom to imaging systems

Agile Focus Designs, of Bozeman, MT increases throughput and enables real-time imaging in microscopes and cameras with their fast focus and zoom technology. The technology proves 100x faster than conventional focus and zoom mechanisms. The MONT facilities enable Agile Focus Designs to locally fabricate voltage controlled micro-electro-mechanical systems mirrors capable of rapid focusing. These mirrors have enhanced various imaging applications, such as wide-field microscopes, confocal microscopes, camera, and optical disk systems by allowing greater imaging flexibility in the sample space. Agile Focus Designs has ongoing R&D efforts, including recent NSF SBIR awards 1548737 and 1819493 and projects through the Montana Board of Research and Commercialization. The company broadens participation and diversity in engineering by exceeding the national company average (13%) of practicing female engineers with a 50% ratio of women to men.



© Kelly Gorham

Dr. Sarah Lukes, founder and CEO, in the MONT facility inspecting a micro-electro-mechanical systems (MEMS) mirror capable of electronically actuated focus control. Agile Focus Designs is commercializing fast focus and zoom devices to enable real-time imaging in microscopes, cameras, and surgical instruments.

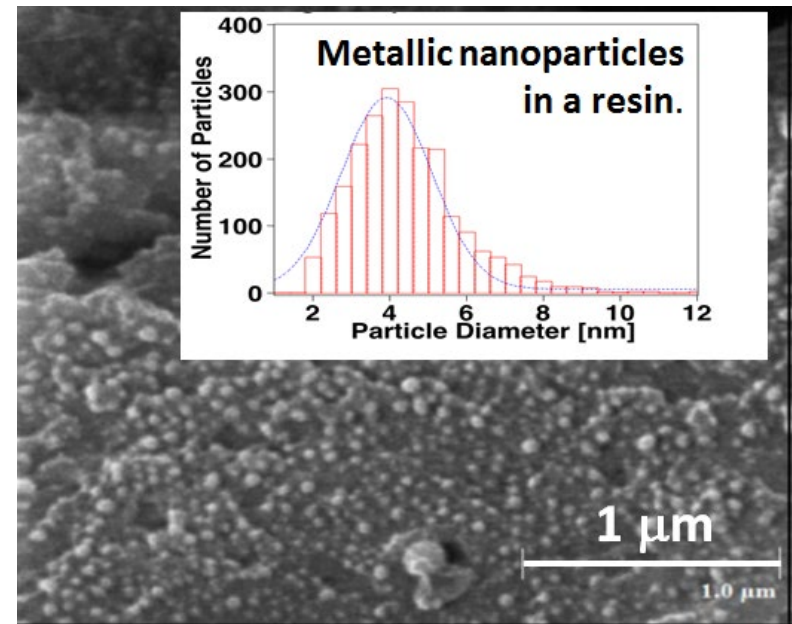
Sarah Lukes, Agile Focus Designs, LLC, Bozeman, MT
Work performed at Montana State University, MONT facilities MMF and ICAL

This work supported by NSF SBIR awards 1548737 and 1819493.

Metallic Nanoparticle Distribution

Objective: Determination of the size distribution of metallic nanoparticles distributed in a polymer resin.

By combining Auger Nanoprobe and the transmission electron microscopy the size distribution of metallic nanoparticles have been determined as shown in figure on the right. The work is done at the MONT/ICAL facility at MSU.



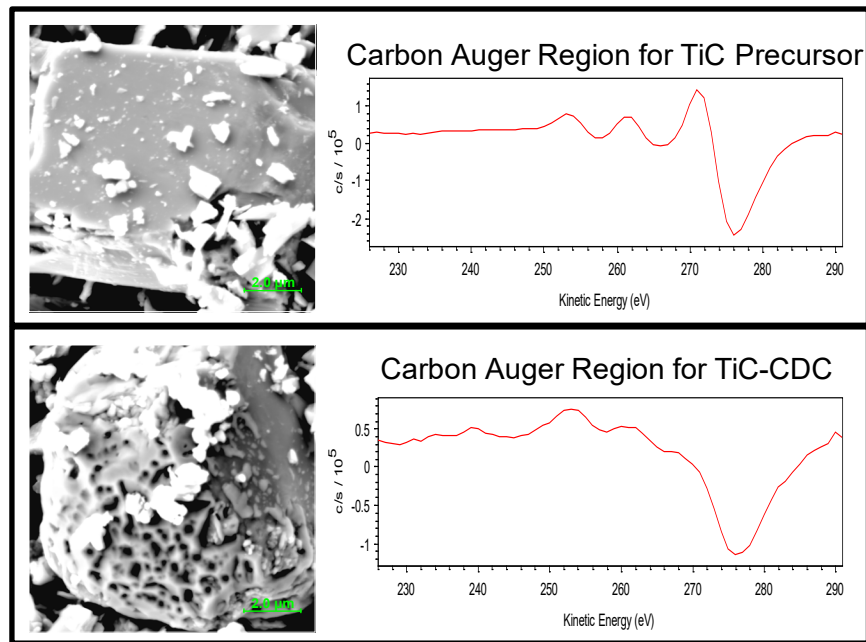
Metallic nanoparticles and size distribution in a polymer resin. The SEM image is obtained by Auger Nanoprobe.



Work performed at Montana State University, ICAL
Work funded by Sterisil, Palmer Lake, CO.

Identifying Structural Changes of Metal Carbides Transitioning to Carbide-Derived Carbons Using Auger Scanning Spectroscopy

Our research investigates an alternative carbide-derived carbon (CDC) synthesis route using an inexpensive halogen-containing etchant, ammonium chloride (NH_4Cl), to produce porous CDCs with tunable microstructures. To ensure tunable microstructures are achievable through our synthesis method, analytical techniques including scanning electron microscopy (SEM), energy dispersive spectroscopy (EDS), and auger electron spectroscopy (AES) are used. SEM images are used to show a developing porous layer on the surface of the Me_xC . AES of the carbon KLL region is used to show a transition from a carbide to carbon structure and to determine the resulting allotrope of the Me_xC -CDC powders.



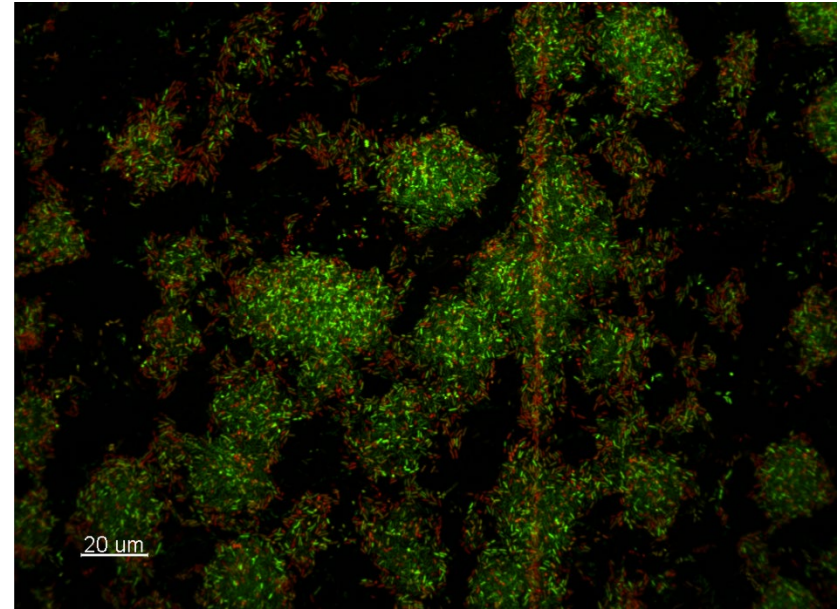
Microstructural changes of TiC precursor to processed TiC-CDC powders are observed via SEM surface images (left) and their corresponding carbon KLL spectra obtained via AES (right).

Emily Remington, Spencer Dansereau, Paul Gannon, Montana State University

This work was performed at Montana State University, MONT facility Imaging and Chemical Analysis Laboratory (ICal)

Immobilized Silver Nanoparticles: An eco-friendly way of preventing biofilm-related health risks?

Developing and testing nanosilver-based coatings for controlling biofilm formation is an important global health challenge of our time. In this project we assessed the efficacy of nanosilver-coated surfaces against microbial colonization in order to evaluate its ranges of application and limitations. Assessment was made of the development and structure of biofilms grown on test samples in a drip flow biofilm reactor system. Fluorescence microscopy was used to visualize the biofilm and assess viability of microorganisms. Our data showed that the coatings were not efficient at preventing biofilm formation. Therefore, it is important that novel antimicrobial surface coatings undergo testing to confirm their efficacy and to provide scientific evidence to support any claims that the manufacturer wishes to make about them.



Pseudomonas aeruginosa biofilm formed on nanosilver coated polyethylene coupon stained with LIVE/DEAD BacLight viability kit and visualized using a confocal laser-scanning microscopy.

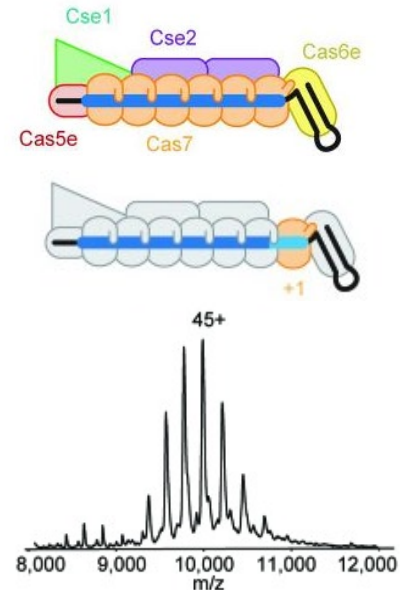
Marketa Hulkova, Fulbright Scholar, Masaryk University, Czech Republic
Work performed at Montana State University, Center for Biofilm Engineering (CBE)

Work supported by MONT User Grant, NSF ECCS-1542210

Investigation of multi-protein complexes in native conditions using gold-coated glass capillaries

Analysis of non-covalent protein complexes is performed by means of nano-flow electro spray ionization, using glass or quartz capillaries which have been pulled to a fine tip ($\sim 1 \mu\text{m}$ inner diameter), and coated with conductive material (gold). Precision application of the coating improves the stability of the current and electro spray.

This technique allows protein complexes to be transferred from liquid to gas phase (and ionized) without disruption of non-covalent interactions when coupled with mass spectrometry. Therefore it can be used to answer a range of fundamental questions such as complex stability (transhydrogenases), protein and cofactor component stoichiometry (CRISPR/Cas complex), general complex topology and architecture (Fix complexes, Nitrogenase systems) via investigation of protein-protein interactions.



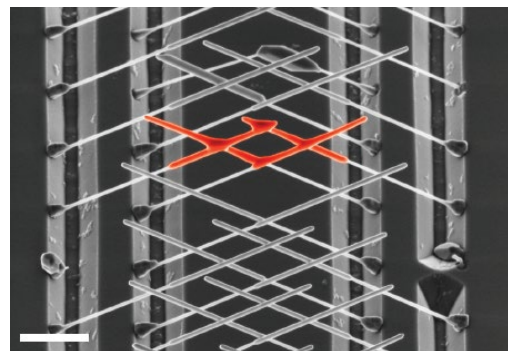
Monika Tokmina-Lukaszewska, Angela Patterson, Luke Berry, Brian Bothner, Montana State University
Work performed at MSU, MMF & Mass Spectrometry Facility.

Funded by DOE DE-SC00012518, NIH IDEA program grant P20GM103474 & Murdock Charitable Trust
Tokmina-Lukaszewska, M. et al., *Front. Microbiol.* 5,9:1397 (2018); Harris, D.F. et al., *Biochemistry* 57, 701-710 (2018);
Peters, J.W. et al., *Curr. Opin. Chem. Biol.* Vol47, 32-38 (2018).

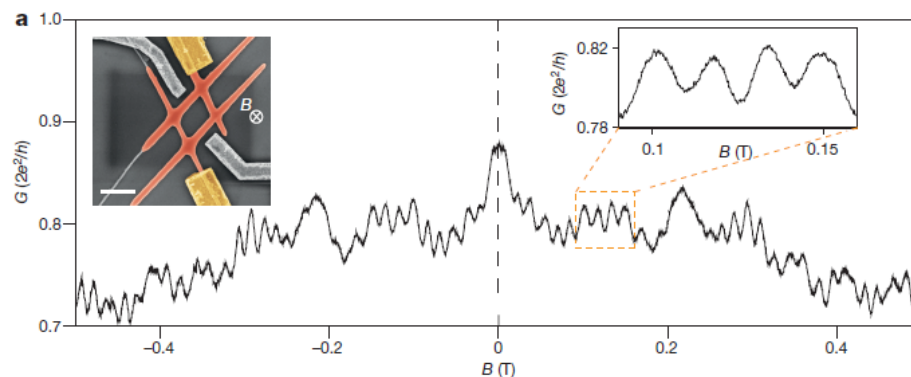
Nanotechnology Collaborative Infrastructure Southwest (NCI-SW)

Epitaxy of Advanced Nanowire Quantum Devices

Semiconductor nanowires are ideal for realizing various low dimensional quantum devices. Here we demonstrate a technique for generic bottom-up synthesis of complex quantum devices with a special focus on nanowire networks with a predefined number of superconducting islands. Structural analysis confirms the high crystalline quality of the nanowire junctions, as well as an epitaxial superconductor–semiconductor interface. Quantum transport measurements of nanowire ‘hashtags’ reveal Aharonov–Bohm and weak antilocalization effects, indicating a phase-coherent system with strong spin–orbit coupling. Our approach opens up new avenues for the realization of epitaxial 3D quantum architectures that have the potential to become key components of various quantum devices.



A scanning electron microscopy image of InP nanowires forming a four wire ‘hashtag’ structure.



Magnetococonductance of a hashtag (inset) shows periodic Aharonov–Bohm oscillations and a weak-anti-localization peak at $B = 0$ T.

Chris J. Palmstrom, Materials Department, UC Santa Barbara
Work performed at NCI-SW

The work at UCSB was supported in part by NSF Award # DMR 11–21053
Gazibegovic et al. *Nature*, vol. 548, p. 434 (2017)

Dispersion Free 450-V p GaN-Gated CAVETs With Mg-ion Implanted Blocking Layer

In this work a GaN-based current aperture vertical electron transistor (CAVET) with a p-type gate layer and an implantation-based current blocking structure is presented. The devices measured showed a breakdown voltage of 450 V and no dispersion. The factors limiting higher breakdown voltages in these devices were carefully studied and discussed. The devices were grown on sapphire and relied on a box-shaped Mg implanted current blocking scheme. This is the first demonstration of an implantation based CAVET, grown on sapphire, with a blocking voltage of 450 V and respectable on-state characteristics.

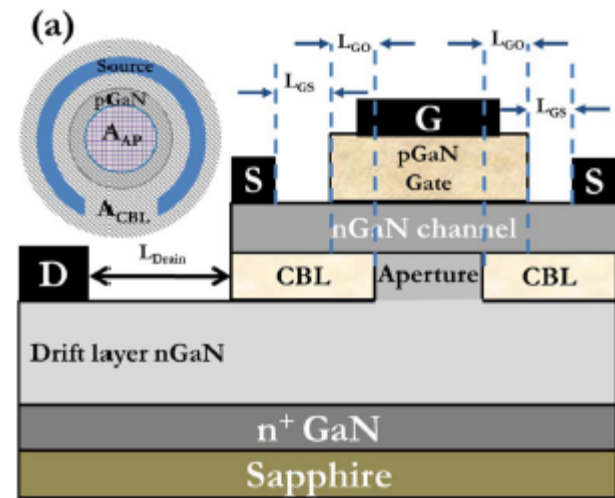


Fig 1. Schematic cross-section of the GaN CAVET device

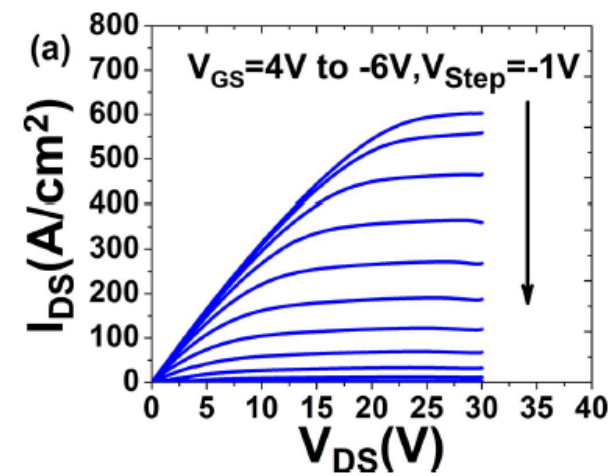


Fig 2. Output characteristics of the CAVET device.

Srabanti Chowdhury, Dept. of ECE, UC Davis
 Work performed at NCI-SW

The work at UC Davis was supported in part by DARPA grant # D15AP00092
 S. Mandal et al. *IEEE Electron Device Letters*, vol. 38, pp. 933–936 (2017)

Demonstration of GaN Static Induction Transistor (SIT) Using Self-Aligned Process

RF power electronics requires amplifiers operating at high frequency with high output power. GaN-based HEMTs as RF devices have made continuous progress in the last two decades showing great potential for working up to G band range. However, a vertical structure is preferred to obtain higher output power. In this work, we have designed and fabricated GaN static induction transistors using a self-aligned technology. Both dry and wet etch techniques were investigated to reduce the gate leakage on the etched surface. Careful control of the etch process can effectively reduce the etch damage, decrease the gate leakage and enhance the gate control over the channel.

Srabanti Chowdhury, Dept. of ECE, UC Davis
Work performed at NCI-SW

The work at UC Davis was supported, in part, by DARPA under grant # D15AP00092W.

Li et al. *J. of the Electron Devices Society*, vol. 5, pp. 485–490 (2017)

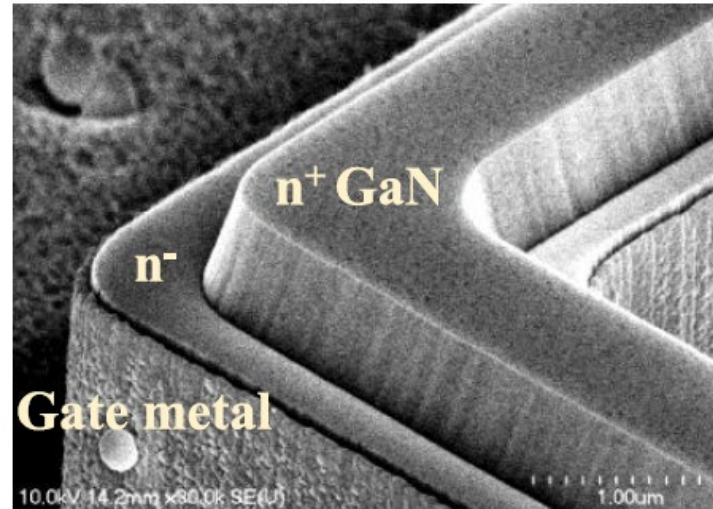


Fig 1. SEM image of the fully processed device

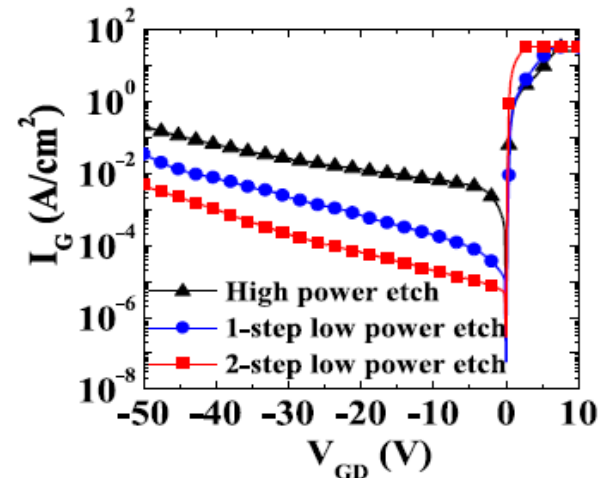
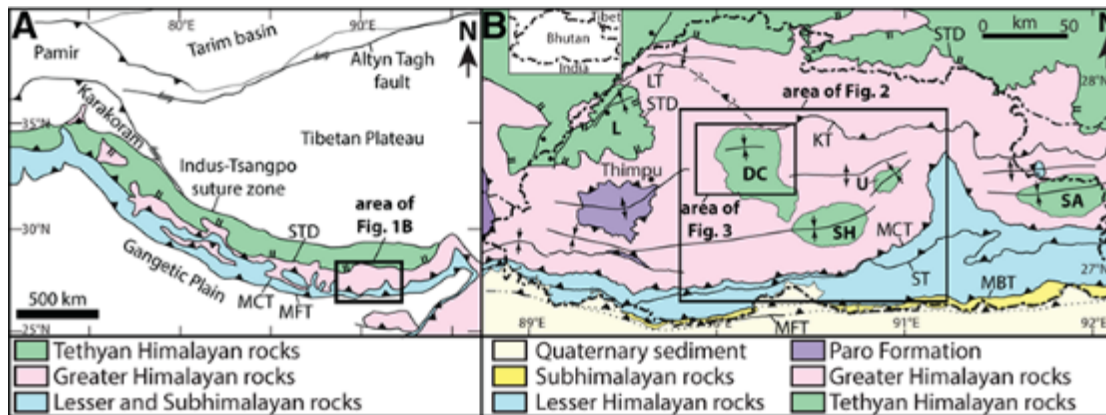


Fig 2. I - V characteristics of the Schottky diodes fabricated on different etched surfaces

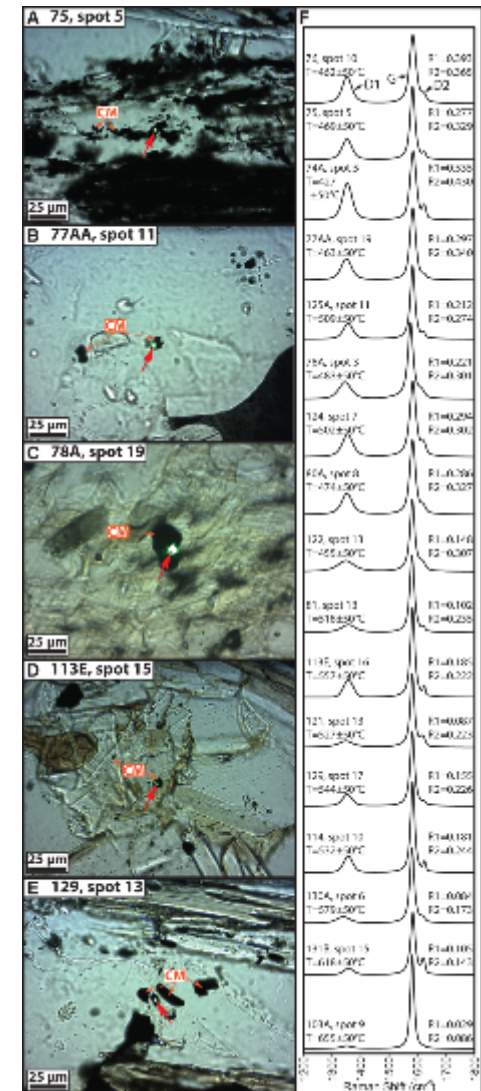
Distributed North-Vergent Shear and Flattening through Greater and Tethyan Himalayan Rocks

The debate over the location of the South Tibetan detachment fault (STD in bottom figure) is addressed using a combination of temperature, pressure and shear strain data. Raman spectroscopy, done at the Eyring Materials Center at ASU, was used to determine metamorphic temperatures in carbon-bearing rocks. The figure on the right shows how the graphite peak intensifies and sharpens with increasing metamorphic temperature while the carbon defect peak decreases.



S. P. Long, School of the Environment, Washington State University, and S. M. Gordon, Dept. of Geological Sciences and Eng., University of Nevada
Work performed at NCI-SW

This work was supported, in part, by the NSF under grant # EAR-1220300
S. P. Long et al. *Lithosphere* vol. 5, pp.774-795 (2017)



A Nonmagnetic Differentiated Early Planetary Body

Paleomagnetic studies of meteorites have shown that many early planetary bodies generated dynamo magnetic fields and until now, there has been no evidence for an achondrite parent body without a dynamo. This study used paleomagnetic measurements of achondrite NWA 7325 to show that it last cooled in a near-zero field ($< \sim 1.7 \mu\text{T}$), 4563.09 \pm 0.26 million years ago (Ma). Scanning and transmission electron microscopy was done at ASU Eyring Materials Center to characterize structure and twinning in martensite grains, the primary ferromagnetic mineral in the sample. The results confirm a recent conclusion that the solar nebula had dissipated by ~ 4 million years after solar system formation.

B. P. Weiss, Dept. of Earth, Atmospheric, and Planetary Sciences,
Massachusetts Institute of Technology
Work performed at NCI-SW

The work at MIT was supported, in part, by NASA under grants
#NNX15AH72G and #NNA14AB01A.

B. P. Weiss et al. *Earth and Planetary Letters*, vol. 468, pp. 119–132
(2017)

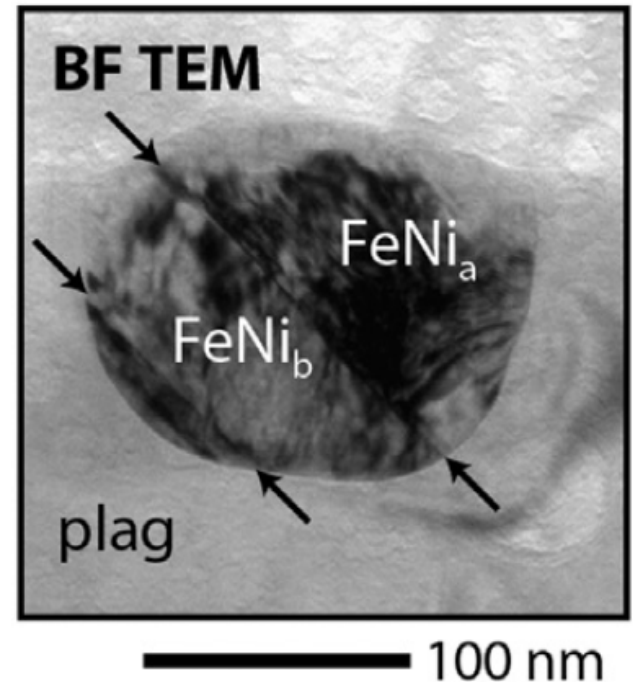
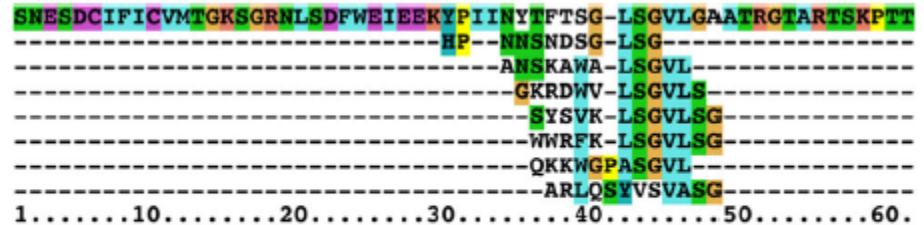


Fig 1. TEM image of an FeNi particle showing a lamellar twin bounded by planar twin boundaries (arrows). The FeNi_a twin domain (dark) is imaged along the $[113]$ zone axis and the FeNi_b domain is imaged nearly along $[113]$. Local variations in diffraction contrast within the twin domains indicate local lattice strain associated with a high density of defects.

Using a Random Peptide Microarray to Diagnose Chronic Fatigue Syndrome

Chronic fatigue syndrome (CFS) affects as many as 2.5 million individuals, underscoring the importance of CFS as a major public health concern. Presently, there are no unique physical symptoms or reproducible biomarkers that can delineate this disease. We present a proof-of-concept study where random peptide arrays show utility in delineating CFS cases from healthy controls. The ultimate goal of this work is the development of a non-subjective clinical tool for diagnosing patients with CFS.



A peptide motif characteristic of individuals suffering from chronic fatigue syndrome that can be used to delineate between CFS cases and healthy controls.

To this end, we used a random peptide array custom designed at ASU, which has previously produced immunosignatures for other chronic and complicated diseases that are difficult to diagnose such as cancer, valley fever, and Alzheimer's disease. Our study has identified a conserved peptide motif that is preferentially recognized by serum antibodies in a large number of CFS cases over that of healthy controls.

Sahajpreet Singh and Vincent Lombardi, Nevada Center for Biomedical Research and the Dept. of Chemistry and Molecular Biology, University of Nevada, Reno, NV
Work performed at NCI-SW

Singh et al. *Mol. Neurobiology*, vol. 55, pp. 633-641 (2018)

Design, Fabrication, and Testing of Stellar Coronagraphs for Exoplanet Imaging

Complex-mask coronagraphs destructively interfere unwanted starlight with itself to enable direct imaging of exoplanets. This is accomplished using a focal plane mask (FPM). We explore methods of fabrication of complex FPMs for a Phased-Induced Amplitude Apodization Complex-Mask Coronagraph (PIAACMC). We present FPMs fabricated using several process paths, including deep reactive ion etching and focused ion beam etching using a silicon substrate. The characteristic size of the mask features is $5\ \mu\text{m}$ with depths ranging over $1\ \mu\text{m}$. The masks are characterized for manufacturing quality using an optical interferometer and a scanning electron microscope. Initial testing is performed at the Subaru Extreme Adaptive Optics testbed, providing a baseline for future experiments to determine and improve coronagraph performance within fabrication tolerances.

J. M. Knight, College of Optical Sciences, University of Arizona, Tucson, AZ

Work performed at NCI-SW

J. M. Knight et al. *Proc. SPIE 10400, Techniques and Instrumentation for Detection of Exoplanets VIII*, 104000N (12 September 2017)

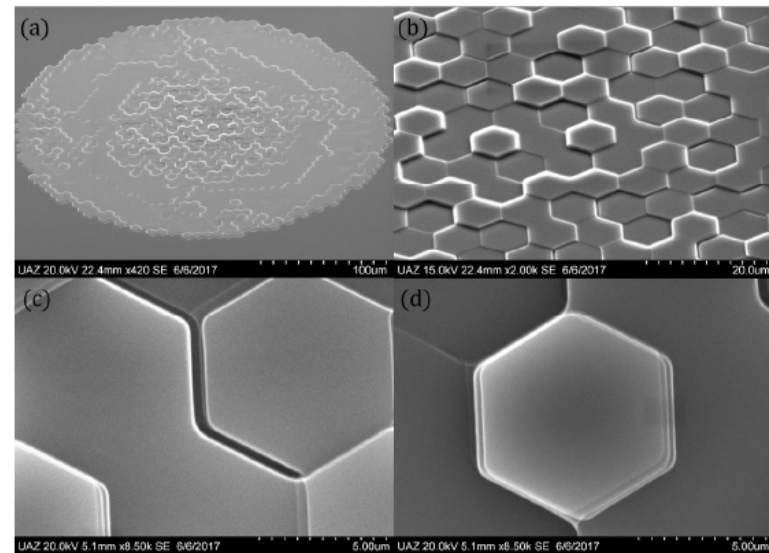


Fig 1. (a) SEM image at a 60 degree tilt of an entire complex FPM. (b) Large scale demonstration of line-on-line mis-registrations between process steps. (c) A 500 nm gap between levels creates an edge feature which may better modeling to see its effect on the mask's performance. (d) Misalignment between multiple levels effectively increases the size of this hexagon creating non-ideal edge effects.

Organic Passivation of Silicon Surfaces and Fabrication of a Hybrid Organic/Semiconductor Solar Cells

Benzoquinone has been demonstrated to provide a remarkable surface passivation and to induce a junction on n-type silicon wafers. Silicon/Organic material-hybrid devices, as schematically shown in Fig1, were fabricated. These devices showed the power efficiencies of 11%. This structure/process is unique in that it doesn't need boron diffusion to create a p+n junction. In addition to this, the organic layer itself acts as a surface passivation layer. This device was used to explore eventual commercialization of this potentially high efficiency, low-cost process.

The comparison of quantum efficiency of the hybrid device with conventional diffused junction solar cells (Fig2) shows that the front response of this device is significantly better than the diffused junction Al-BSF solar cells.

Abhishek Iyer and Robert Opila, Dept. of ECE and Dept. of Material Science and Engineering, University of Delaware, Newark, DE
Work performed at NCI-SW

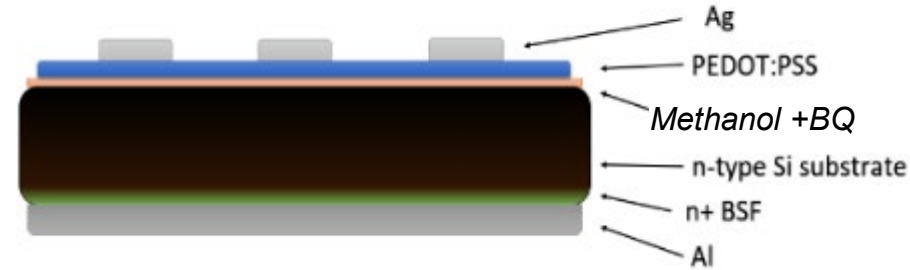


Fig 1. Schematic device structure of a silicon-organic heterojunction solar cell with an inversion layer induced by organic passivants, using PEDOT:PSS as the hole-transfer layer

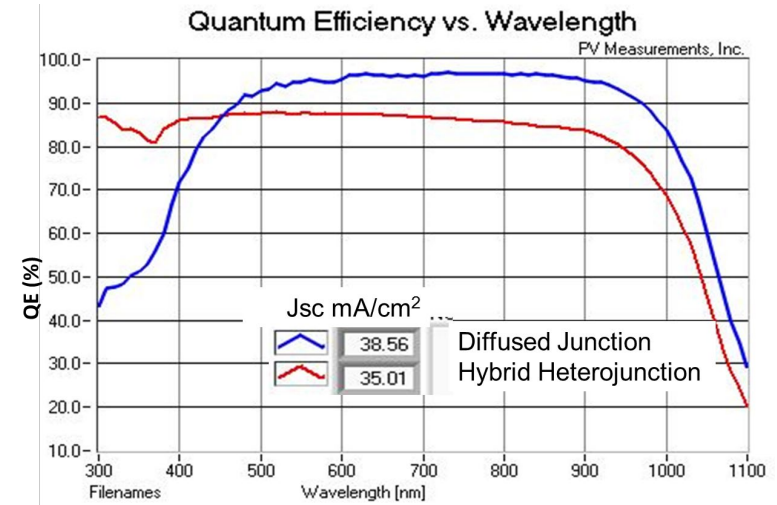


Fig 2. Quantum Efficiency of hybrid cell compared with conventional diffused junction cell. The hybrid cell shows high power conversion at low wavelengths.

Elastically Stretchable Metal Conductors

Microcracked gold films on elastomeric substrates can function as stretchable and deformable interconnects and sensors. This research examines the change in resistance upon bending of a microcracked conductor and compares the results with stretching such a conductor. The resistance depends on the strain in the film, which, for bending, is a function of the bending radius and the location of the film within the structure with respect to the neutral plane. The resistance decreases when the gold conductor is under compression and increases when it is under tension. These results provide guidance for the design of interconnects for flexible and stretchable electronics and for flexible sensors to monitor the magnitude and direction of bending or stretching.

Oliver Graudejus, BioMedical Sustainable Elastic Electronic Devices LLC, Tempe, AZ
Work performed at NCI-SW

Graudejus et al. *Appl. Phys. Letts.*, vol. 110, p. 221906 (2017)

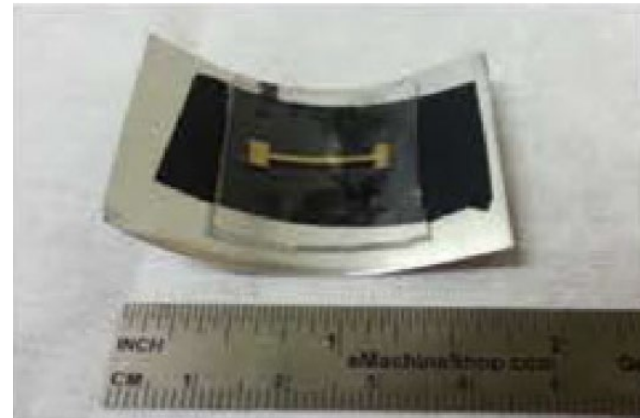


Fig 1. A bent microcracked gold conductor under moderate compression

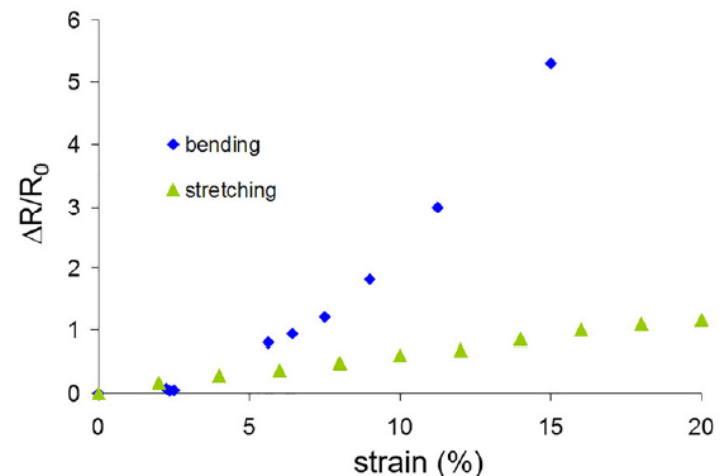


Fig 2. Comparison of the normalized change in resistance ($\Delta R/R_0$) vs. strain for bending and stretching a microcracked gold conductor.

Prospecting Nanomaterials in Aqueous Environments by Cloud Point Extraction

Increasing application of engineered nano-materials (ENMs) in industry and consumer products inevitably lead to their release into and impact on aquatic environments. To characterize the engineered nanomaterials efficiently in surface water, a fast and simple method is needed to separate and concentrate nanomaterials from the aqueous matrix without altering their shape and size. Applying cloud-point extraction (CPE) using the surfactant Triton 114 to an array of ENMs with different sizes or capping agents in nanopure water resulted in extraction efficiency of greater than 83%. This study applied CPE with transmission electron microscopy (TEM) to enrich and analyze popular nanoparticles such as SiO_2 and TiO_2 from natural waters.

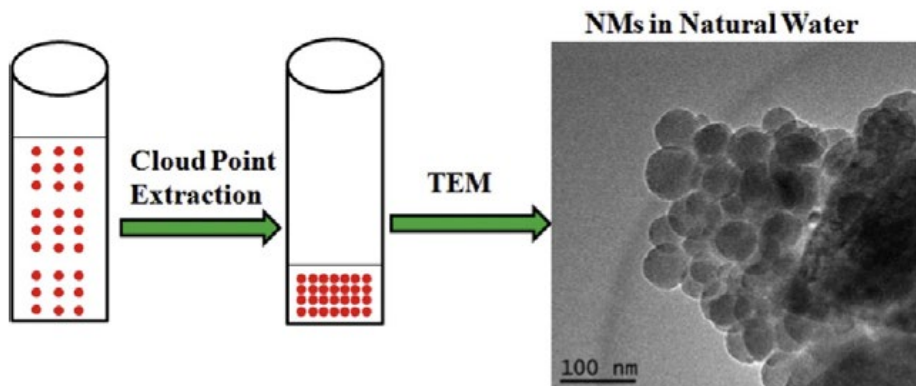


Fig 1. Cloud point extraction uses a small volume of surfactant in a larger volume of water. The combined solution is heated above the cloud temperature of surfactant to form micelles of surfactant and targeted nanoparticles.

P. Westerhoff, Center for the Life-Cycle of Nanomaterials in the Environment, Arizona State University, Tempe, AZ
Work performed at NCI-SW

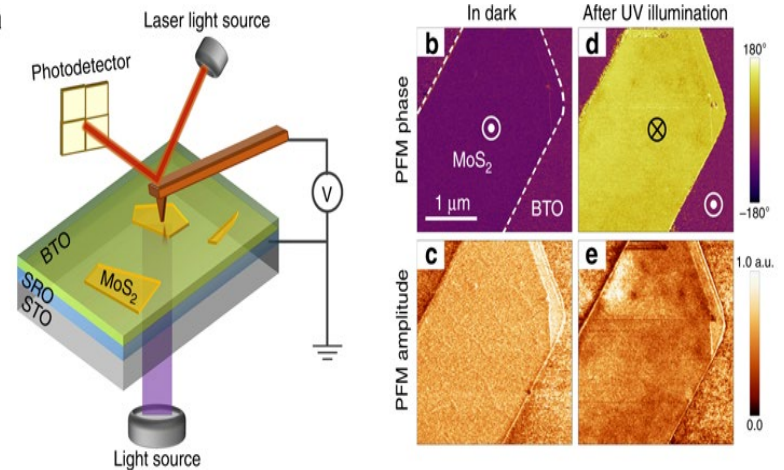
The work was supported by grants from the U.S. Geological Survey (#2013AZ517B), the NSF (#EEC-1449500), and U.S. Environmental Protection Agency (#RD83558001).

Y. Yang et al. *Science of the Total Environment* vol. 584–585 pp. 515–522 (2017)

Nebraska Nanoscale Facility (NNF)

Optical Control of Polarization in Ferroelectric Heterostructures

Tao Li and co-workers demonstrated optically induced polarization switching in BaTiO₃-based ferroelectric heterostructures utilizing a two-dimensional narrow-gap semiconductor MoS₂ as a top electrode. This effect is attributed to the redistribution of the photo-generated carriers and screening charges at the MoS₂/BaTiO₃ interface. Specifically, a two-step process which involves formation of intra-layer excitons during light absorption followed by their decay into inter-layer excitons results in the positive charge accumulation at the interface forcing the polarization reversal from the upward to the downward direction. Theoretical modeling of the MoS₂ optical absorption spectra with and without the applied electric field provides quantitative support for the proposed mechanism. It is suggested that the discovered effect is of general nature and should be observable in any heterostructure comprising a ferroelectric and a narrow gap semiconductor.



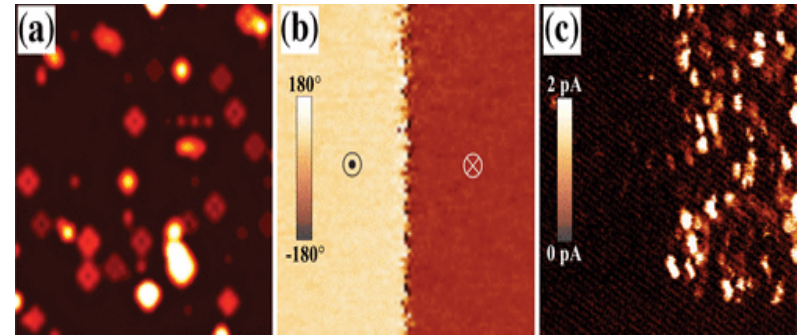
Optically induced changes of the polarization in MoS₂/BaTiO₃/SrRuO₃ junctions. **a** A sketch of the experiment geometry. **b–e** PFM phase (**b**, **d**) and amplitude (**c**, **e**) images acquired in the dark before and after UV illumination. The MoS₂ flake boundary is indicated by the dashed lines in **b**. The BTO film underneath MoS₂ was electrically poled to the upward polarization before illumination.

Tao Li, Alexey Lipatov, Haidong Lu, Hyungwoo Lee, Jung-Woo Lee, Engin Torun, Ludger Wirtz, Chang-Beom Eom, Jorge Íñiguez, Alexander Sinitskii & Alexei Gruverman. UW-Madison, LIST Luxembourg, Univ. of Luxembourg & Univ. of Nebraska–Lincoln. Departments of Chemistry, Physics, Mat. Sci. Eng.

This work was supported by the NSF through MRSEC Grant DMR-1420645 (tunnel junction fabrication) and Grant ECCS-1509874 (electrical characterization), and was performed in part at NNF. *Nature Comm.* **9**, 3344 (2018).

Tunneling Hot Spots in Ferroelectric SrTiO₃

Gruverman and co-workers discovered room-temperature ferroelectricity in strain-free ultrathin films of SrTiO₃ driven by the Ti_{Sr} antisite defects, which generate a local dipole moment polarizing the surrounding nanoregion. They demonstrated that these polar defects are not only responsible for ferroelectricity, but also propel the appearance of highly conductive channels, “hot spots”, in the ultrathin SrTiO₃ films. Using a combination of scanning probe microscopy experimental studies and theoretical modeling, they showed that the hot spots emerge due to resonant tunneling through localized electronic states created by the polar defects and that the tunneling conductance of the hot spots is controlled by ferroelectric polarization. It is also shown that the conductivity of the hot spots can be modulated by mechanical stress, opening a possibility for development of conceptually new electronic devices with mechanically tunable resistive states.



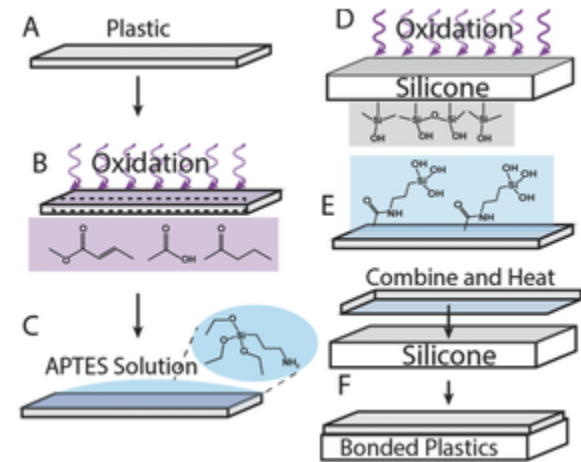
“Hot spots”, in the ultrathin SrTiO₃ films

Haidong Lu, Daesu Lee, Konstantin Klyukin, Lingling Tao, Bo Wang, Hyungwoo Lee, Jungwoo Lee, Tula R. Paudel, Long-Qing Chen, Evgeny Y. Tsymbal, Vitaly Alexandrov, Chang-Beom Eom, and Alexei Gruverman. Penn State Univ., Univ. of Wisconsin-Madison & University of Nebraska-Lincoln. Departments of Physics, Materials Science, Chemical Engineering.

This work was supported by the National Science Foundation (NSF) through Materials Research Science and Engineering Center (MRSEC) under Grant DMR-1420645, and was performed in part at NNF. *Nano Lett.* 18, 491 (2018).

Covalent Bonding of Thermoplastics to Rubbers for Printable, R2R Processing in Soft Robotics and Microfluidics

The disparate mechanical and chemical properties of these materials have made it challenging to develop universal synthetic procedures capable of reliably adhering to these classes of materials together. Morin and co-workers developed a simple and scalable procedure that is capable of covalently laminating a variety of commodity thermoplastic sheets to silicone rubber films. When combined with laser printing, the nonbonding sites can be “printed” onto the thermoplastic sheets, enabling the direct fabrication of microfluidic systems for actuation and liquid handling applications. The versatility of this approach in generating thin, multifunctional laminates is demonstrated through the fabrication of milliscale soft actuators and grippers with hinged articulation and microfluidic channels with built-in optical filtering and pressure-dependent geometries. The concepts and strategies presented herein are broadly applicable to the soft robotics, microfluidics, and advanced and additive manufacturing communities where hybrid rubber/plastic structures are prevalent.



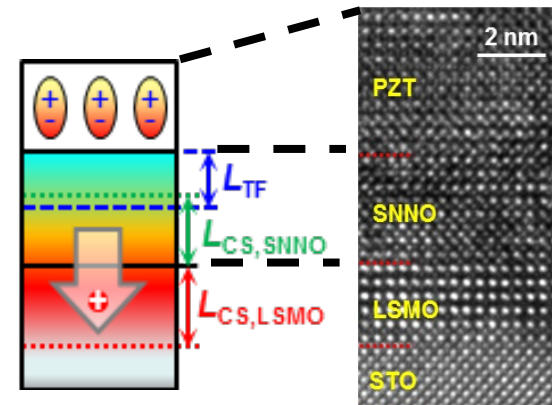
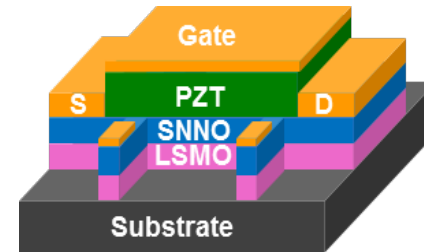
Lamination procedure and surface spectroscopy. A–C) The commodity polymer was oxidized with either O₂ plasma or UVO and then immersed into a solution of APTES to aminate the plastic. D) PDMS was also oxidized. E) The two materials were combined and heated in an oven bonding the plastic to the silicone rubber.

Jay M. Taylor, Karla Perez–Toralla, Ruby Aispuro and Stephen A. Morin. Dept. of Chemistry, University of Nebraska.

This work was supported by the NSF Grant No. 1555356, and was performed in part at NNF. *Advanced Materials* **30**, 1705333 (2018).

Interfacial Charge Engineering for Ferroelectric-Control of Mott Transistors

The objective of this work is to engineer complex oxide interfaces for enhancement of the ferroelectric (FE) field effect in a prototype Mott field-effect transistor. By switching the polarization field of a FE PZT gate, nonvolatile resistance modulation is induced. The device concept has been investigated over the last two decades for examining charge density-driven quantum phase transitions and interfacial magnetoelectric coupling. Here a PZT gated Mott transistors based on a couple of nmr-thick $\text{Sm}_{0.5}\text{Nd}_{0.5}\text{NiO}_3$ (SNNO) and $\text{La}_{0.67}\text{Sr}_{0.33}\text{MnO}_3$ (LSMO) composite channels is fabricated. It employs the charge transfer effect at the SNNO/LSMO interface to engineer the carrier density profile in the channel. It leads to up to two orders of magnitude enhancement in the room temperature resistance switching ratio. This study shows how tailored electronic states can be achieved through atomistic design of complex oxide interfaces.



PZT-gated ferroelectric FET (top) with the key innovation of an engineered complex oxide heterostructure (bottom) for enhanced ferroelectric field control.

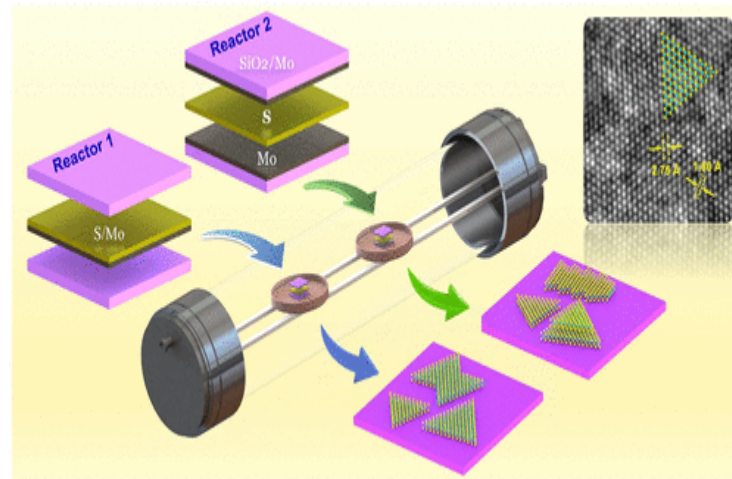
X. Chen, X. Zhang, M.A. Koten, H. Chen, Z. Xiao, L. Zhang, J.E. Shield, P.A. Dowben, X. Hong. University of Nebraska-Lincoln. Departments of Mechanical and Materials Engineering, Physics.

This work was supported by NSF Grants DMR-1420645 and 1148783, DOE Grant DESC0006153, and was performed in part at NNF.

Adv. Funct. Mater. **29**, 1701385 (2017).

Sulfurization Strategy for Growth of High-Quality Ultrathin Molybdenum Disulfide Single Crystals

Yongfeng Lu and co-workers developed a novel approach for direct formation of high-quality, monolayer and few-layer MoS_2 single crystal domains via a single-step rapid thermal processing of a sandwiched reactor with sulfur and molybdenum (Mo) film in a confined reaction space. An all-solid-phase growth mechanism was proposed and experimentally/theoretically evidenced by analyzing the surface potential and morphology mapping. Compared with the conventional chemical vapor deposition approaches, our method involves no complicated gas-phase reactant transfer or reactions and requires very small amount of solid precursors [e.g., Mo ($\sim 3 \mu\text{g}$)], no carrier gas, no pretreatment of the precursor, no complex equipment design, thereby facilitating a simple, low-cost, and environmentally friendly growth. For the first time, we observed that the SFG (peak intensity/position) polarization can be used as a sensitive probe to identify the orientation of TMDs' crystallographic axes.



Growth of monolayer and few-layer MoS_2 single crystals through space-confined, solid-phase sulfurization strategy. (a) Schematic drawing of two sandwich-structured reactor configurations for space-confined solid-phase growth of highly crystalline MoS_2 atomic layers.

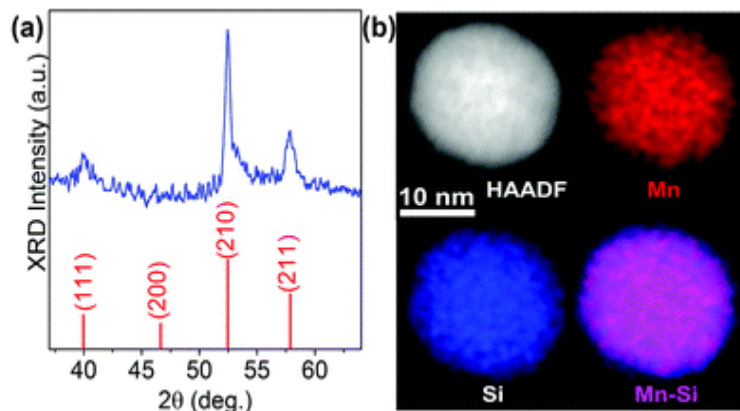
Reactor Type 1: substrate/Mo-S/substrate. Reactor Type 2: substrate-Mo/S/Mo-substrate

Dawei Li, Zhiyong Xiao, Sai Mu, Fei Wang, Ying Liu, Jingfeng Song, Xi Huang, Lijia Jiang, Jun Xiao, Lei Liu, Stephen Ducharme, Bai Cui, Xia Hong, Lan Jiang, Jean-Francois Silvain, and Yongfeng Lu. ORNL Tennessee, BIT Beijing, ICMCB France & Univ. of Nebraska – Lincoln. Departments of Physics, Materials Eng., Electrical Eng.

This research was supported by NSF (CMMI 1129613, CMMI 126512) and the Nebraska Center for Energy Science Research, and was performed in part at NNF. *Nano Lett.* **18**, 2021 (2018).

Effect of Size Confinement on Skyrmionic Properties of MnSi Nanomagnets

The control of skyrmion spin structures in the 10 nm size ranges is essential to explore them for spintronics, ultra-high-density magnetic recording, and other applications. In this study, Das and co-workers have fabricated MnSi nanoparticles with average sizes of 9.7, 13.1 and 17.7 nm and investigated their structural and magnetic properties. X-ray diffraction and transmission electron microscope studies show that the MnSi nanoparticles crystallize in the cubic B20 structure. Field-dependent dc susceptibility data of the MnSi samples with average particle sizes of 17.7 and 13.1 nm show anomalies in limited field (about 25–400 Oe) and temperature (25 K–43 K) ranges. These features are similar to the signature of the skyrmion-like spin structures observed below the Curie temperature of MnSi. Our results also show that this anomalous behavior is size-dependent and suppressed in the smallest nanoparticles (9.7 nm), and this suppression is interpreted as a confinement effect that leads to a truncation of the skyrmion structure.



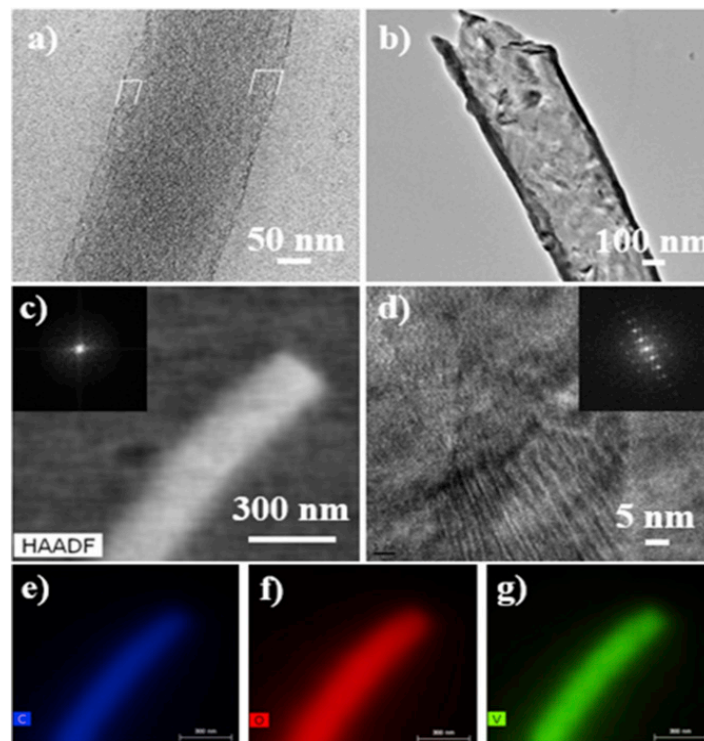
(a) X-ray diffraction pattern of 17.7 nm MnSi nanoparticles. The vertical lines represent the standard peak positions and corresponding relative intensities of the X-ray diffraction peaks of MnSi.¹⁵ (b) A high-angle annular dark-field (HAADF) image with atomic number (Z) contrast and the corresponding EDX elemental color mappings showing Mn, Si, and Mn and Si distributions

Bhaskar Das, Balamurugan Balasubramanian, Ralph Skomski, Pinaki Mukherjee, Shah R. Valloppilly, George C. Hadjipanayis and David J. Sellmyer. Univ. of Delaware & Univ. of Nebraska – Lincoln. Departments of Physics, NCMN.

This research was supported by the U.S. DOE DE-FG02-04ER46152 and DE-FG02-04ER4612, and was performed in part at NNF. *Nanoscale* **10**, 9504 (2018).

Facilitating High-Capacity V_2O_5 Cathodes with Stable Two and Three Li^+ Insertion

Jun Li and co-workers at Kansas State Univ. reported an approach to achieving stable 2 and 3 Li^+ insertion, respectively, into vanadium pentoxide (V_2O_5) as lithium-ion battery (LIB) cathode materials using a core-shell structure based on a self-standing carbon nanofiber (CNF) membrane fabricated by an electrospinning process. Uniform coaxial V_2O_5 shells are coated onto continuous CNF cores via a pulsed electrodeposition. SEM and TEM images indicate that the uniform 30–50 nm thick V_2O_5 shell forms an intimate interface with the CNF core. Lithium insertion capacities up to 291 and 429 $mAh\ g^{-1}$ are achieved in the voltage ranges of 4.0–2.0 V and 4.0–1.5 V, respectively. Moreover, after 100 cycles, remarkable retention rates of 97% and 70% are obtained for 2 Li^+/V_2O_5 and 3 Li^+/V_2O_5 insertion, respectively. These results reveal that it is potentially feasible to fabricate the core-shell structure with electrospinning and electrodeposition processes to break the intrinsic limits of V_2O_5 and enabling this high-capacity cathode materials for future LIBs.



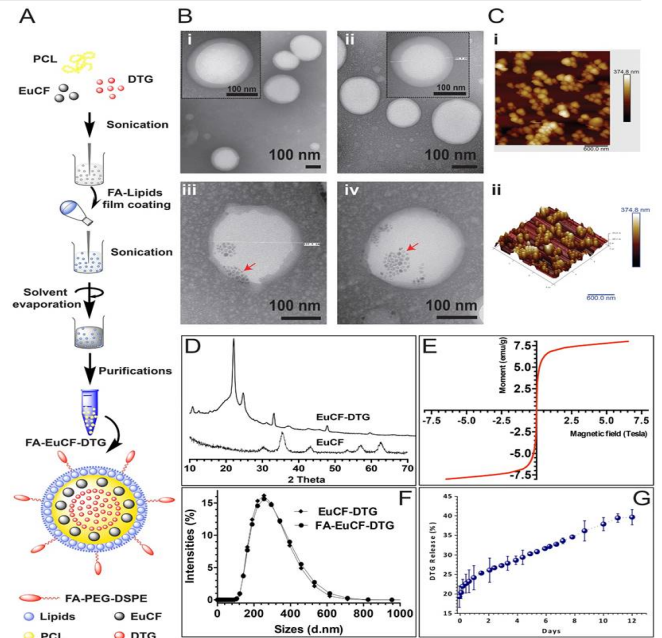
HRTEM images of V_2O_5 shell and EDS mapping of CNF V_2O_5 nanofiber.

Emery Brown, Seok-Hwan Park, Ayyappan Elangovan, Yue Yuan, Jooyoun Kim, Xiuzhi Susan Sun, Xiaoming Zhang, Guohong Wang, Jun Li. Kansas State University, Kansas. Departments of Chemistry, Textiles, Grain Science.

This work was supported by NASA Grant NNX13AD42A and NSF Grants CBET-1703263 and DMR-1707585, and was performed in part at NNF. *Electrochimica Acta* **269**, 144 (2018).

Multimodal Theranostic Nanoformulations Permit Magnetic Resonance Bioimaging of Antiretroviral Drug Particle Tissue-Cell Biodistribution

Long-acting slow effective release antiretroviral therapy (LASER ART) was developed to improve patient regimen adherence, prevent new infections, and facilitate drug delivery to human immunodeficiency virus cell and tissue reservoirs. To facilitate LASER ART development, “multimodal imaging theranostic nanoprobes” were created by Kevadiya and co-workers. These allow combined bioimaging, drug pharmacokinetics and tissue biodistribution tests in animal models. Europium (Eu^{3+})-doped cobalt ferrite (CF) dolutegravir (DTG)-loaded (EuCF-DTG) nanoparticles were synthesized then fully characterized based on their size, shape and stability. These were then used as platforms for nanoformulated drug biodistribution. Folic acid (FA) decoration of EuCF-DTG (FA-EuCF-DTG) nanoparticles facilitated macrophage targeting and sped drug entry across cell barriers. Drug particles were detected in macrophage Rab compartments by dual fluorescence labeling. Replicate particles elicited sustained antiretroviral responses. After parenteral injection of FA-EuCF-DTG and EuCF-DTG into rats and rhesus macaques, drug, iron and cobalt levels, measured by LC-MS/MS, magnetic resonance imaging, and ICP-MS were coordinate.



Syn. and charact. of lipid-coated core-shell nanoparticles. (A) Schematic illustration of multimodal core-shell nanoparticles (B) TEM images (C) Characterization by AFM. (D) XRD patterns (E) Evaluation of the magnetic properties using SQUID.

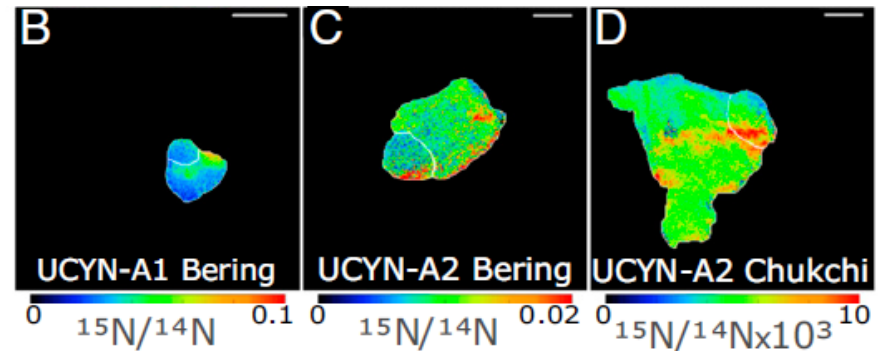
Bhavesh D. Kevadiya, Howard E. Gendelman et al., Pharmacology, University of Nebraska Medical Center–Omaha

This work was supported, in part, by NIH Grants AG043540, DA028555, NS036126, NS034239, MH064570, NS043985, MH062261, AG043540, AI113883 and DOD Grant 421-20-09A, the Carol Swarts Emerging Neuroscience Fund and the Nebraska Research Initiative, and was performed in part at NNF. *Theranostic* 8, 256 (2018).

NNCI Site @ Stanford (nano@stanford)

Symbiotic unicellular cyanobacteria fix nitrogen in the Arctic Ocean

Biological dinitrogen (N_2) fixation (BNF) is an important source of nitrogen in marine systems. Until recently, it was believed to be primarily limited to subtropical open oceans. Marine BNF is mainly attributed to cyanobacteria. However, recently an unusual N_2 -fixing unicellular cyanobacteria (UCYN-A)/haptophyte symbiosis was reported with a broader temperature range than other N_2 -fixing cyanobacteria. We report that the UCYN-A symbiosis is present and fixing N_2 in the Western Arctic and Bering Seas, further north than any previously reported N_2 -fixing marine cyanobacteria. Nanoscale secondary ion mass spectrometry enabled us to directly show that the symbiosis was fixing N_2 . These results show that N_2 -fixing cyanobacteria are not constrained to subtropical waters and challenge commonly held ideas about global marine N_2 fixation.



UCYN-A symbioses fix $^{15}N_2$ in western Arctic waters. UCYN-A cell specific ^{15}N enrichment from nanoSIMS measurements after incubating natural populations in seawater with $^{15}N_2$.

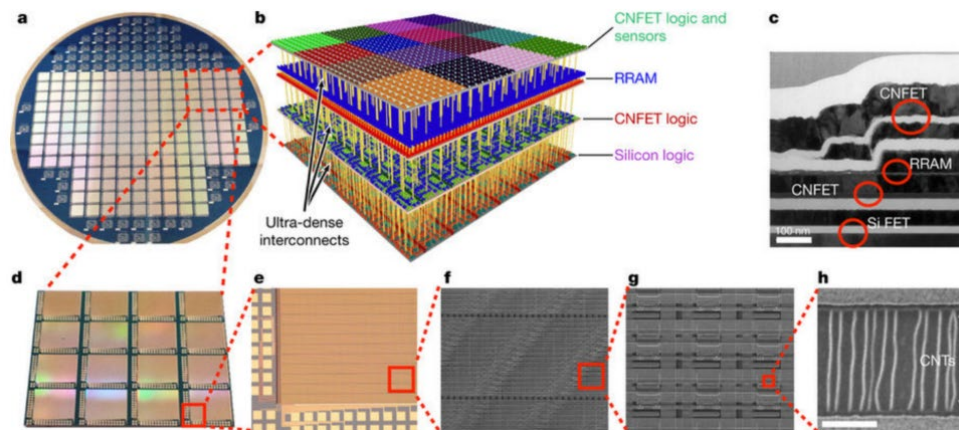
Bars of the same color (A) represent rates measured in individual symbioses (UCYN-A with host alga) from a single station and lineage (noted in underlying cell image). (Scale bar, 2 μm .)

Harding (UCSC), Turk-Kubo (UCSC), Sipler (College of William & Mary, Uni., of Newfoundland), Mills (Stanford), Bronk (College of William & Mary, Bigelow Laboratory for Ocean Sciences), Zehr (UCSC). Work performed at the NNCI Site@Stanford.

Supported by NSF Awards OPP-1503614, 1241093, 1559152, OPP-1504307; NanoSIMS MRI: ECCS-0922648
PNAS, 2018

3D integration for computing and data storage on a single chip

Transformative nanosystems, which use new nanotechnologies to simultaneously realize improved devices and new integrated circuit architectures was fabricated. The device consists of more than one million resistive random-access memory cells and more than two million carbon-nanotube field-effect transistors—promising new nanotechnologies for use in energy-efficient digital logic circuits and for dense data storage —fabricated on vertically stacked layers in a single chip. Unlike conventional integrated circuit architectures, the layered fabrication realizes a three-dimensional integrated circuit architecture with fine-grained and dense vertical connectivity between layers of computing, data storage, and input and output (in this instance, sensing).



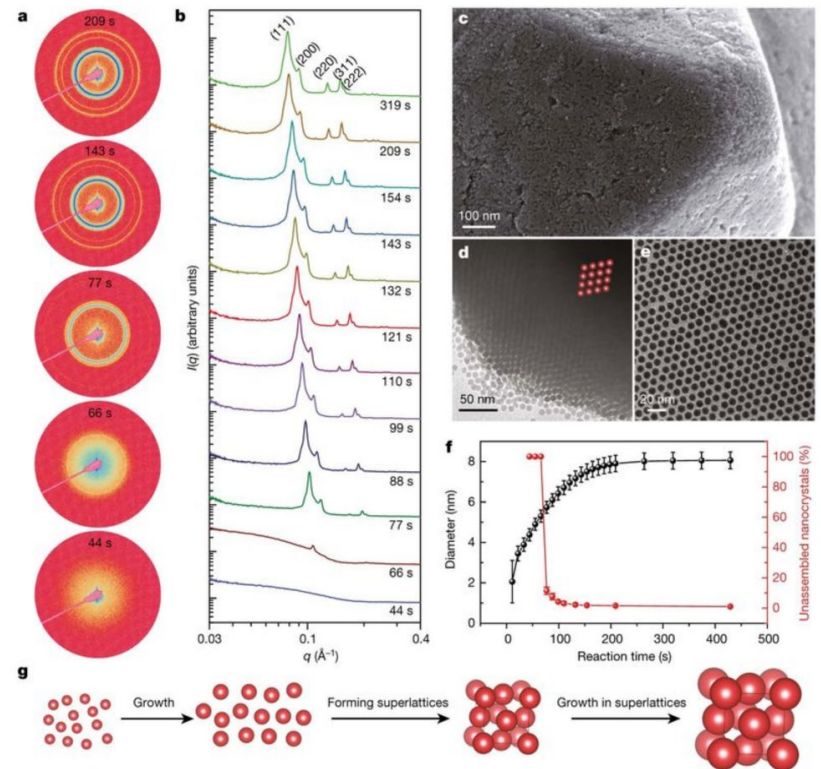
a, A 100-mm-wide wafer on which the integrated circuits are fabricated; b, Illustration of the nanosystem; c, Cross-sectional TEM image of the four-layer chip; d–h, Progressively magnified top views of the nanosystem

Shulaker (MIT), Hills, Park, Howe, Saraswat, Wong, and Mitra (Stanford). Work performed at the NNCI Site @ Stanford.

Supported by NSF Award CNS-1059020, DARPA W909MY-16-1-0001
Nature volume 547, pages 74–78 (06 July 2017)

High-temperature crystallization of nanocrystals into 3D superlattices

Crystallization of colloidal nanocrystals into superlattices represents a practical bottom-up process with which to create ordered metamaterials with emergent functionalities. With precise control over the size, shape and composition of individual nanocrystals, various single- and multi-component nanocrystal superlattices have been produced, the lattice structures and chemical compositions of which can be accurately engineered. The team reported the rapid growth (seconds) of micrometre-sized, face-centred-cubic, three-dimensional nanocrystal superlattices during colloidal synthesis at high temperatures. The rational assembly of various nanocrystal systems into novel materials is thus facilitated for both fundamental research and for practical applications in the fields of magnetics, electronics and catalysis.



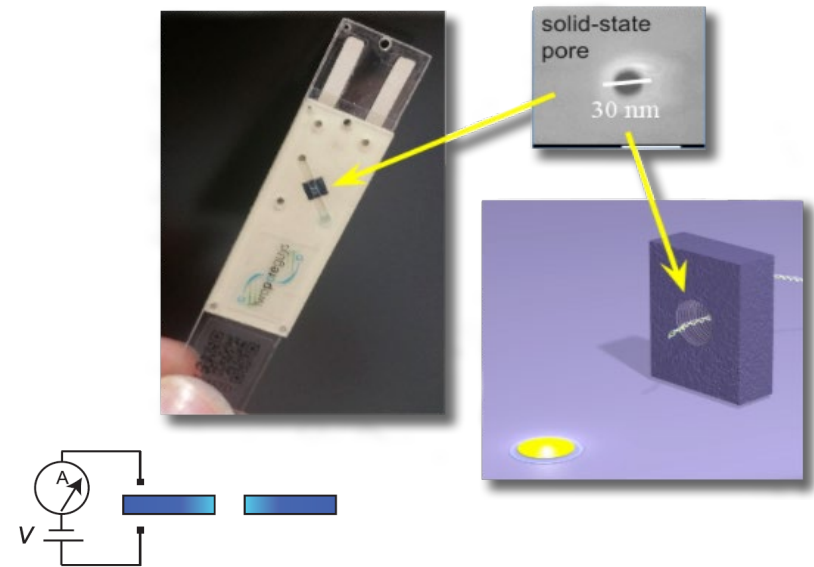
Wu (SLAC), Willis, McKay, Diroll (Argonne), Qin, Cargnello, Tassone (SLAC) (Stanford). Work performed at the NNCI Site @ Stanford.

Supported by DoE, DoD
Nature volume 548, pages 197–201 (10 August 2017)

TwoPoreGuys

Two Pore Guys is developing a handheld, single-molecule sensing platform with the accuracy, precision, and sensitivity of reference lab equipment and sample-in, results-out capability. The core technology includes solid-state, nanopore-based sensors that can detect nucleic acids and proteins and other analytes in human, animal, agriculture, and environmental samples.

Several employees use the nano-fabrication and characterization facilities at the NNCI Site @ Stanford to develop prototypes of the solid state nanopore devices deployed in food crop testing, molecular diagnostics, DNA sequencing and genome mapping.



A small volume of fluid from blood or saliva which has DNA, RNA, Protein and other antibodies are introduced in the two-pore chip. The Silicon Nitride membrane has hole 20-30nm diameter, called as solid-state nanopore.

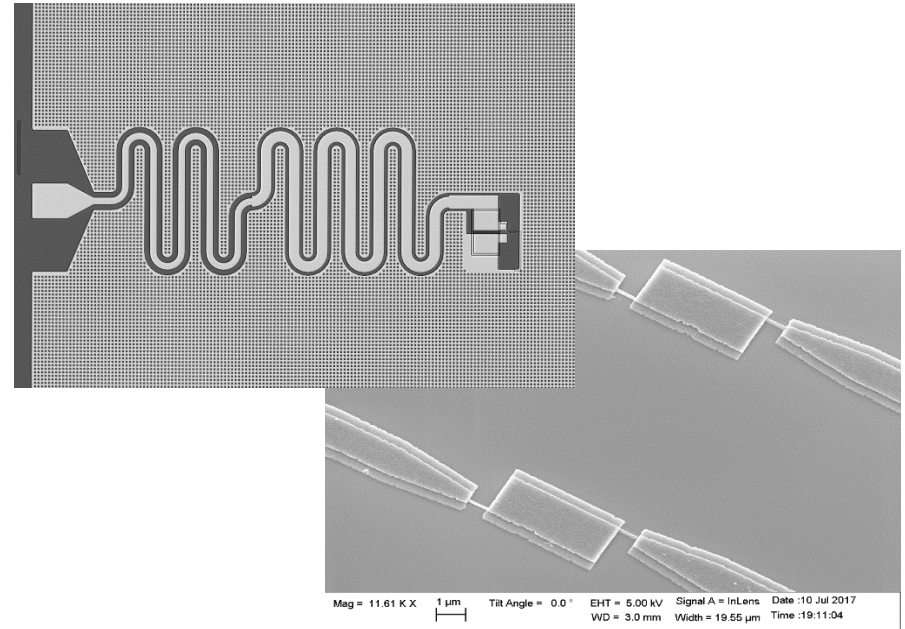
Work performed at the NNCI Site @ Stanford.

Two Pore Guys was founded in 2011 and initial funding was received through SBIR grant. In 2017, the company raised \$51 million. Two Pore Guys currently has 200 employees.

Rigetti Quantum Computing

Rigetti Quantum Computing is developing a full-stack scalable quantum computing platform based on superconducting microwave circuits. The high-fidelity readout of these circuits requires custom-built low-temperature amplifiers based on the Josephson effect.

At the NNCI Site @ Stanford, Rigetti has been researching Josephson junction design and fabrication techniques for the fabrication and testing of Josephson parametric amplifiers (JPAs), which consists of a large capacitor in parallel with a superconducting quantum interference device (SQUID), all connected to a transmission line.



Top: A Josephson parametric amplifier developed at Rigetti Computing. A meandering transmission line connects the input/output port to a capacitor and a SQUID in parallel, all surrounded by ground plane. Bottom: The SQUID of a JPA after metallization, with both aluminum layers easily visible.

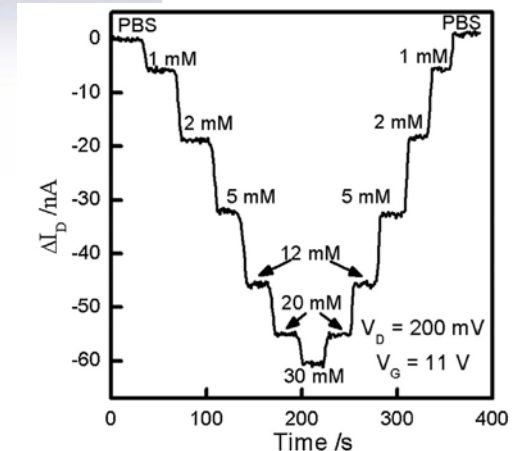
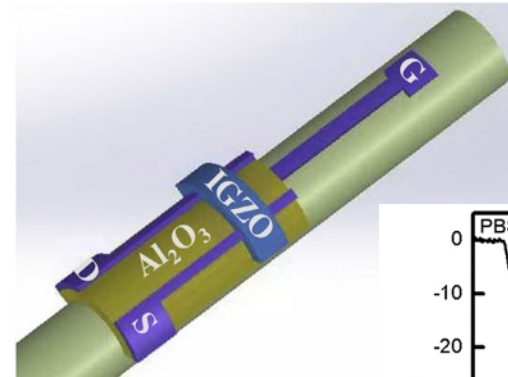
Work performed at the NNCI Site @ Stanford.

Rigetti Computing has recently raised \$70M to develop quantum computers. The company was founded in 2013 and has currently about 200 employees.

Northwest Nanotechnology Infrastructure (NNI)

Transparent Glucose Sensors Fabricated Directly on Curved Substrates

The Herman Group fabricates fully transparent electronics. These are of increasing interest for biological applications, where the combination of sensing and imaging can potentially improve patient healthcare diagnostics. We report high-performance, fully-transparent amorphous In-Ga-Zn-O field-effect transistor (a-IGZO FET) based biosensors fabricated directly on highly-curved glass substrates. The glucose limit of detection is 170 μ M. These results provide insight into new methods for fabricating a-IGZO FETs and a-IGZO FET biosensors on non-planar substrates, and may open a range of new applications, including transparent sensing catheters, flexible active transparent electrode sensing arrays, and integration of FET based biosensors on optical fibers.



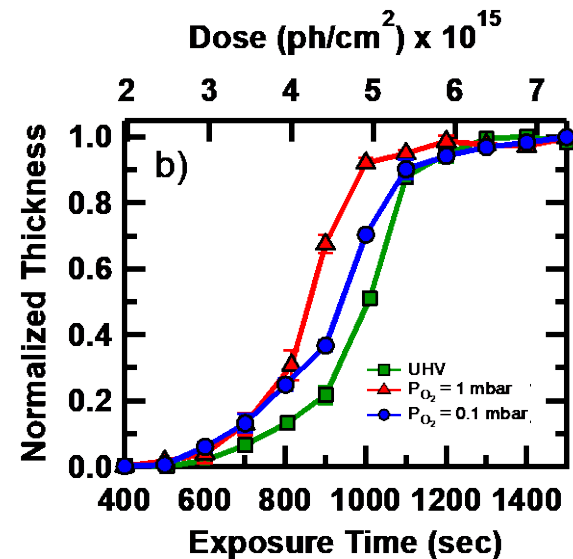
Schematic illustration of a field effect sensor structure fabricated directly on a catheter. Continuous monitoring of ΔI_D versus time for various glucose concentrations.

Xiaosong Du and Gregory Herman, School of Chemical, Biological and Environmental Engineering, Oregon State University. Work performed at OSU's Materials Synthesis and Characterization Facility and Advanced Technology and Manufacturing Institute.

This work was supported by NSF Award # ECCS-1542101.
X. Du, G.S. Herman, *Sensors and Actuators B* 268 (2018) 123–128 .

Characterization of Tin-based Inorganic EUV Resists

Organotin clusters have shown promise for use as EUV resists, where they have high absorption coefficient Sn centers and radiation sensitive organic ligands. The Herman Group uses ambient pressure X-ray photoelectron spectroscopy (APXPS) to investigate the contrast properties of β -Keggin butyl-Sn cluster resists in ultrahigh vacuum (UHV) and ambient oxygen. We found significant changes in the contrast curves, where the presence of an oxygen ambient improved the sensitivity of the photoresist. These results may have significance for EUV and e-beam lithography processing parameters, as well as implications for cluster design and ligand chemistries.



Contrast curve showing normalized insoluble spot thickness versus exposure dose for different ambients.

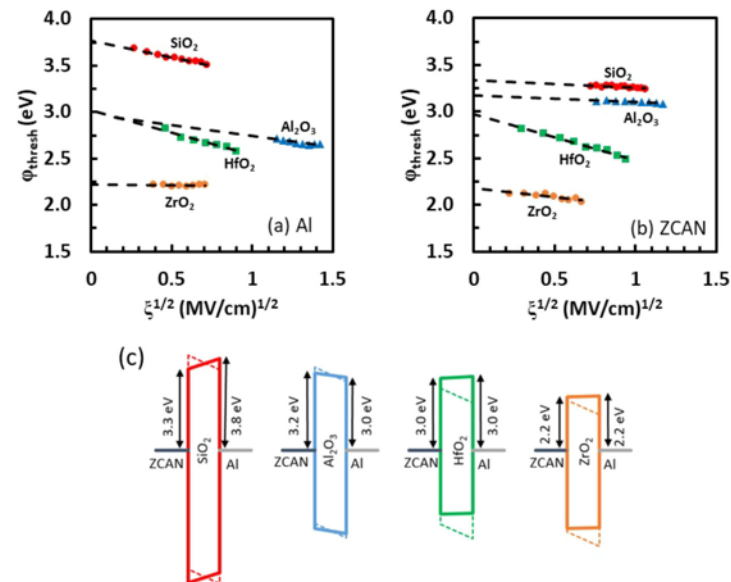
Ryan Frederick, Trey Diulus, Igor Lyubinetsky, Danielle Hutchison, Morgan Olsen, May Nyman, and Gregory Herman, School of Chemical, Biological and Environmental Engineering and the Department of Chemistry, Oregon State University. Work performed at OSU's Ambient Pressure Surface Characterization Laboratory and Materials Synthesis and Characterization Facility.

This work was supported by NSF Award # ECCS-1542101.

Proc. SPIE 10586, Advances in Patterning Materials and Processes XXXV, 1058607 (2018).

Assessment of Energy Barriers Between Amorphous Metal and ALD Insulators

The Conley Materials Group at OSU studies the energy barrier heights between an ultra-smooth amorphous metal electrode, ZrCuAlNi, and several atomic layer deposited (ALD) insulators by measuring internal photoemission (IPE) spectroscopy. ZrCuAlNi-insulator barriers are characterized within metal-insulator-metal (MIM) stacks with Al top contacts. The measured barrier heights are consistent with the electron affinity of the respective oxides. However, barriers for SiO₂ and Al₂O₃ are smaller than expected based on the reported vacuum work function of ZrCuAlNi. These results indicate that ZrCuAlNi has a smaller effective work function in these device structures. These results demonstrate that bulk vacuum parameters are insufficient to accurately predict barrier heights and device performance in MIM device structures.



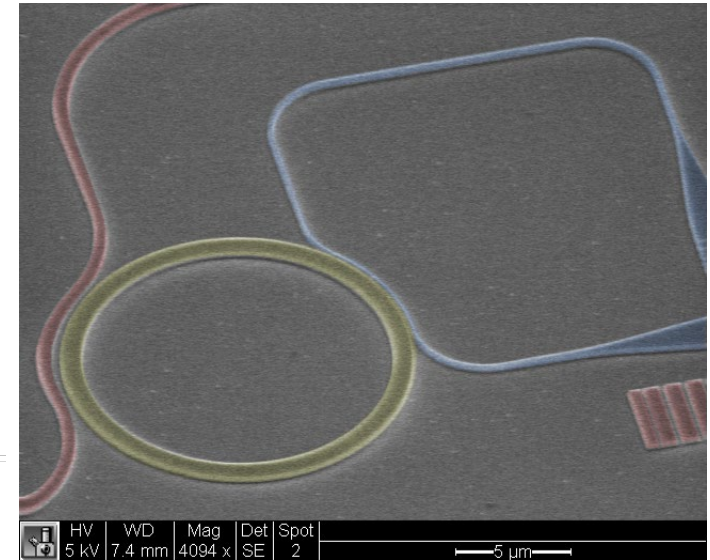
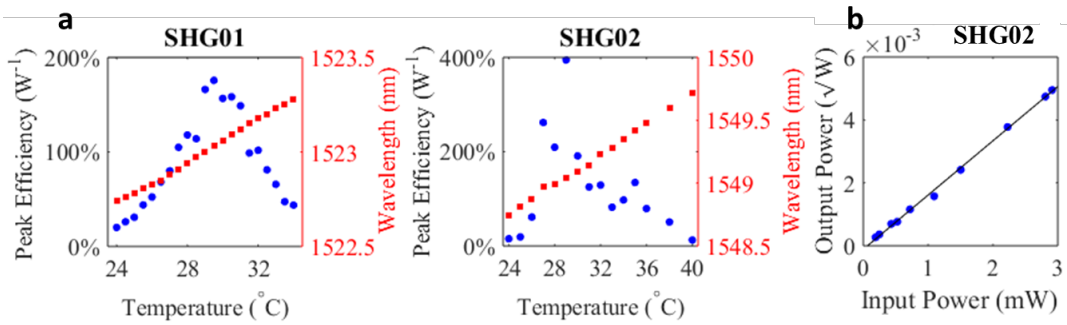
Schottky plots of ϕ_{thres} versus $\xi^{1/2}$ for (a) negative bias IPE (emission from Al interface) and (b) positive bias (emission from ZrCuAlNi interface). Resulting energy band diagrams of all devices based on IPE barrier heights measured in this work.

Melanie Jenkins, Tyler Klarr, Dustin Austin, Wei Li, Nhan Nguyen, and John Conley, School of Electrical Engineering and Computer Science, Oregon State University. Work performed at OSU's Materials Synthesis and Characterization Facility.

This work was supported by NSF Award # ECCS-1542101. *Physica Status Solidi-Rapid Research Letters* 12, 1700437 (2018).

400%/W Second Harmonic Conversion Efficiency in 14 μ m-diameter GaP-on-oxide Resonators

The Majumdar and Fu groups at the UW investigate second harmonic conversion from 1550 nm to 775 nm and show an efficiency of 400% W^{-1} in a gallium phosphide (GaP) on oxide integrated photonic platform. The platform consists of doubly-resonant, phase-matched ring resonators with quality factors $Q \sim 10^4$, low mode volumes $V \sim 30(\lambda/n)^3$, and high nonlinear mode overlaps. Measurements and simulations indicate that conversion efficiencies can be increased by a factor of 20 by improving the waveguide-cavity coupling to achieve critical coupling in current devices.



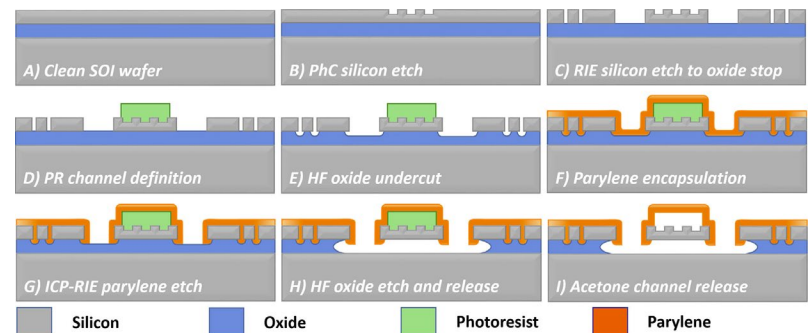
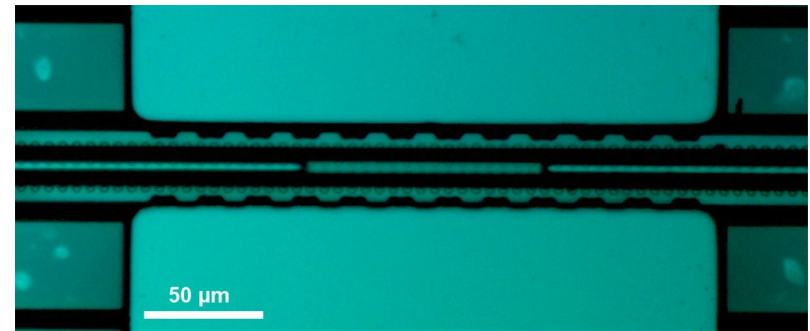
(Top) A 14 μ m GaP-on-oxide resonator.
(Left, a) Maximum conversion efficiency as a function of temperature for two resonators.
(Left, b) Second harmonic output power as a function of input power.

Alan D. Logan, Michael Gould, Arka Majumdar, and Kai-Mei Fu, Department of Electrical and Computer Engineering, University of Washington. Emma Schmidgall, Department of Physics, University of Washington. Karine Hestroffer and Fariba Hatami, Department of Physics, Humboldt University of Berlin. Zin Lin, Weiliang Jin, and Alejandro W. Rodriguez, Department of Electrical Engineering, Princeton University. Work performed at the Washington Nanofabrication Facility.

This work was supported by NSF Award # EFMA-1640986 and #DMR-1454836. Results will be published as Logan et al. in *Optics Express* (manuscript in press, 2018).

High-accuracy MEMS Mass Sensor with Integrated Optical Trapping

The Lin Group investigates optical manipulation of particles in fluid as a viable method to achieve better experimental fidelity and extend the application of integrated-fluidic resonant-mass sensing. Fluctuations in sample position or trajectory can lead to measurement error, thereby degrading the resolution with which these devices can accurately characterize mass. Optical trapping offers precise location control in such fluidic environments and can define and fix position within the channel to mitigate such variability, but requires a novel approach to design, fabrication, and biological viability concerns. This work details specific design and fabrication considerations embodied by unique devices that demonstrate compatibility with optical trapping and mass sensing utilizing photonic crystal (PhC) nanostructures. The effect of optical trapping on the enhancement of mass-sensing accuracy is demonstrated.



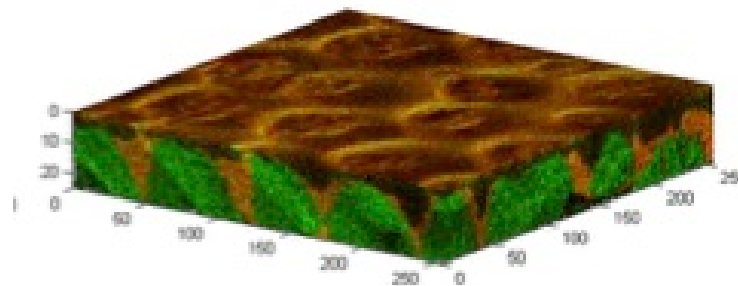
(Top) MEMS bridge resonator with an integrated parylene fluidic channel (guiding fluid) and the underlying PhC.
(Bottom) Fabrication process.

Ethan G. Keeler, Peifeng Jing, Chen Zou, and Lih Y. Lin, Department of Electrical and Computer Engineering, University of Washington. Work performed at the Washington Nanofabrication Facility (WNF).

This work was supported by NSF Award # DBI-1353718 and GRFP DGE-1256082.
IEEE Transaction on Nanotechnology 17(4): 714-718 (2018)

Dealing with Image Shifting in 3D ToF-SIMS Depth Profiles

The Gamble Group examines the high sputter efficiency and low damage of gas cluster ion beams that enable depth profiling to greater depths within organic samples using time-of-flight secondary ion mass spectrometry (ToF-SIMS). Due to the typically fixed geometry of the ion sources used in ToF-SIMS, as one digs into a surface, the position sampled by ion beams shifts laterally. This causes a lateral shift in the resulting images that can become quite significant when profiling down more than one micron. In this work, three methods to compensate for this image shift are presented in order to more accurately stack the images to present a 3D representation. Using these methods, features from spherical objects that were ellipsoidal prior to shifting were seen to be spherical after correction. A combination of hardware and software shift correction can enable correction for a wide range of samples and profiling depths. The scripts required for the software shifting demonstrated in this work are provided along with tutorials in the supplementary material of the recent publication.



ToF-SIMS 3D depth profile data from PHEMA filled with OCT. RG overlays shows PHEMA in Red ($m/z = 19$ (H_3O^+), 45 ($C_2H_5O^+$), 58 ($C_3H_6O^+$)) and OCT in Green ($m/z = 29$ ($C_2H_5^+$), 69 ($C_4H_5O^+$), 87 ($C_4H_7O_2^+$)) for the shifted data. Image is 200 micron \times 200 micron \times ~25 micron at 256 pixels \times 256 pixels per layer.

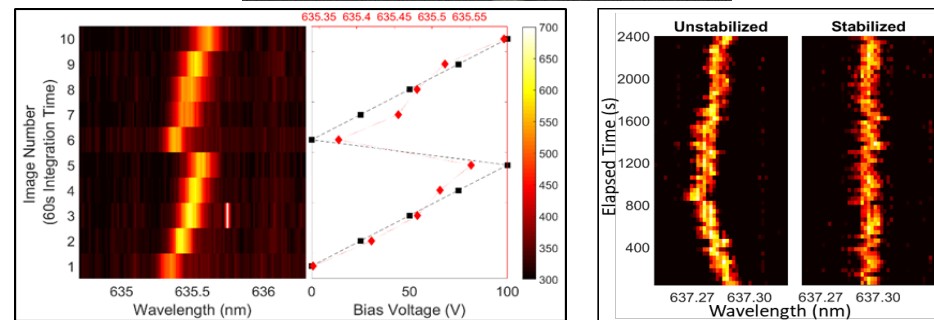
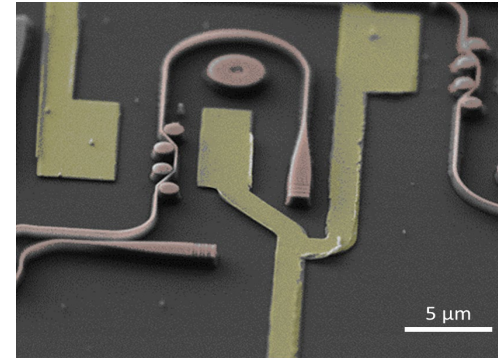
Dan J. Graham and Lara J. Gamble, Bioengineering, University of Washington. Work performed at the UW MAF.

This work was supported by NSF Award # ECCS-123456.

D. J. Graham and L. J. Gamble, *Biointerphases* 2018, 13 (6) 06E402.

Frequency Control of Single Quantum Emitters in Integrated Photonic Circuits

The Fu Group at UW is generating entangled graph states of qubits requiring high entanglement rates with efficient detection of multiple indistinguishable photons from separate qubits. Integrating defect-based qubits into photonic devices results in an enhanced photon collection efficiency, however, typically at the cost of a reduced defect emission energy homogeneity. We demonstrated that the reduction in defect homogeneity in an integrated device can be partially offset by electric field tuning. Using photonic device-coupled implanted nitrogen vacancy (NV) centers in a GaP-on-diamond platform, we demonstrate large field-dependent tuning ranges and partial stabilization of defect emission energies. These results address some of the challenges of chip-scale entanglement generation.



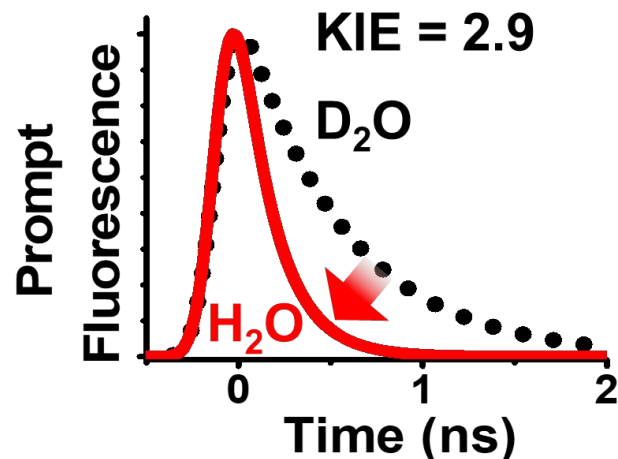
(Top) The integrated device. (Left) Demonstration of a large field-dependent tuning range. (Right) Demonstration of emission energy stabilization.

Emma R. Schmidgall, Srivatsa Chakravarthi, Michael Gould, Ian Christen, and Kai-Mei C. Fu, Department of Physics, University of Washington. Karine Hestroffer and Fariba Hatami, Department of Physics, Humboldt University of Berlin. Work performed at the Washington Nanofabrication Facility.

This work was supported by NSF Award # ECCS-1506473 and DARPA Award #W31P4Q-15-1-0010. Schmidgall et al. *Nano Letters* **18**, 1175-1179 (2018).

Proton-coupled Electron Transfer in a Model Heptazine-based Photocatalyst

To gain mechanistic understanding of metal-free photochemistry, we synthesized and studied triisole-heptazine (TAHz), a model molecular photocatalyst chemically related to carbon nitride. Based on time-resolved photoluminescence (TR-PL) spectroscopy, the Schlenker Group kinetically reveals a new feature that emerges in aqueous dispersions. Using global target analysis, we spectrally and kinetically resolve the new emission feature to be blueshifted from the steady state luminescence, and observe a fast decay component exhibiting a kinetic isotope effect (KIE) of 2.9 in H_2O versus D_2O , not observed on longer timescales. The KIE suggests excited state is quenching by proton-coupled electron transfer, liberating hydroxyl radicals that we detect using terephthalic acid. Our findings are consistent with recent theoretical predictions that heptazine-based photocatalysts can participate in proton-coupled electron transfer with H_2O .



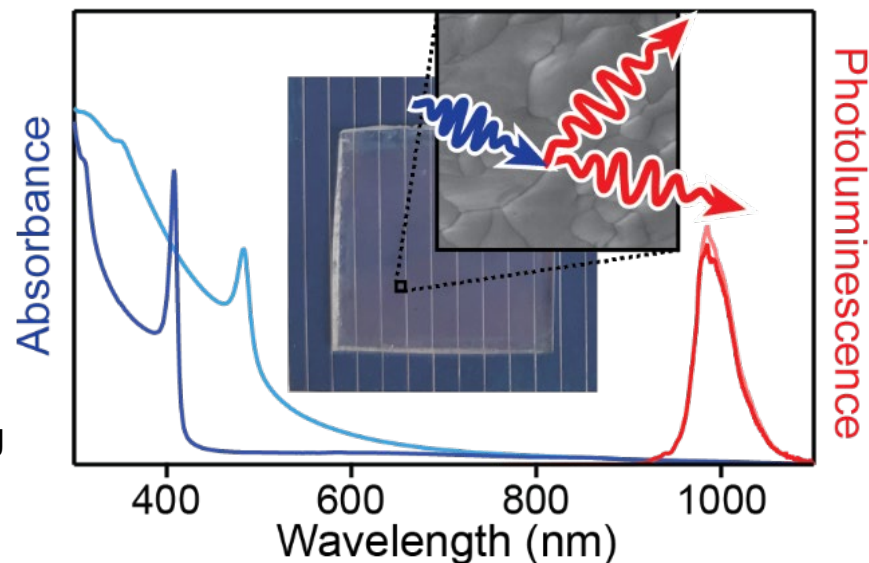
Decay components of TAHz emission in H_2O versus D_2O show a significant kinetic isotope effect (KIE) on the pico- to nanosecond timescale. This provided the first spectroscopic evidence for proton-coupled electron transfer driven by heptazine.

Emily Rabe¹, Katie Corp¹, Andrzej Sobolewski², Wolfgang Domcke³, Cody Schlenker.¹ ¹Department of Chemistry, University of Washington, ²Institute of Physics, Polish Academy of Sciences, ³Department of Chemistry, Technical University of Munich

This work was supported by NSF Award # NNCI-1542101.
J. Phys. Chem. Lett. **2018**, *9*, 6257-6261.

Quantum-cutting Ytterbium-doped $\text{CsPb}(\text{Cl}_{1-x}\text{Br}_x)_3$ Perovskite Thin Films with Photoluminescence Quantum Yields over 190%

The Gamelin Group at UW utilizes a two-step solution-deposition method for preparing ytterbium-doped (Yb^{3+}) $\text{CsPb}(\text{Cl}_{1-x}\text{Br}_x)_3$ perovskite thin films. Yb^{3+} -doped $\text{CsPb}(\text{Cl}_{1-x}\text{Br}_x)_3$ films are made that exhibit intense near-infrared photoluminescence with extremely high quantum yields reaching over 190%, stemming from efficient quantum cutting that generates two emitted near-infrared photons for each absorbed visible photon. The near-infrared Yb^{3+} $f-f$ photoluminescence is largely independent of the anion content (x) in $\text{CsPb}(\text{Cl}_{1-x}\text{Br}_x)_3$ films with energy gaps above the quantum-cutting threshold of twice the Yb^{3+} $f-f$ transition energy, but it decreases abruptly when the perovskite energy gap becomes too small to generate two Yb^{3+} excitations. Excitation power dependence measurements show facile saturation of the Yb^{3+} luminescence intensity, identifying a major challenge for future solar applications of these materials.



Absorbance spectra (blue) and photoluminescence spectra (red) of ytterbium-doped $\text{CsPb}(\text{Cl}_{1-x}\text{Br}_x)_3$ perovskite thin films. Inset shows an optical and scanning electron microscope image of a perovskite thin film.

Daniel M. Kroupa, Joo Yeon Roh, Tyler J. Milstein, Sidney E. Creutz, and Daniel R. Gamelin, Department of Chemistry, University of Washington. Work performed at University of Washington's Molecular Analysis Facility.

This work was supported by NSF Award # ECC-1542101. *ACS Energy Letters*. 2018, 3, 2390-2395.

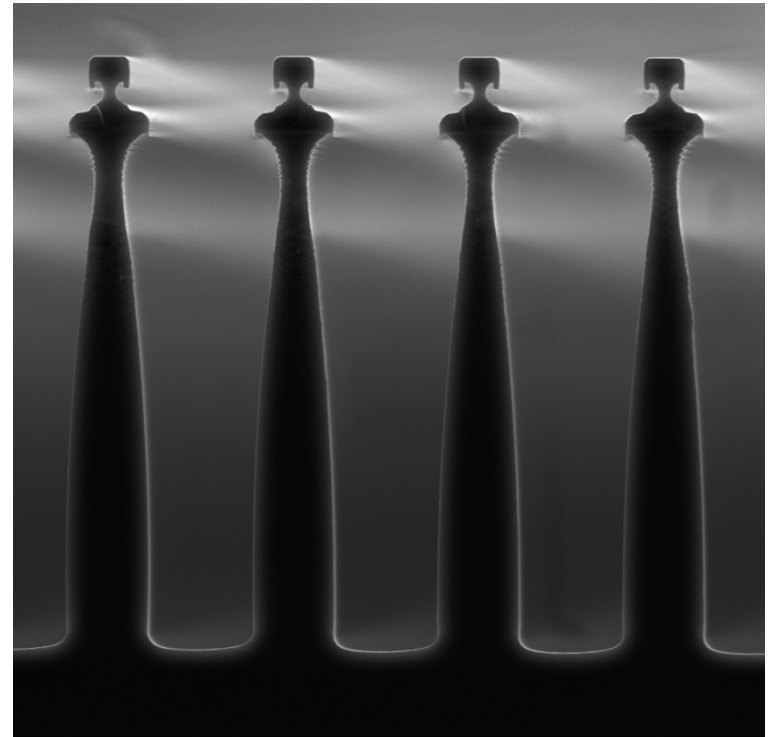
Enhanced Electron Collection in Advanced Thermionic Generators

Modern Electron is an energy technology startup based in the Seattle area. Our mission is to generate affordable, scalable, and reliable electricity via direct heat-to-electricity generation with advanced thermionic energy converters.

We have used the **WNF** consistently for three years, and currently have four and a half full time users at the facility.

We use microfabrication techniques to build electrodes for thermionic converters that draw electrons across a vacuum gap and funnel them into an anode.

The image to the right shows grids electrically isolated from one another on top of silicon anodes. The prototypes were entirely fabricated in the UW WNF cleanroom.



SEM micrograph showing the collector of an advanced thermionic generator, with electrostatic grids.

Jason Parker, Mark Stone, Gary Foley, Amy Chiu, Andrew Lingley, Max Mankin, Tony Pan, and the rest of the Modern Electron team.

Work performed at the Washington Nanofabrication Facility.

Research Triangle Nanotechnology Network (RTNN)

Nanofluidic Platforms for Analyzing Genomic DNA

Development of nanofluidic platforms for isolating large genomic DNA molecules and detecting structural variants in these molecules

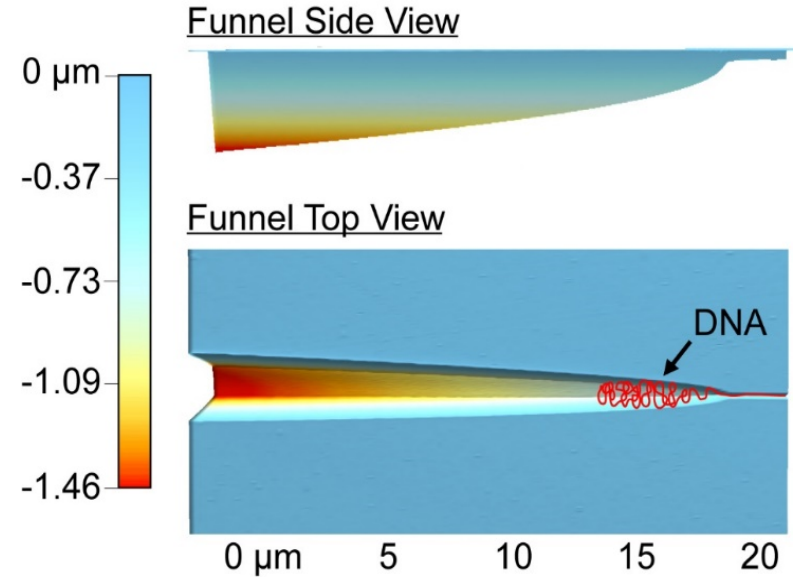
Three-dimensional nanofunnels gently introduce DNA molecules into nanochannels

Enzyme cuts molecules at sequence specific sites

Positions of cuts measured revealing

Long-range structure of the genome

Presence and identity of structural variants



AFM profiles of a FIB-synthesized three-dimensional nanochannel interfaced with a cartoon of DNA imposed on the top-view image

Jinsheng Zhou and Laurent Menard, Genturi Inc.

Work performed at UNC's Chapel Hill Analytical and Nanofabrication Laboratory

Supported by NIH Award #'s R01HG002647, P01-HL108808 and 1UH2HL123645; NSF Award #'s DMR-1309892, DMR-1436201, and DMR-1121107, and the Cystic Fibrosis Foundation.

Zhou, J. et al., *Nat. Commun.*, 8 (2017).

Dynamically Reconfigurable Active Thin Film Silicon Microparticles

Designed, fabricated, and powered millions of custom silicon microparticles, p-n junctions, and microdiodes

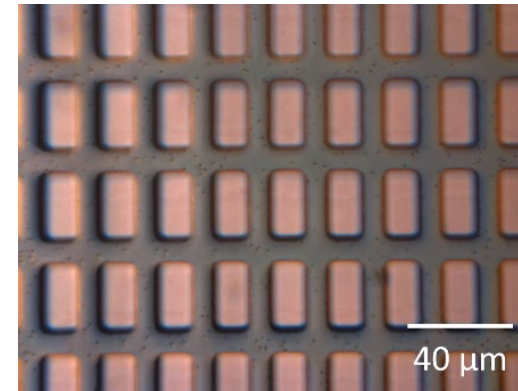
10 x 20 μm in surface area and 3.5 μm thick

100 times smaller than commercial devices

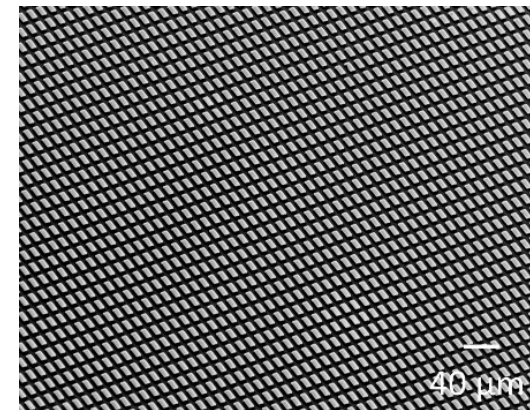
Microparticles fabricated from silicon-on-insulator (SOI) wafers

Active microparticles can dynamically assemble, disassemble, and reassemble on-demand when applying AC electric field gradients

Ugonna Ohiri and Nan Jokerst, Department of Electrical and Computer Engineering, Duke University & Orlin Velev, Department of Chemical and Biomolecular Engineering, NC State University.
Work performed at Duke's Shared Materials Instrumentation Facility
Work supported by NSF Award # DMR-1121107
Ohiri, U. et al., *Nat. Commun.*, 9 (2018).



Optical micrograph of etched monodisperse p-n junction silicon microparticles on SOI



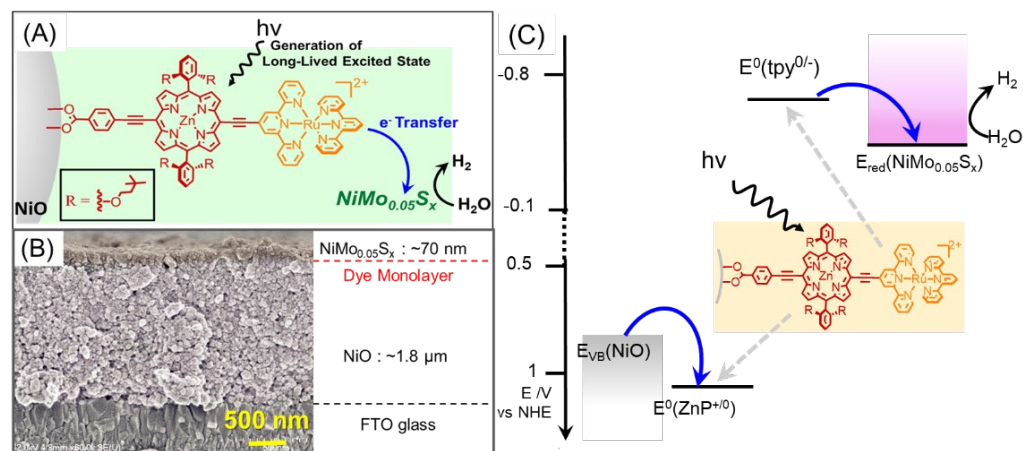
Scanning electron microscope image of etched monodisperse p-n junction silicon microparticles

Photoelectrocatalytic Water Splitting by an Integrated Dye-sensitized Photoelectrode

Dye-sensitized photoelectrodes combining surface-immobilized catalysts for water splitting or CO₂ reduction present strategy for solar fuel generation

New structure designed based on surface-bound chromophore that generates a long-lived, redox-separated state directly at its excited state for transferring electrons to an electrodeposited, hydrogen evolution catalyst and holes to a p-type electrode substrate

Photocathode shows enhanced photoelectrocatalytic performance



The structure (A) and cross-section scanning electron microscopic (SEM) image (B) of the photocathode (C) Energy diagram illustrating the light-induced electron transfer reactions in the photocathode

Bing Shan, Animesh Nayak, and Thomas Meyer, Department of Chemistry, UNC-Chapel Hill. Work performed at UNC's Chapel Hill Analytical and Nanofabrication Laboratory

Work supported by DOE Award #'s DE-SC0015739 and DE-SC0001011.

Shan, B. et al., *Energy Environ. Sci.*, 11 (2018).

Enhanced Endosomal Escape by Light-Fueled Liquid-Metal Transformer

New method to deliver drugs intracellularly

Nanospheres coated with graphene quantum dots (GQDs) absorb light to transform from nanospheres to hollow nanorods

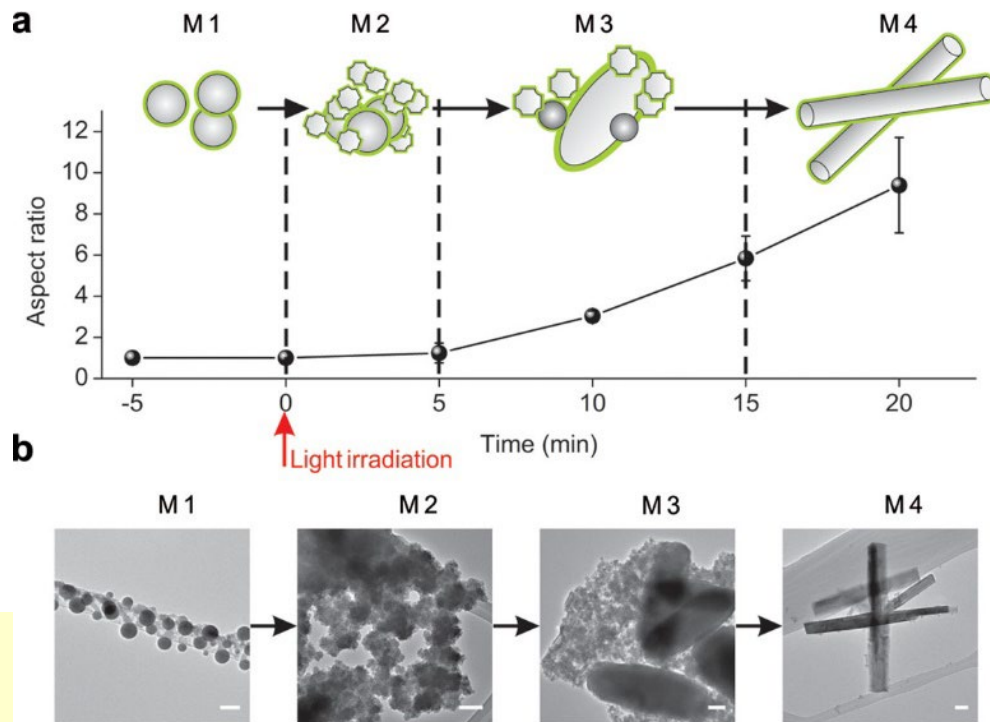
Swift change in shape disrupts the endosomal membrane and allows cargo to escape into the cell

Novel platform to achieve efficient, spatiotemporally-controlled drug delivery

Yue Lu and Zhen Gao, Joint Department of Biomedical Engineering, NC State University and UNC-Chapel Hill. Work performed at NC State's Analytical Instrumentation Facility

Work supported by NSF Award # DMR-1121107

Lu, Y., et al., *Nano Lett.*, 17 (2017).



- GQD-coated nanospheres change transform to rod shape upon light irradiation
- Representative TEM images of nanoparticles before and after irradiation (Scale bar = 100 nm)

Detection of Pathogen RNA using an Integrated Lab-in-a-Stick Device and Nanorattles

Nanorattles detect biomarkers in body fluids without target amplification

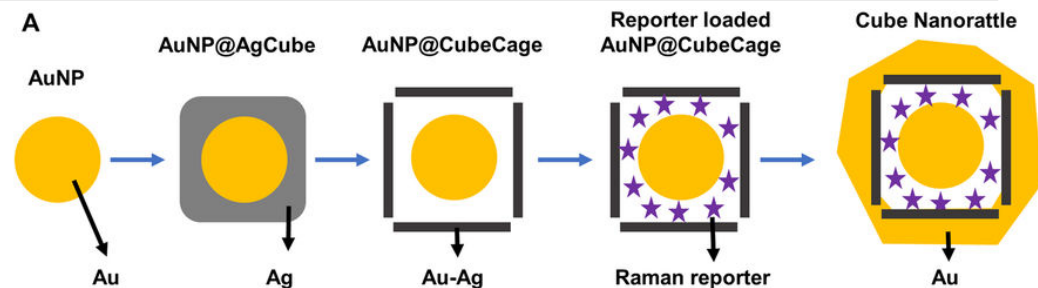
Bioassay developed that uses surface-enhanced Raman spectroscopy (SERS)-based detection integrated in a “lab-in-a-stick” portable device

Signal amplified in two ways:

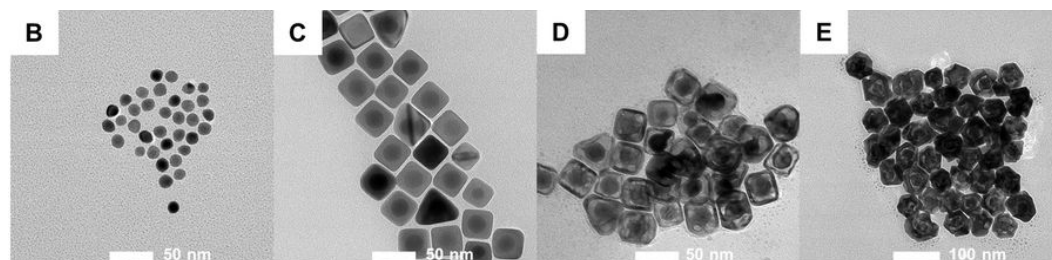
Target RNA sequence tagged with SERS-encoded nanorattle with ultrahigh SERS signals

Tagged sequences concentrated with magnetic microbeads

Detect malaria parasite RNA in infected red blood cells lysate: first time reported without nucleic acid extraction or target amplification



A. Cubic nanorattle synthesis process.



TEM images

B. AuNP

C. AuNP@AgCube

D. Reporter loaded

AuNP@CubeCage

E. Cube nanorattles

Hoan Ngo and Tuan Vo-Dinh, Department of Biomedical Engineering, Duke University. Work performed at Duke's Shared Materials Instrumentation Facility

Work supported by NIH Award #s R21 AI120981-01 and K08AI100924 and the Duke Faculty Exploratory Research Fund.

Ngo, HT, et al., *Sci. Rep.*, 8 (2018).

Size and Composition Control of CoNi Nanoparticles and Conversion into Phosphides

Mixed metal phosphide nanoparticles (NPs) studied for numerous uses including electrocatalysts for hydrogen evolution reactions and materials for Li-ion batteries

Optimized synthesis strategies needed to control and tailor the NP composition and structure

Binary CoNi NPs synthesized by heating mixtures of Ni(acetylacetonate)₂ and Co(acetylacetonate)₂, oleylamine, trioctylphosphine, and trioctylphosphine oxide

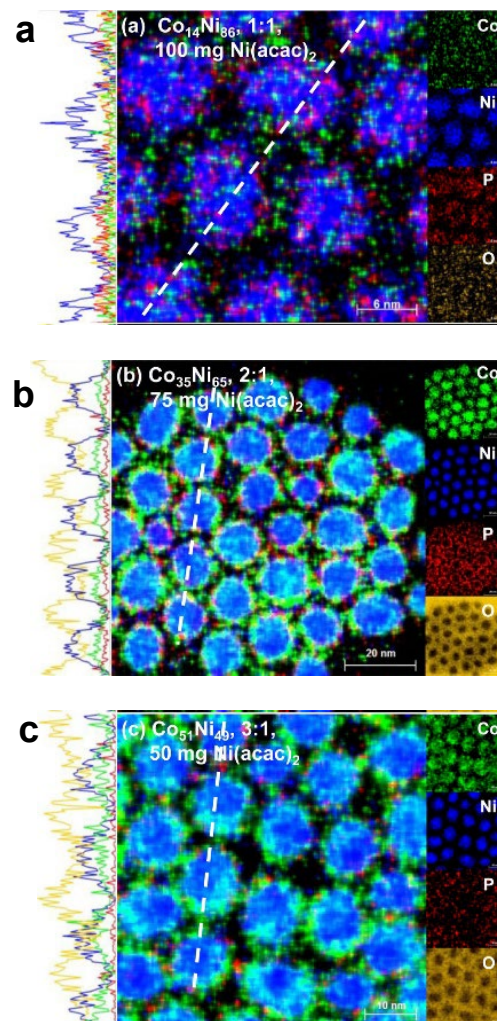
Resulting NPs are enriched with Ni; Co localizes to the NP shells

Synthesis at 300°C formed Co-enriched branched NPs

Kate Marusak and Joe Tracy, Department of Materials Science and Engineering, NC State University. Work performed at NC State's Analytical Instrumentation Facility

Work supported by NSF Award # DMR-1056653

Marusak, K. et al., *Chem. Mater.*, 29 (2017).



EDS maps of three samples of similar sizes and different compositions (Co:Ni precursor mass ratios of a. 1:1, b. 2:1, and c. 3:1)

*Left: line scans
Center: composite EDS maps (excluding oxygen)
Right: EDS maps over the same region from which the composite images were composed.*

Thermoelectric Generators for Self-Powered Wearable Health Monitoring Systems

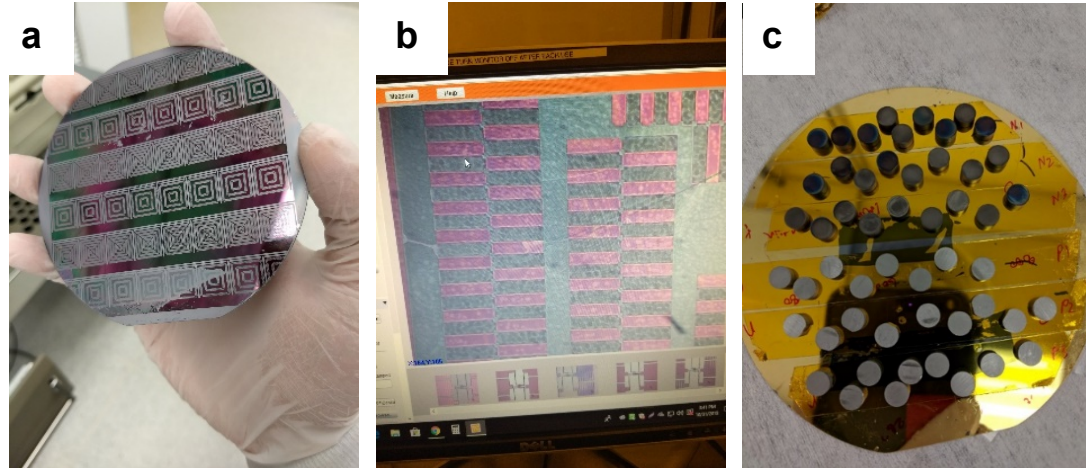
Objective: develop CMOS compatible, wafer-scale microfabrication process that relies on mature processes and techniques used in MEMS integration

Novel device structure enables high-efficiency thin-film thermoelectric devices

Power generation from small temperature gradients

Several thousands of micro-scale elements can generate >1000x larger voltage than conventional devices

Provisional patent application recently filed for this technology



- Thermoelectric rings post spin-on doping process*
- Microscopic view of the n and p legs before metallization*
- Thermoelectric wafers mounted for the sputtering step.*

Abhishek Malhotra, Prithu Bhatnagar, and Daryoosh Vashae, Department of Electrical and Computer Engineering, NC State University. Work performed at NC State's Nanofabrication Facility

Work supported by the National Science Foundation (NSF) Award #'s EEC-1160483 and ECCS-1351533.

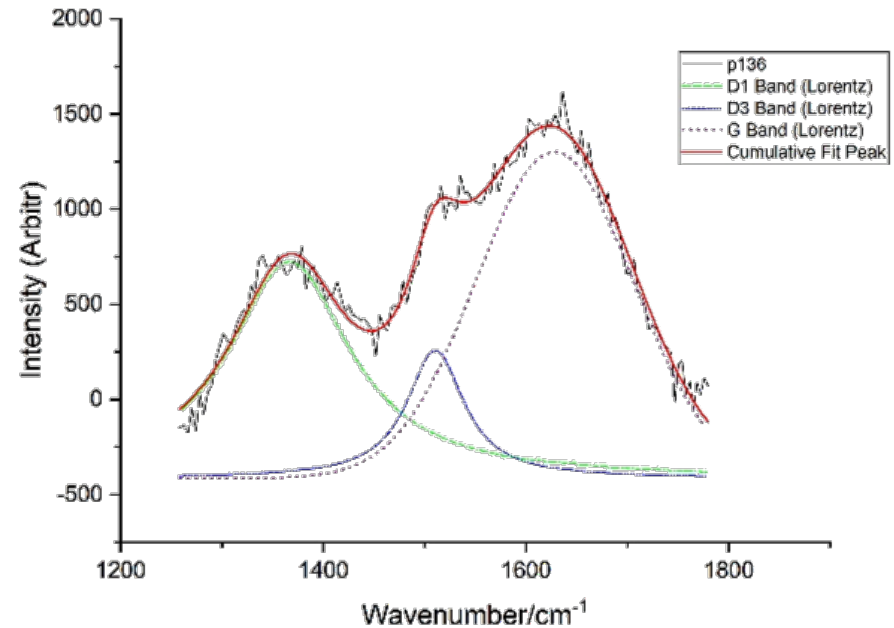
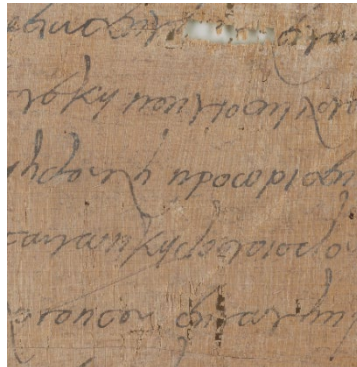
Study of Ancient Carbon-Based Ink in Greek Papyri through Micro-Raman Spectroscopy

Investigating non-destructive means to identify material components of carbon-based inks used on ancient papyrus

Data used to identify anachronistic composition of ink for authentication and date ink

Initial tests comparing a modern mock-up papyrus with a sixth-century Greek papyrus have provided a starting point for further investigation

Detail of P. Duke Inv. 1377 (GA 136), Greek text written in a chancery hand



Raman spectra for the carbon ink of the manuscript presented in a three-peak plot, where the D-band peaks represent disordered carbon and the G band represents hexagonal graphite

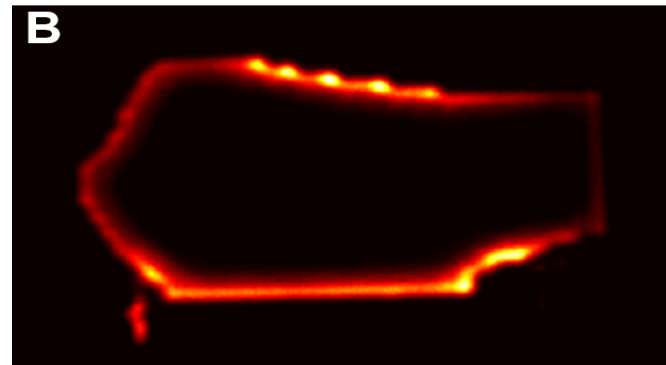
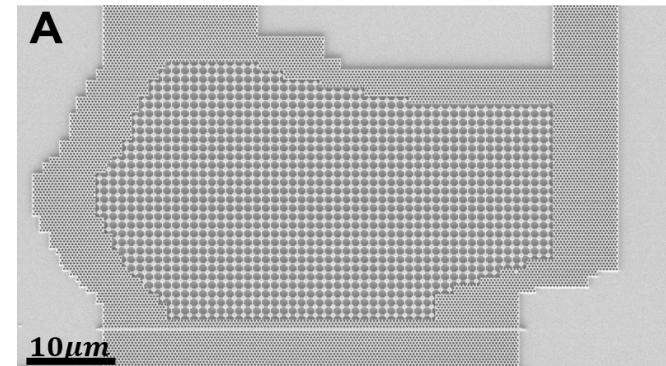
W. Andrew Smith and Valerie Smith, Shepherds Theological Seminary. Work performed at Duke's Shared Materials Instrumentation Facility

Work supported by RTNN's Kickstarter Program (NSF Award # ECCS-1542015)

San Diego Nanotechnology Infrastructure (SDNI)

Topological Light Sources

The lack of self-protected laser necessitates using complex methods and bulky optical components to protect integrated laser from parasitic reflections. These reflections can lead to instabilities of emission or even irreversible damages in systems. Current sources mainly include an optical component known as an isolator before the optical output. Such components require precise alignment. We proposed and demonstrated for the first topological cavities and lasers that are single mode and non-reciprocally couple light to selected waveguide outputs. The laser thus does not need isolators. Furthermore, the cavity can have arbitrary shapes and maintain its properties. The proposed platform opens novel perspectives in integrated photonics, in which, information can robustly flow between sectors characterized by different topological indices.



A. Top-view SEM of a fabricated arbitrarily shaped topological cavity with a geometry approximating a flipped USA-like map.

B. Real space image of the lasing of the edge mode when the entire structure is optically pumped from the top.

B. Bahari, A. Ndao, F. Vallini, A. El Amili, Y. Fainman, B. Kanté, Department of Electrical and Computer Engineering, University of California-San Diego. Work performed at University California-San Diego

This work was supported by NSF Award # ECCS-123456.

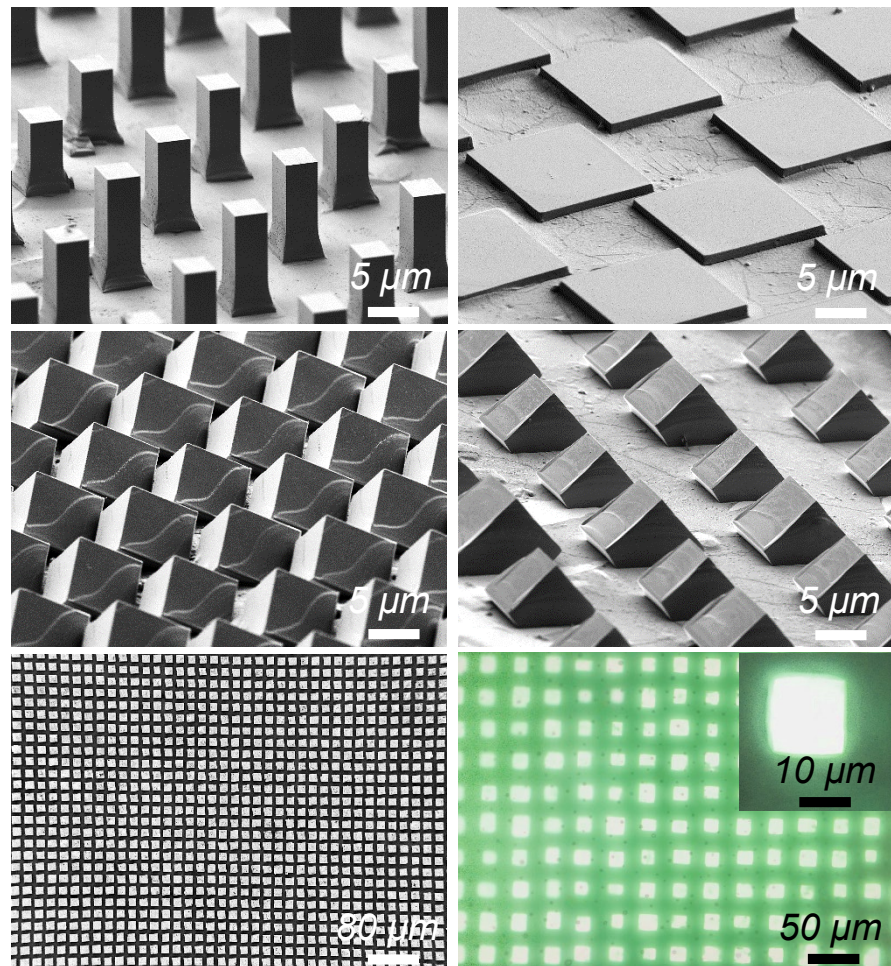
B. Bahari et al., *Science* 358, 636-640 (2017).

Controlled Homo-Epitaxy Growth of Hybrid Halide Perovskites (HHPs)

Organic–inorganic hybrid perovskites have demonstrated tremendous potential for the next-generation electronic and optoelectronic devices due to their remarkable carrier dynamics. Current studies are focusing on polycrystals, since controlled growth of device compatible single crystals is extremely challenging. In this work, the first chemical epitaxial growth of single crystal $\text{CH}_3\text{NH}_3\text{PbBr}_3$ with controlled locations, morphologies, and orientations, using combined strategies of advanced microfabrication, homoepitaxy, and low temperature solution method is reported. The growth is found to follow a layer-by-layer model. A light emitting diode array, with each $\text{CH}_3\text{NH}_3\text{PbBr}_3$ crystal as a single pixel, with enhanced quantum efficiencies than its polycrystalline counterparts is demonstrated.

Yusheng Lei, Yimu Chen, and Sheng Xu, Department of Nanoengineering, University of California-San Diego. Work performed at the San Diego Nanotechnology Infrastructure.

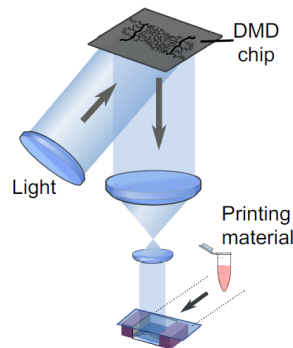
This work was supported by the UCSD startup fund.
Advanced Materials 30 (20), 1705992



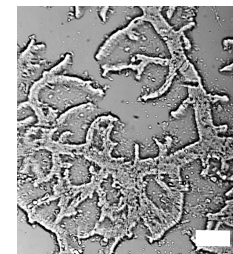
SEM micrographs of single crystalline HHPs in different morphologies and orientations, and photograph of working light emitting diode.

Scanningless and Continuous 3D Bioprinting of Human Tissues

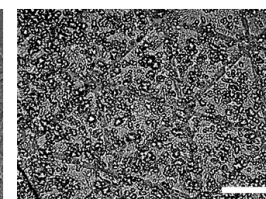
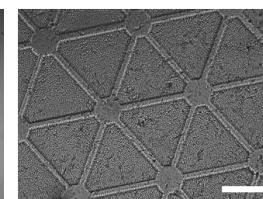
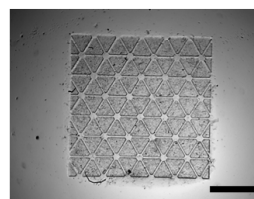
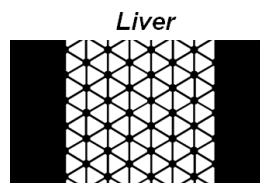
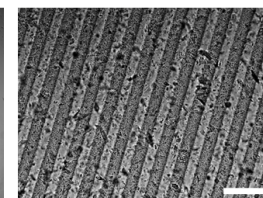
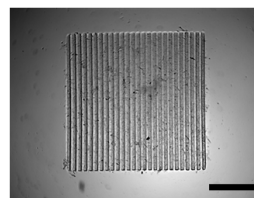
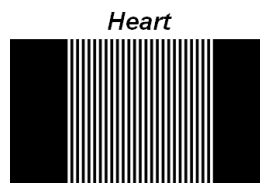
This work presents a (DLP)-based scanningless and continuous 3D bioprinting method to rapidly 3D print photocrosslinkable bioinks made of decellularized extracellular matrix (dECM). Biomimetically patterned heart and liver tissues were demonstrated using human induced pluripotent stem cells (hiPSCs)-derived cardiomyocytes and hepatocytes. The high control over detailed complex microscale tissue architecture as well as tunable mechanical properties achieved with our approach facilitated proper cellular morphology and function. Such engineered human tissue models could be used for drug screening, personalized medicine, and the elucidation of disease mechanisms.



Scale bar =
500 μ m



Scale bar =
250 μ m

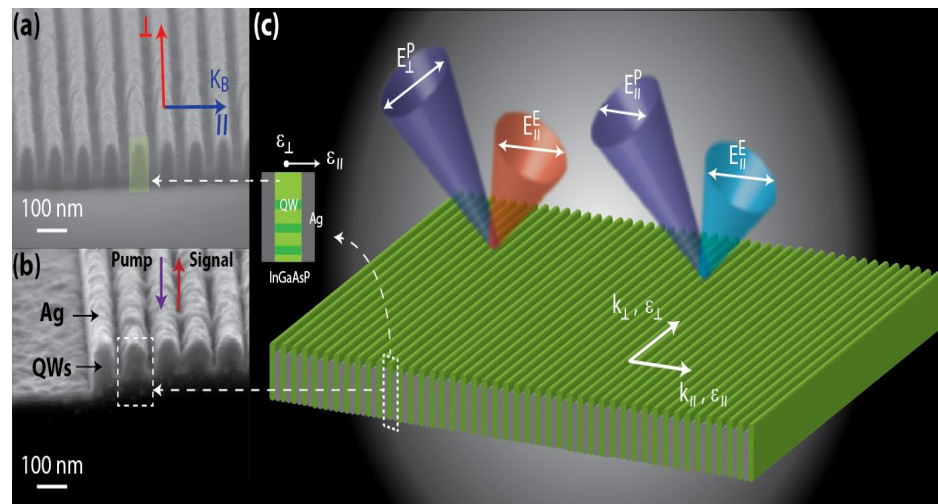


C. Yu, X. Ma, W. Zhu, P. Wang, K. Miller, J. Stupin, A. Koroleva-Maharajh, A. Hairadedian, S. C. Chen, Nanoengineering, UCSD. Work performed at SDNI.

This work was supported by an NIH RO1 grant.
Biomaterials, 194, 1-13, 2019

Luminescent Hyperbolic Metasurfaces

This work targets to achieve hyperbolic metasurfaces by combining the properties of hyperbolic dispersion with the potential for chip-scale integration offered by planar metasurfaces. While studies have proposed using gain to offset losses, bulk hyperbolic metamaterials (HMM) have incorporated light emitters only in addition to their constituent metallic and dielectric components. Herein, we demonstrate luminescent hyperbolic metasurfaces (LuHMS), in which semiconductor quantum heterostructures, distributed within the entire HMM, simultaneously function as light-emitters and the constituent dielectric. The unique design of the LuHMS maximizes light-matter interactions and enables verification of broadband hyperbolic dispersion by extreme polarization anisotropy of photoluminescence.



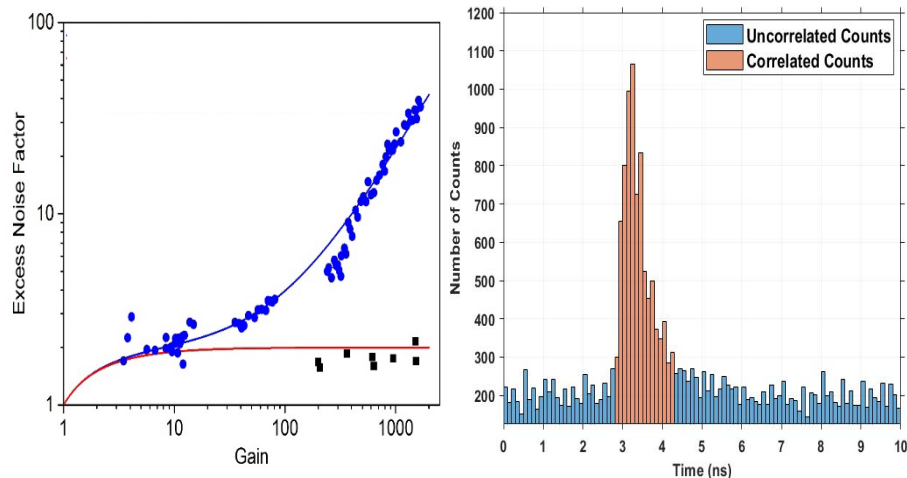
Luminescent hyperbolic metasurface (LuHMS) based on nanostructured Ag/InGaAsP MQW: (a) InGaAsP MQW pillars of 100 nm height and 40 nm width, separated by 40 nm trenches, defined by E-beam lithography and RIE. (b) Ag is deposited to create a multilayer LuHMS with 80 nm period. (c) Optical pumping of the LuHMS results in emission polarized parallel to the metacrystal Bloch vector, K_B . The wavelength of peak emission and PL intensity depend strongly on pump polarization. PL spectra of the LuHMS differ significantly from that of control MQW, regardless of pump polarization.

J. S. T. Smalley, F. Vallini, S. Montoya, L. Ferrari, S. Shahin, C. T. Riley, B. Kanté, E. E. Fullerton, Z. Liu and Y. Fainman
Department of ECE, University of California San Diego. Work performed at San Diego Nanotechnology Infrastructure.

This work was supported by NSF Award # ECCS-1542148.
Nature Communications 7, 13793 (2017).

Single Photon Detector with a Mesoscopic Cycling Excitation Design

Conventional semiconductor single photon detectors are Geiger-mode avalanche photodiodes made of high-quality crystalline semiconductors and require external quenching circuits. Here we report a design of single photon detector having dual gain sections to obtain mesoscopic cycling excitation and an amorphous/crystalline heterointerface to form an electron transport barrier that suppresses gain fluctuations. At 100 MHz, the device shows single photon detection efficiency greater than 11%, self-recovery time of less than 1ns at an average gain as high as 75,000 under 8.5V bias. The device concept and technology offer a promising direction for solid-state single photon detectors for applications that benefit from very high optical sensitivity down to the level of single photons.



Left: Excess noise factor dependence on gain. The measured excess noise factor of the device (black) is orders of magnitude lower than the state-of-the-art APD (blue dots).

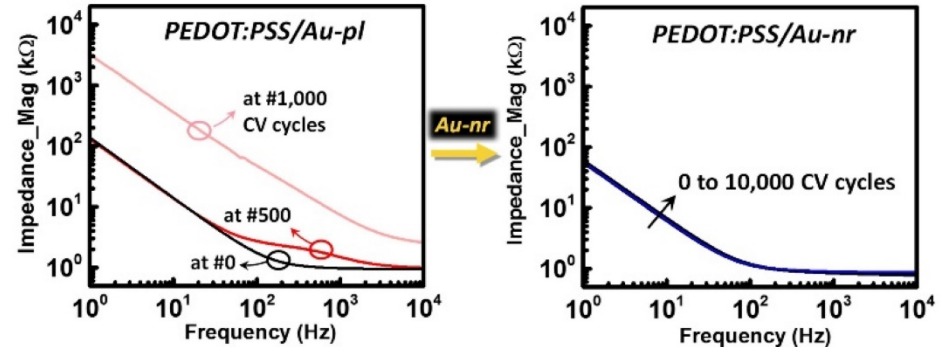
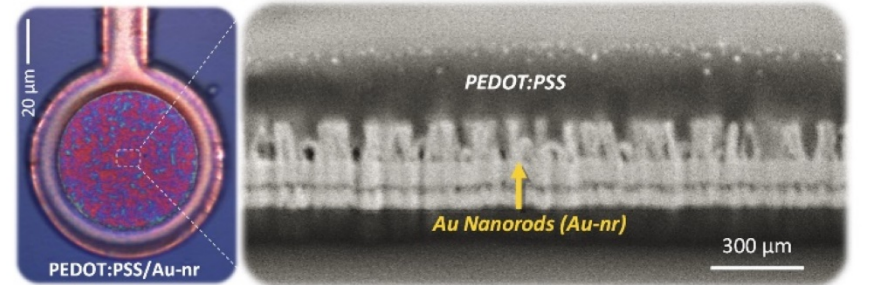
Right: Time-correlated photon counting histograms. The orange counts represent detector response to single photons at 100MHz.

Lujiang Yan, Yugang Yu, Alex Ce Zhang, David Hall, Iftikhar Ahmad Niaz, Mohammad Abu Raihan Miah, Yu-Hsin Liu, and Yu-Hwa Lo. Work performed at San Diego Nanotechnology Infrastructure

This work was supported by Office of Naval Research (N00014-18-1-2486), DARPA MTO (No. N00014-16-1-3206). *Appl. Phys. Lett.* 111, 101104 (2017)

Detection of Anti-IgG Using Cantilever-Type Resonant Microstructures

Poly (3,4-ethylenedioxythiophene) or PEDOT, is a promising candidate for next-generation neuronal electrode materials but its weak adhesion to underlying metallic conductors impedes its potential. We used an effective method of mechanically anchoring the PEDOT within a Au nanorod (Au-nr) structure and demonstrate that it provides enhanced adhesion and overall PEDOT layer stability permitting 10,000 CV cycles of coated PEDOT film in phosphate buffered saline solution without delamination (compared to 1,000 cycles on planar Au – see right panel), stability for 5 weeks of accelerated aging tests at 60 ° C (92% channel survival compared to only 25% survival on planar films), and stability after a 10-week chronic implantation onto mouse barrel cortex (no delamination compared to 100% partial or full delamination on planar films).



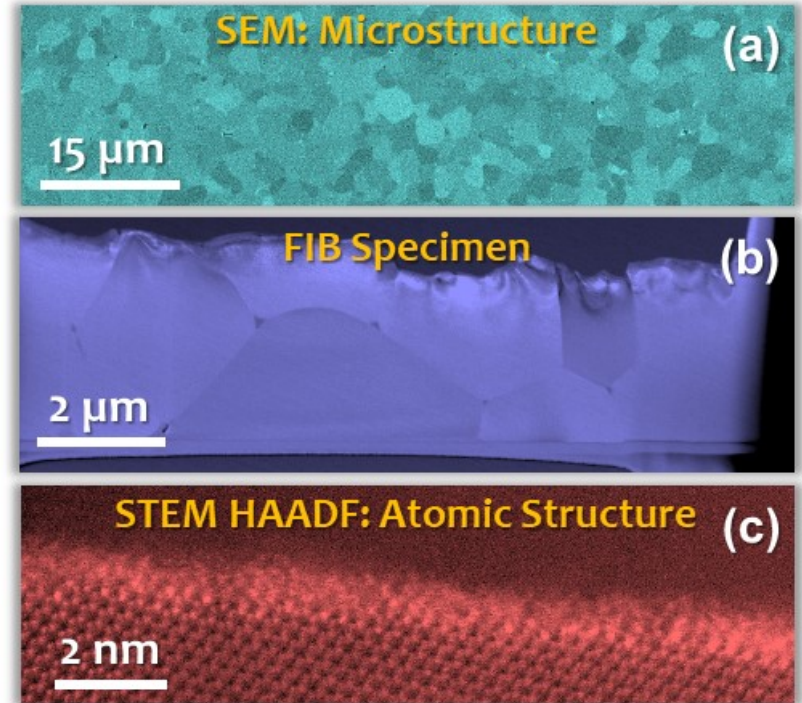
Top: Optical image and cross-sectional SEM image of PEDOT:PSS anchored in Au nanorods. This structure stabilizes PEDOT under cyclic voltammetry stress (bottom right, compared to planar, bottom left), accelerated aging, and in-vivo experiments.

Mehran Ganji, Lorraine Hossain, Atsunori Tanaka, Martin Thunemann, Eric Halgren, Anna Devor and Shadi A. Dayeh, Department of Electrical and Computer Engineering, UCSD. Work performed at the San Diego National Infrastructure.

This work was supported by NSF EAGER Award # ECCS- 1743694.
Adv. Healthcare Mater, 1800923, 2018.

Understand and Control Interfaces to Enable Innovative Ceramic Processing Using Electric Fields

This work aims to understand and control the effects of electric fields in innovative materials fabrication via altering the atomic-level interfacial (grain boundary) structures using ZnO as a model system. The FEI Scios DualBeam FIB/SEM system at Nano3 was used to prepare specimens. Such basic scientific research enabled by advanced tools available at the National Nanotechnology Coordinated Infrastructures such as Nano3 lead to the development of innovative, energy-saving, ceramic fabrication methods. For example, our prior work showed that an electric field plus water vapor can “flash” ZnO ($T_m = 1975^\circ\text{C}$) at room temperature to subsequently sinter it to ~98% density in 30 seconds, while the conventional sintering of ZnO takes place at $>1000^\circ\text{C}$ for hours. Our ongoing study with an example shown here further aims to understand the fundamental underlying mechanisms.

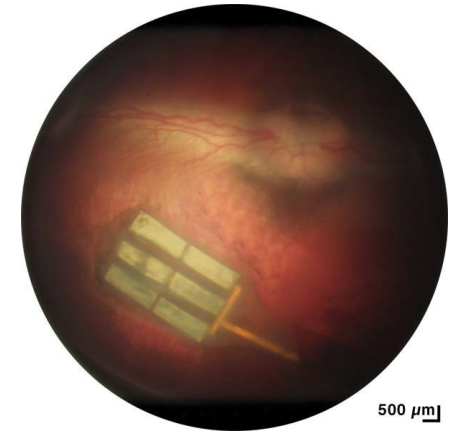
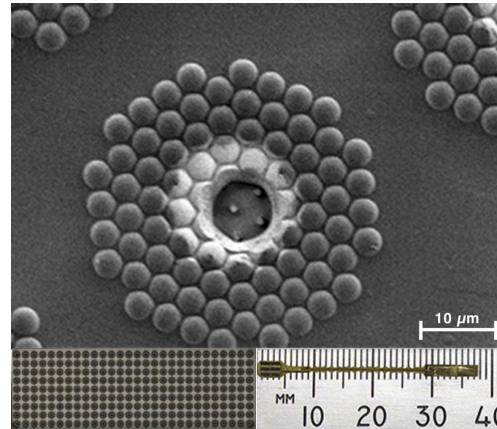


(a) SEM micrograph of the microstructure of a polycrystalline doped ZnO specimen fabricated with an applied electric current, (b) a FIB specimen prepared at Nano3, and (c) the atomic-level interfacial structure in STEM HAADF imaging.

Jiuyuan Nie and Jian Luo, Department of NanoEngineering, University of California, San Diego. This specimen was prepared at UCSD's Nano3 Analytical Lab.

In Vivo Photovoltaic Performance of a Silicon Nanowire Photodiode–Based Retinal Prosthesis

For more than 20 years, there has been an international, multidisciplinary effort to develop retinal prostheses to restore functional vision to patients blinded by retinal degeneration. We developed a novel subretinal prosthesis with 1512 optically addressed silicon nanowire photodiodes, which transduce incident light into an electrical stimulation of the remaining retinal circuitry. This study was conducted to evaluate the efficacy of optically driving the subretinal prosthesis to produce visual cortex activation via electrical stimulation of the retina. The results show that subretinal electrical stimulation with nanowire electrodes can elicit EEPs in the visual cortex, providing evidence for the viability of a subretinal nanowire prosthetic approach for vision restoration.



Left: The retinal prosthesis consists of six tiles on a polyimide substrate (bottom right). Each tile has 252 electrodes (bottom left). Each of the electrodes has 85 silicon nanowires capped with iridium oxide (top).

Right: Fundus photograph showing retina covering the six-tiled nanowire implant following surgical placement into the subretinal space.

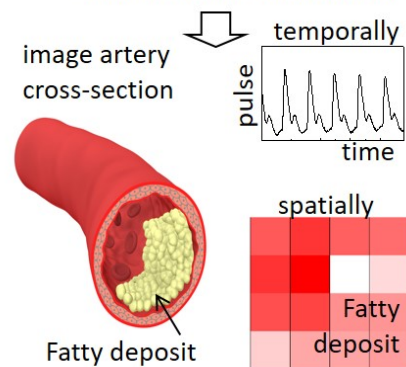
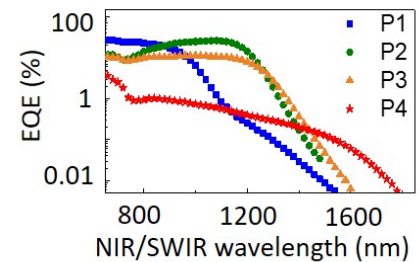
B. Bosse, S. Damle, A. Akinin, Yi Jing, Dirk-Uwe Bartsch, L. Cheng, N. Oesch, Y. Lo, G. Cauwenberghs, and W. R. Freeman. Nanovision Biosciences, University of California, San Diego. This device fabrication was performed at the San Diego National Infrastructure (SDNI) facilities.

Retina, iovs/937686/2018

Emerging Design and Characterization of Polymer-Based Infrared Photodetectors

Infrared photodetectors are essential to many applications including surveillance, communications, process monitoring, and biological imaging. The shortwave infrared spectral region (SWIR: 1-3 μm) is particularly powerful for health monitoring and medical diagnostics. Solution-processable semiconductors are being developed for infrared detectors to enable direct deposition and facilitate monolithic integration and resolution not achievable by using current technologies.

As progress is made towards overcoming challenges associated with losses due to recombination and increasing noise at progressively narrow bandgaps, the performance of organic SWIR photodetectors is steadily rising with detectivity exceeding 10^{11} Jones, comparable to commercial germanium photodiodes. The organic photodetectors are easily integrated within a wide range of portable systems as illustrated in the figure showing physiological monitoring applications.



(Top) External quantum efficiency versus wavelength of organic photodiodes. (Bottom) Potential applications of photoplethysmogram and tissue differentiation.

Zhengkui Wu, Weichuan Yao, Hyonwoong Kim, Yichen Zhai, Tse Nga Ng. Department of Electrical and Computer Engineering, University of California San Diego. Work performed at UCSD San Diego Nanotechnology Infrastructure.

This work was supported by NSF Award # ECCS-1839361.

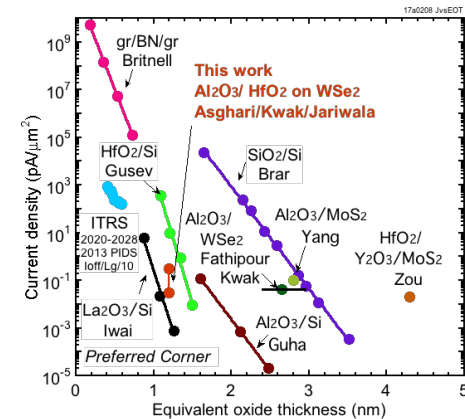
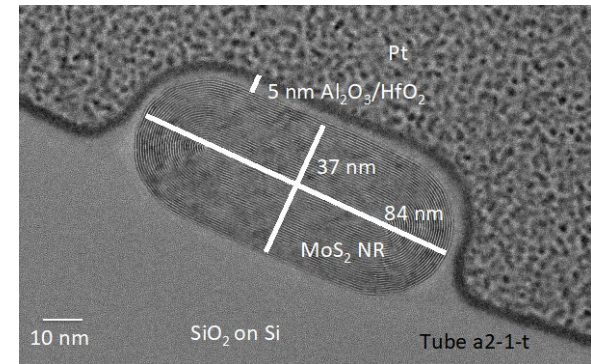
Acc. Chem. Res. 2018, 51,12, 3144-3153. *Adv. Func. Mater.* 2018, 28, 50, 1805738. *Adv. Func. Mater.* 2018, 28, 18, 1800391. *Adv. Optical Mater.* 2018, 6, 7, 1701138.

Nanofog for High K Gate oxides on 2D Materials

Background - Conventional ALD techniques usually result in poor quality oxides on 2D materials due to lack of dangling bonds. A ALD nucleation is needed which does not damage 2D materials.

- (a) Nanofog to nucleate ALD - Short Purge time (green) and long pulse time (blue and yellow) allow both TMA and H₂O to slightly intermix in the gas mixer. The nanofog is sprayed onto the sample which nucleates the ALD and a second higher K electric can then be deposited.
- (b) Bilayer gate oxide deposited on MoS₂ nanoribbons. Note conformality.
- (c) Benchmarking study of gate oxide scaling with nanofog + high T HfO₂ grown in Nano3

Next – New grant from TSMC joint with Prab Bandaru (UCSD) to apply to CNT transistors



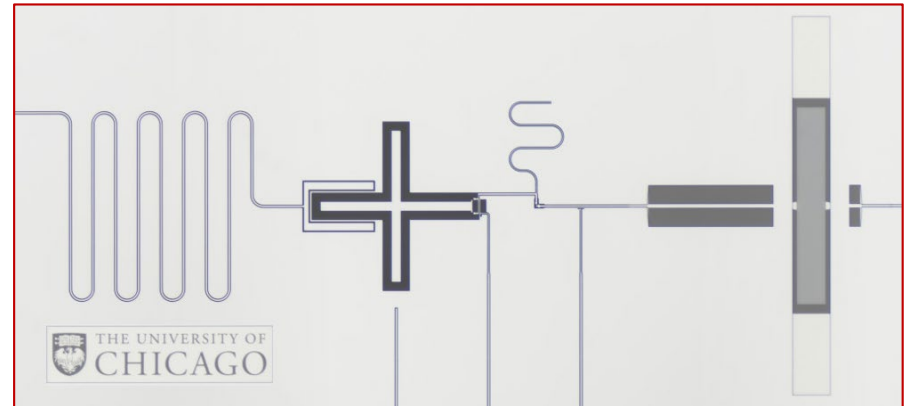
Iljo Kwak, Jun Hong Park, Larry Grissom, Bernd Fruhberger, Andrew C, Kummel, ECS Transactions **75 (5)** 143-151 (2016)
 Sara Fathipour, Paolo Paletti, Bhakti Jariwala, Jun Hong Park, Andrew Kummel, Joshua Robinson, Susan Fullerton-Shirey,
 and Alan Seabaugh, Proceeding of DRC 2018. Work performed at SDNI

The work was supported by SRC and TSMC.

Soft and Hybrid Nanotechnology Experimental (SHyNE) Resource

Quantum Control of Surface Acoustic Wave Phonons

This work demonstrates that a microfabricated assembly comprising a superconducting qubit and a surface acoustic wave resonator can be used to quantum-control, at the single phonon level, the surface acoustic wave excitations in the resonator. Lithographic patterning was used to pattern a superconducting qubit and a “variable coupler” on a low-loss sapphire substrate, and in parallel, a microwave frequency surface acoustic resonator patterned on a separate lithium niobite substrate. The two were assembled using a flip-chip process, and the whole operated on a cryostat at a temperature of 10 mK. The qubit afforded the ability for the controlled emission of single phonons, and the qubit then employed to probe the resulting quantum acoustic states.



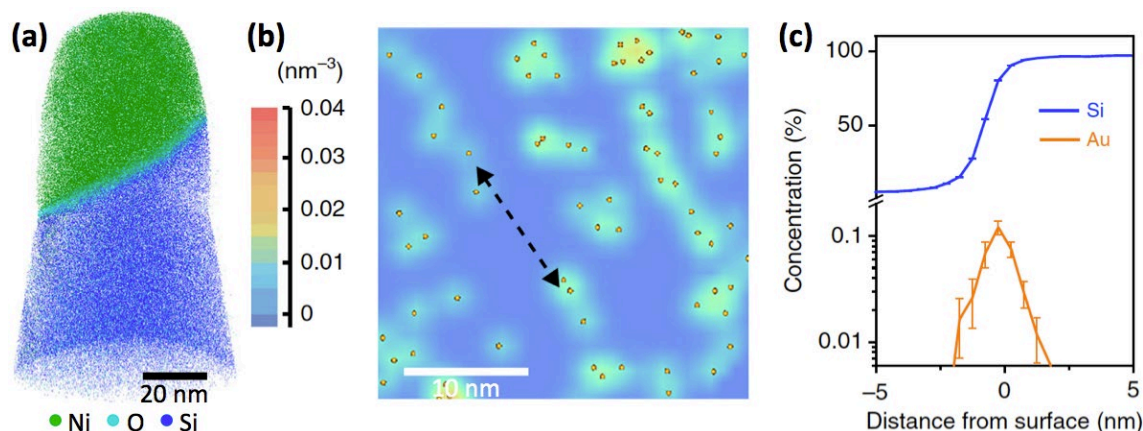
Optical micrograph of assembled device yielding quantum-controlled surface acoustic wave phonons. An xmon-style qubit (cross shaped structure on left) is connected through an electronically controlled coupler (center) to an acoustic cavity formed by an interdigitated transducer facing IDT mirrors on either side (right). The qubit structure is fabricated on a separate sapphire substrate from the IDT structure on a LiNbO₃ substrate, which is viewed looking through the transparent sapphire substrate. The two are assembled using a flip-chip technique. A similar device was used in the publication below.

K.J. Satzinger, Y.P. Zhong, H.-S. Chang, G.A. Peairs, A. Bienfait, M.-H. Chou, A.Y. Cleland, C.R. Conner, E. Dumur, J. Grebel, I. Gutierrez, B.H. November, R.G. Povey, S.J. Whiteley, D.D. Awschalom, D.I. Schuster, and A. N. Cleland, University of Chicago and Argonne National Laboratory.

Work supported by AFOSR, ARL, DOE, MRSEC and GRFP, ANL, Packard Foundation and NSF NNCI-1542205.
Nature **563**, 661–665 (2018).

3D Arrays of Atomic Gold Catalyst Imaged by Atom-Probe Tomography

Large-scale assembly of individual atoms over smooth surfaces is difficult to achieve. An atom reservoir, from which individual atoms can be readily extracted, may address this challenge. In this work, we demonstrate that a liquid gold–silicon alloy established in classical vapor–liquid–solid growth can deposit uniform patterns of isolated or small groups of gold atoms on the sidewalls of a silicon nanowire.



(a) 3D atom-by-atom atom-probe tomography (APT) reconstruction of a silicon nanowire sidewall surface region. Nickel capping is added for preparation. (b) 2D map of gold atomic density exhibiting a chain-like arrangement, indicated by a black dashed arrow. Orange spheres represent the positions of individual gold atoms. (c) Concentration profile of Si and Au in the direction normal to the nanowire surface.

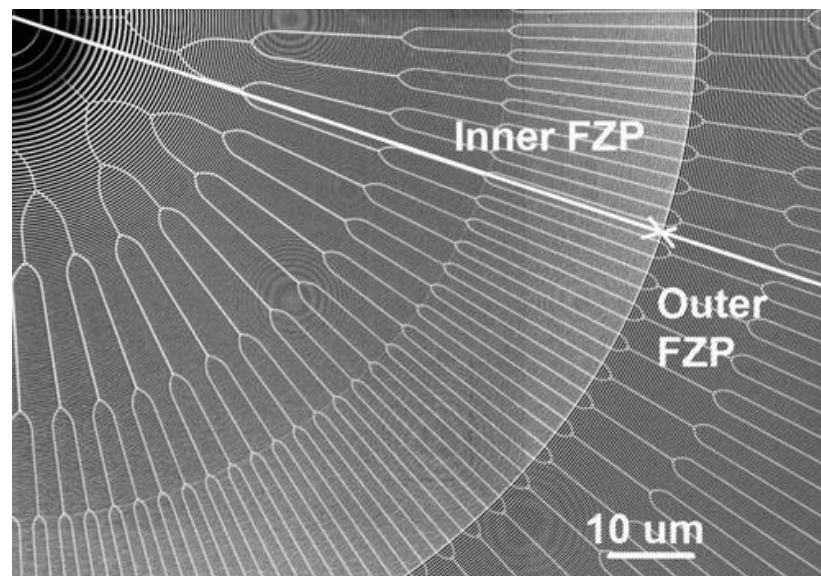
Atom-probe tomography of a Si nanowire surface region revealed presence and distribution of individual Au atoms, isolated or in small clusters, with a tendency for chain-like arrangements, and local peak volume concentration of 0.01–0.03 atoms nm⁻³. These results highlight the possibility of atom array patterning during a VLS process.

Yin Fang, Yuanwen Jiang, Bozhi Tian, Department of Chemistry, and The James Franck Institute, The University of Chicago. Atom probe work performed at SHyNE facilities.

This work was supported NSF Award # DMR-1420709 and NSF NNCI-1542205
Nature Communications **8** (2017).

Atomic layer deposition frequency-multiplied Fresnel zone plates for hard x-rays focusing

This work reported the design and fabrication of Fresnel zone plates for hard x-ray focusing up to 25 keV photon energies with better than 50 nm imaging half-pitch resolution. The fabrication process is 1) form an ultrananocrystalline diamond (UNCD) scaffold by chemical vapor-deposited UNCD, electron beam lithography, and deep-reactive ion etching of diamond to desired specifications, 2) coat it with atomic layer deposition (ALD) with an absorber/phase shifting material of Ir, Pt, or W, 3) backside etching of Si to form a diamond membrane device. The yield can reach 121 device chips per 4 inch wafer. X-ray tests with such plates allowed resolving 50 nm lines and spaces, at the limit of the available resolution test structures.



SEM image of the composite zone plate structure with novel buttresses configuration

Nicolaie Moldovan, Advanced Diamond Technologies, Inc.. Part of this work was performed in SHyNE Facilities.

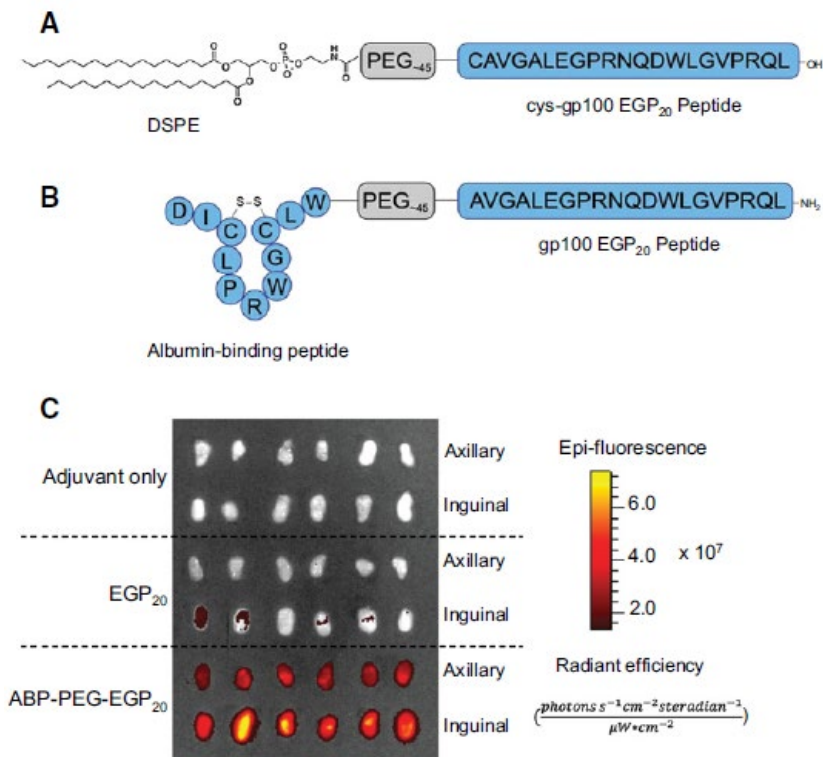
Work supported by DOE and NSF NNCI-1542205.

Journal of Vacuum Science & Technology A **36**, 01A124 (2018).

Peptide Vaccine Development: Enhancement of Immunogenicity with Peptide Conjugates

This work uses phospholipid, albumin-binding peptides, and polyethylene glycol (PEG) modified peptide conjugate structures as delivery vehicles of the peptide adjuvant sequence to the lymph nodes where T-cell responses are generated. Building on prior work, new linkage chemistries were used that proved important for ease and variety of synthetic options available to make the peptide amphiphiles. New albumin-binding moieties that were added showed enhanced accumulation in the lymph nodes and thus a stronger immune response which gives promise to this approach being used for the next generation of peptide vaccines.

A) Schematic of the phospholipid-PEG-peptide conjugate, B) Schematic of an albumin-binding peptide bound to the target peptide through a PEG-linkage. C) Lymph node fluorescence showing targeting of the peptide conjugates compared to the peptide alone.



Mark Karver of the SQI Peptide Synthesis Core collaborated with MIT researchers on this work.

Work supported by NSF, NIH, Koch Institute, Dana Farber/Harvard Cancer Center, the V Foundation and NSF NNCI-1542205

Cancer Immunol Res 6(9) 1025-1038 (2018).

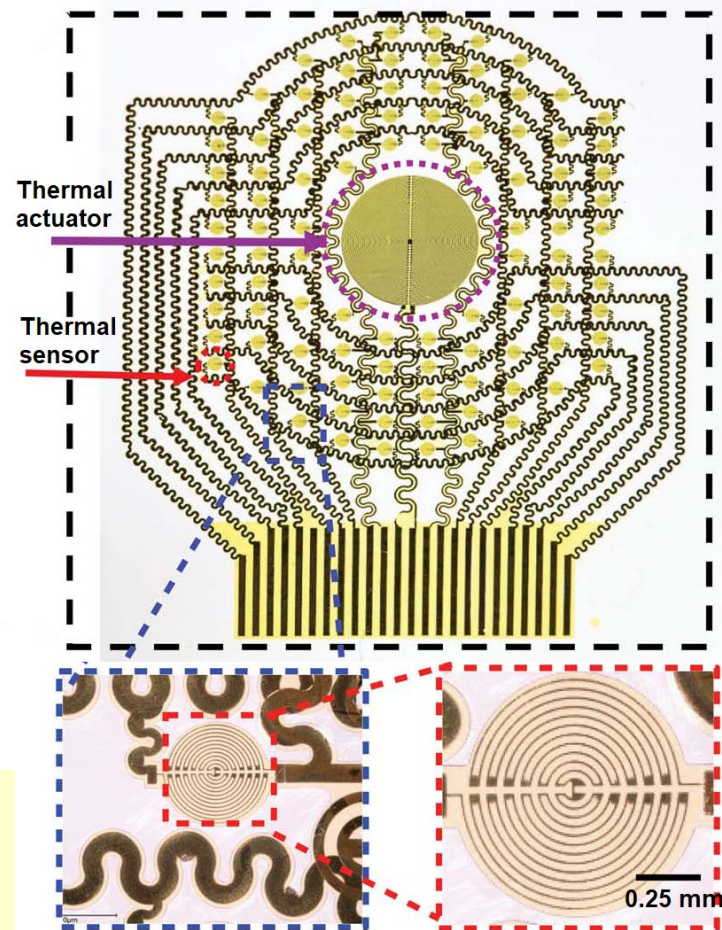
Epidermal electronics for ventricular shunt function assessment in patients with hydrocephalus

This work targets the diagnosis of shunt failure of hydrocephalus treatment. The authors developed and tested a noninvasive, skin-mounted, wearable measurement platform that incorporates arrays of thermal sensors and actuators for precise, continuous, or intermittent measurements of flow through subdermal shunts, without the drawbacks of other methods such as CT and MRI. Systematic theoretical and experimental benchtop studies demonstrate high performance across a range of practical operating conditions. Advanced electronics designs serve as the basis of a wireless embodiment for continuous monitoring based on rechargeable batteries and data transmission using Bluetooth protocols. Clinical studies involving five patients validate the sensor's ability to detect the presence of CSF flow ($P = 0.012$) and further distinguish between baseline flow, diminished flow, and distal shunt failure.

John A. Rogers, Northwestern University and University of Illinois at Urbana-Champaign. The device fabrication was performed in SHyNE Facilities.

Supported by Dixon Translational Research Grants, NSF CMMI, NSF IIP and NSF NNCI-1542205

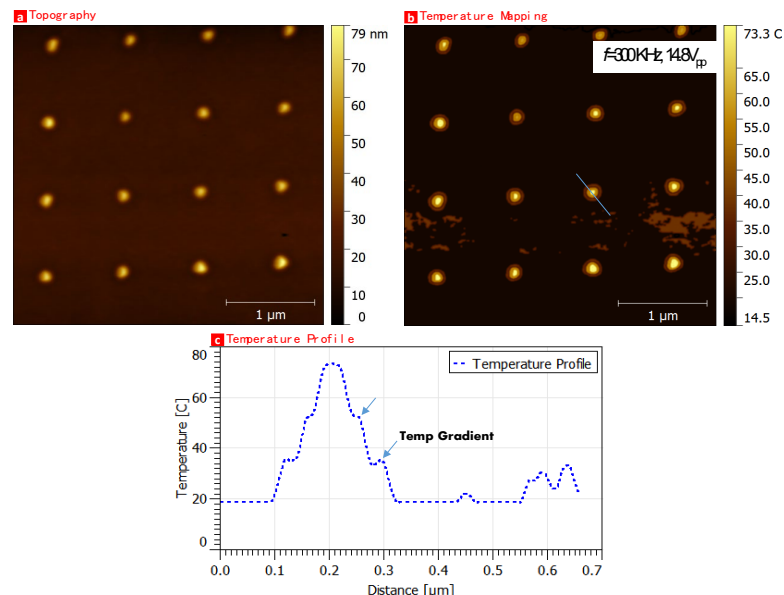
Science Translational Medicine **10**, eaat8437 (2018).



Optical micrograph of the device with enlarged images showing stretchable interconnects (blue dashed line) and individual temperature sensors (red dashed line).

Single Nanoparticle Temperature Mapping for Theranostics

An integrated thermal imaging system was developed for accurate temperature measurement of single MNP as a function of particle size and applied magnetic field. This is made possible by an innovative thermal probe design that has vertically oriented thermocouple that connects to the sample through a nanowire that offers 20 nm resolution in ambient conditions. The ability to accurately map thermal properties of single nanoparticles would further accelerate widespread application of MNPs in biomedicine. On the other hand, localized heating can be exploited for modifying the local properties of the materials, triggering chemical reactions, and developing thermal therapy of nanoparticles. Thus, accurate thermometry with high spatial resolution is essential for understanding the local thermal non-equilibrium processes during device applications and unveiling the thermal transport physics at low dimensions.



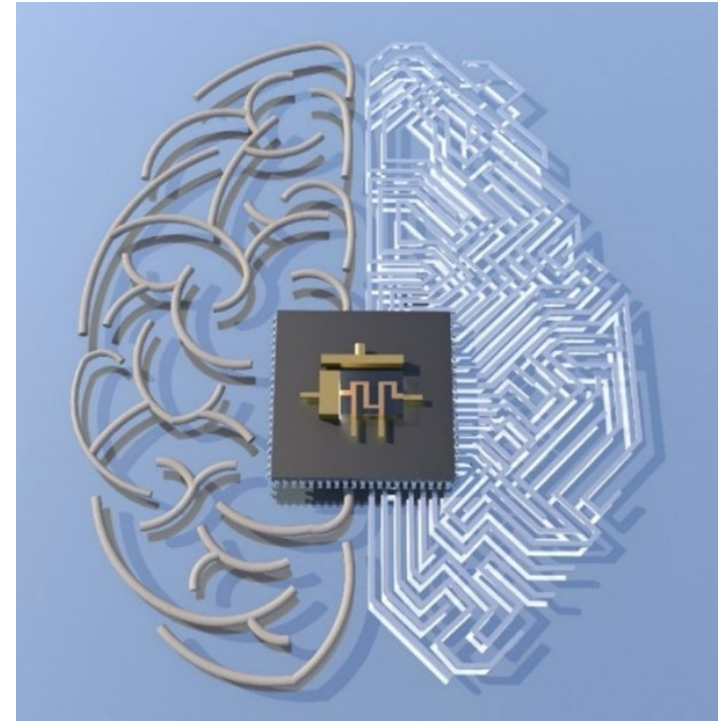
Thermal imaging of 100 nm nickel magnetic nanoparticles under external magnetic field. (a) AFM topography shows uniform patterned Ni dots, (b) depicts the sharp rise in individual nanoparticle temperature when the magnitude of the applied field is increased significantly, and (c) cross sectional profile of image b). The temperature gradient across the nanoparticle is clearly depicted in the profile plot.

Industrial collaboration between SHyNE facilities, NU Department of Materials Science and Engineering and Applied NanoStructures, Inc.

This work was supported by NSF IDBR-1256188, SBIR-1256640 and NNCI-1542205
ACS Nano 12 (2), 1760–1767 (2018)

Polycrystalline MoS₂ Memtransistors for Neuromorphic Computing

Sangwan et al. report the experimental realization of a multi-terminal hybrid memristor and transistor using polycrystalline monolayer molybdenum disulfide (MoS₂) in a scalable fabrication process. The two-dimensional MoS₂ memtransistors show gate tunability in individual resistance states by four orders of magnitude, as well as large switching ratios, high cycling endurance and long-term retention of states. In addition to conventional neural learning behaviour of long-term potentiation/depression, six-terminal MoS₂ memtransistors have gate-tunable heterosynaptic functionality, which is not achievable using two-terminal memristors. Overall, the seamless integration of a memristor and transistor into one multi-terminal device could enable complex neuromorphic learning and the study of the physics of defect kinetics in two-dimensional materials.



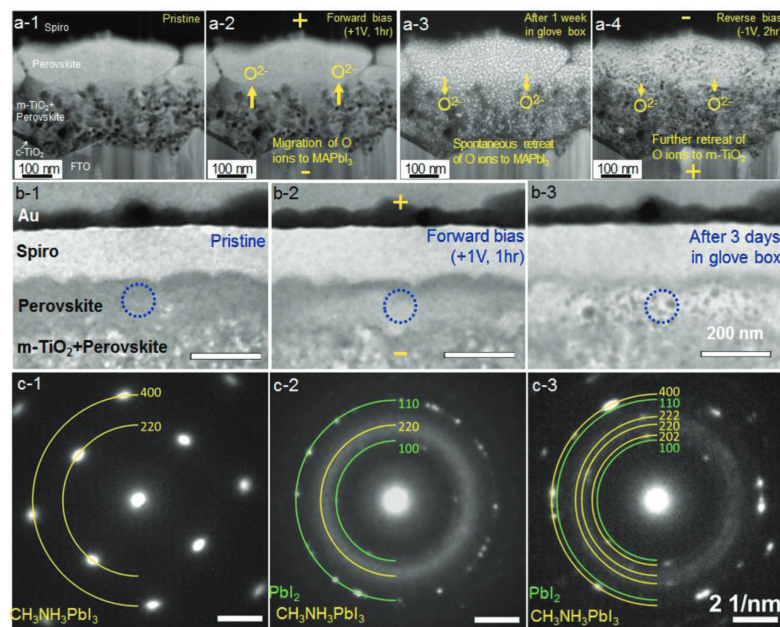
Schematic illustration of memtransistors bringing the world closer to brain-like computing.

Hersam Laboratory, Materials Science and Engineering, Northwestern University. Device fabrication and characterization performed in SHyNE facilities.

Supported by NSF DMR, NSF EFRI, NIST, ONR and NSF NNCI-1542205
Nature, **554** (2018)

Stability of Halide Perovskite Solar Cell Devices: In Situ Observation of Oxygen Diffusion under Biasing

In this work, structural and chemical modification to n-i-p-type MAPbI₃ solar cells are examined with a TiO₂ electron-transporting layer caused by bias in the absence of other stimuli known to affect the physical integrity of MAPbI₃ such as moisture, oxygen, light, and thermal stress. Electron energy loss spectroscopy (EELS) measurements reveal that oxygen ions are released from the TiO₂ and migrate into the MAPbI₃ under a forward bias. The injection of oxygen is accompanied by significant structural transformation; a single-crystalline MAPbI₃ grain becomes amorphous with the appearance of PbI₂. Withdrawal of oxygen back to the TiO₂, and some restoration of the crystallinity of the MAPbI₃, is observed after the storage in dark under no bias. The results indicate negative impacts on the device performance caused by the oxygen migration to the MAPbI₃ under a forward bias.



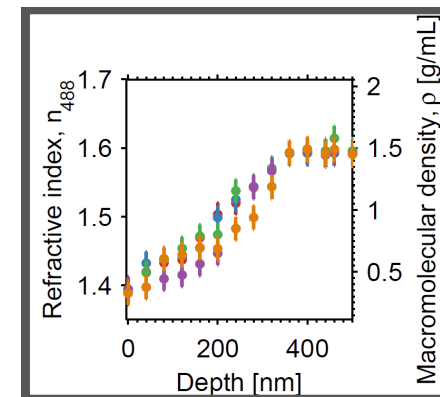
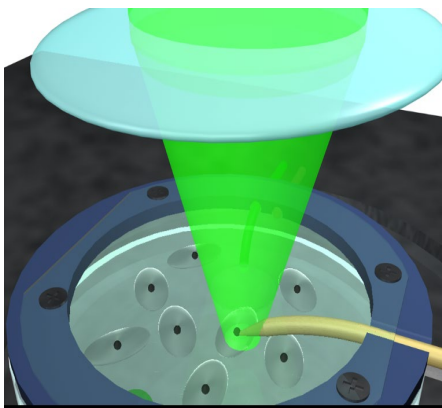
(a) Series of HAADF-STEM, (b) BFTEM, and (c) SAD of MAPbI₃ solar cell devices (1) of the pristine conditions, (2) after applying a forwards bias of +1 V, (3) after the storage for 1 week in a Ar glove box, and (3) after applying a reverse bias of -1 V (4). Note that SADs in c were taken from the same selected area of MAPbI₃ (blue dotted circle) in the BFTEMs in (b), where the yellow rings represent MAPbI₃ and the green rings represent PbI₂.

Daehan Kim and Byungha Shin, Materials Science and Engineering, Korea Advanced Institute of Science and Technology. Electron microscopy carried out in SHyNE Facilities

This work was supported by the KUSTAR-KAIST Institute and NSF NNCI-1542205.
Advanced Materials **30**, 18027692018 (2018).

Development of Optical Nanoprobe for Macromolecular Density in Colon Cancer Cells

We developed high resolution optical nanoprobe for quantification of internal, nanoscale macromolecular density measurements of pulmonary endothelial cells (EC) in response to the EC barrier-disrupting agent, thrombin, barrier-enhancing agent, sphingosine 1-phosphate (S1P) and study the differential disorder strength between two morphologically similar but genetically altered human colon cancer cells, HT29 cells and CSK shRNA transfected HT29 cells and found large variation in refractive index based on degrees of neoplastic aggressiveness. We probe the living cells under their physiological conditions using tapered optical fiber at successive depths of an illuminated sample and collect it with 50 nm fiber probe in near field mode. Directly proportional to refractive index, these data provide quantitative direct measurements of nanoscale macromolecular density within the sub-cellular architectures. The successful development and application reported here will find significant applications in biomedical imaging of living cells and have the potential to improve biological discovery and drug development processes.



(Left) Schematic of Optical Nanoprobe that collects RI within the sub-cellular architectures Optical and **(Right)** Optical nanoprobe based macromolecular density measurements of less aggressive HT 29 colon cancer cells and CSK variant of it which is more aggressive version of HT 29.

Gajendra Shekhawat, Vadim Backman, Steven Dudek+ and Vinayak Dravid. +Department of Medicine, University of Illinois, Chicago. Characterization work performed in SHyNE Facilities.

This work was supported by NSF Award # ECCS-1842662, DBI 1256188 and NNCI-1542205

Southeastern Nanotechnology Infrastructure Corridor (SENIC)

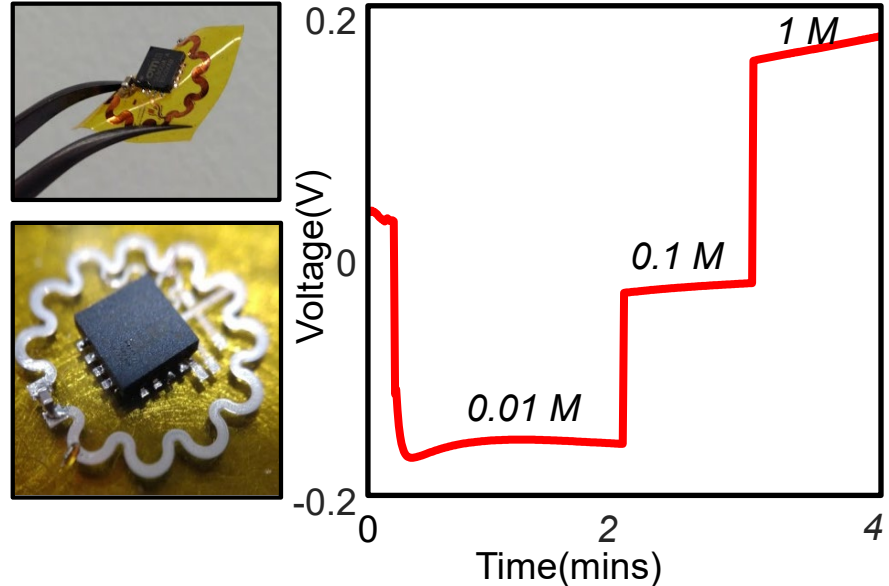
Stretchable Hybrid Electronics for Wireless Monitoring of Salivary Electrolytes

This project developed a batteryless, hybrid electronic sensor platform for analyzing salivary electrolytes.

The device was fabricated by using two different process methods, including aerosol jet printing and material transfer printing. The IC chip allowed for configuration of potentiometric sensors.

The RFID tag fits on a Hawley retainer and reads up to 1 meter in free space.

The current sensor design was electroplated with palladium and Ag/AgCl for measurements of potassium electrolytes. Current sensor configuration could successfully detect potassium as small as 0.01 Mol/L.



Optical images (left) of fabricated hybrid electronics via the combination of microfabrication, transfer printing, and direct writing methods. The graph (right) shows the sensor response according to various solutions with potassium analytes.

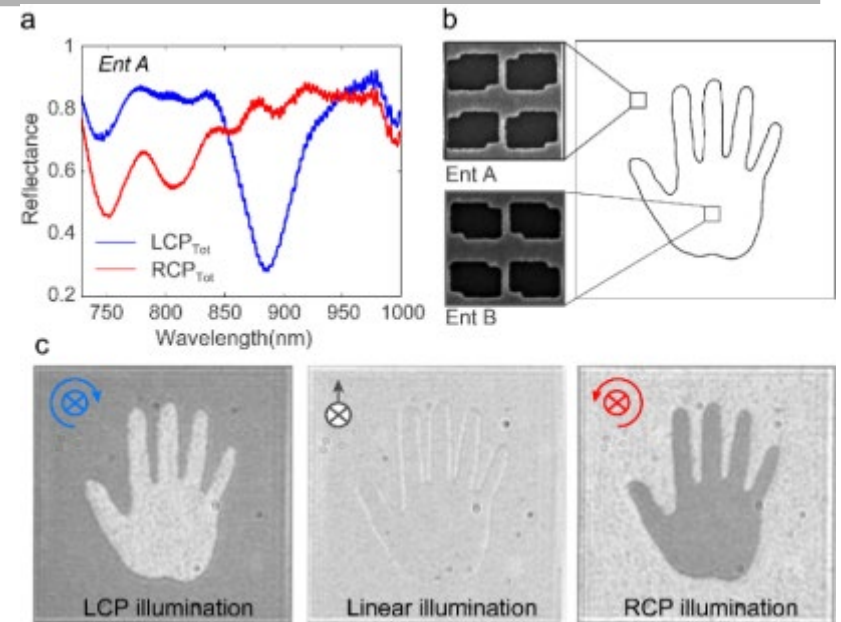
Saswat Mishra and Woon-Hong Yeo, School of Electrical and Computer Engineering, Georgia Institute of Technology. Work performed at Georgia Tech's Institute for Electronics and Nanotechnology.

This work was supported by SENIC Seed Grant (NSF ECCS-1542174).

Y. Lee, et al., *Proceedings of the National Academy of Sciences*, **115**, 5377 (2018)

Chiral Metamaterials for Optical Modulation and Signal Processing

Metamaterials can be designed to exhibit extraordinarily strong chiral responses. We realized a set of photonic metamaterials that possess pronounced chiroptical features in the nonlinear regime. In addition to the gigantic chiral properties such as the circular dichroism and polarization rotation, the metamaterials demonstrate a distinct contrast between second harmonic responses from the two circular polarizations. These structures are further exploited for chiral-selective two-photon luminescence from quantum emitters, photon-drag effect with helicity-sensitive generation of photocurrent, and all-optical modulation of chiroptical responses under a modest level of excitation power.



(a) Measured circular dichroism spectra of a chiral metamaterial. (b) Schematic of enantiomeric placement in the pattern. (c) Imaging of the chiral pattern under linear and circularly polarized lights.

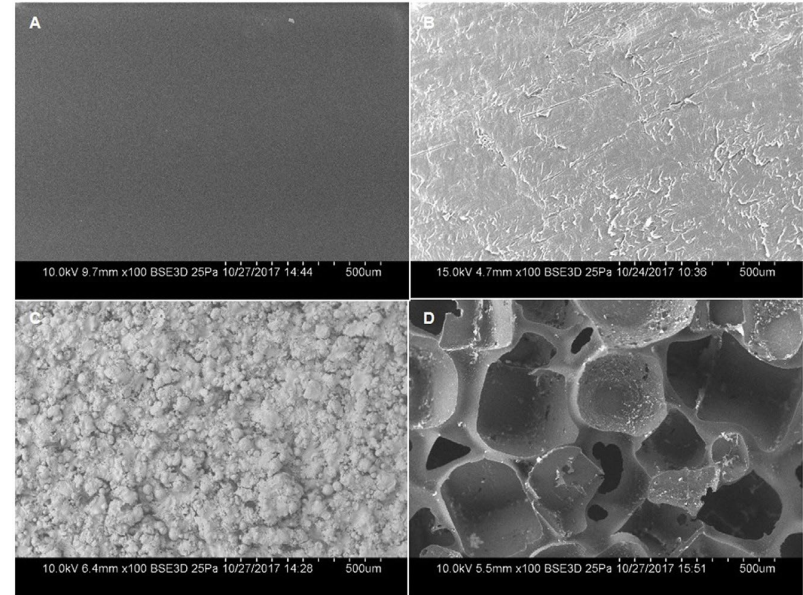
S. P. Rodrigues, L. Kang, and W. Cai, School of Electrical and Computer Engineering, Georgia Institute of Technology. Work performed at Georgia Tech's Institute for Electronics and Nanotechnology.

Project supported by NSF (ECCS-1609567) and ONR (N00014-17-1-2555).

S. P. Rodrigues et al., *Nature Communications*, Vol. 8, 14602 (2017). L. Kang et al., *Nano Letters*, Vol. 17, No. 11, 7102-7109 (2017)

Porous PEEK Improves the Bone-implant Interface Compared to Plasma-sprayed Titanium Coating on PEEK

Polyether-ether-ketone (PEEK) is one of the most common materials used for load-bearing orthopaedic devices due to its radiolucency and favorable mechanical properties. However, current smooth-surfaced PEEK implants can lead to fibrous encapsulation and poor osseointegration. This study compared the in vitro and in vivo bone response to two smooth PEEK alternatives: porous PEEK and plasma-sprayed titanium coatings on PEEK. Overall, porous PEEK was associated with improved osteogenic differentiation in vitro and greater implant fixation in vivo compared to smooth PEEK and Ti-coated PEEK. These results suggest that not all PEEK implants inherently generate a fibrous response and that topography has a central role in determining implant osseointegration.



SEM images depicting the macro-scale topography of injection molded PEEK (A), machined PEEK (B), Ti-coated PEEK (C), and porous PEEK (D).

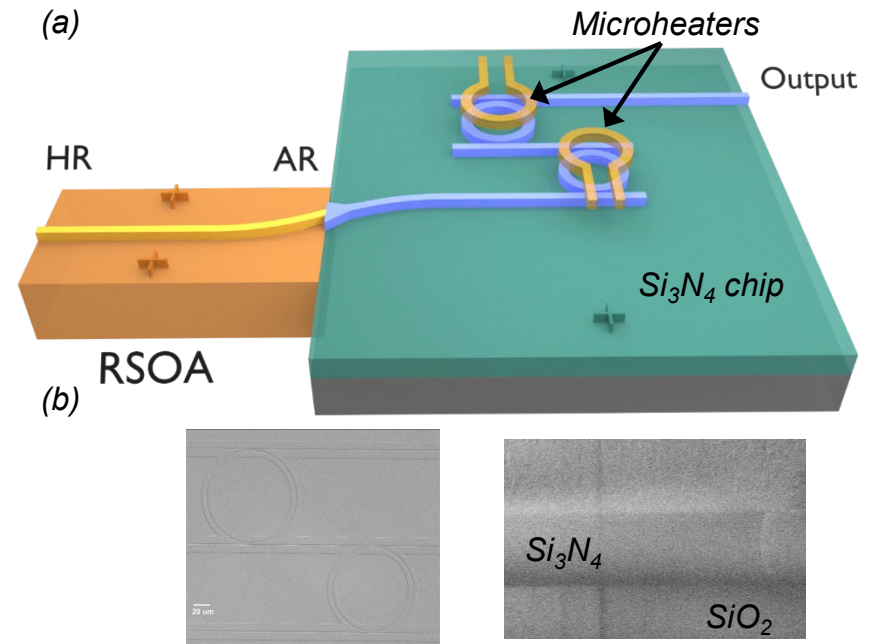
David Safranski, MedShape, Inc.; Todd Sulchek, Robert Guldberg, School of Mechanical Engineering, Georgia Institute of Technology. Work performed at Georgia Tech's Institute for Electronics and Nanotechnology.

This work was supported by Vertera Spine.

Torstrick, FB, Lin, ASP, Potter, D, Safranski, DL, Sulchek, TA, Gall, K, Guldberg, RE., *Biomaterials*. 2018. Vol 185. p. 106-116.

Narrow-linewidth, Tunable External Cavity Diode Lasers through InP-Si₃N₄ Hybrid Integration

Narrow linewidth, tunable diode lasers are important for a wide range of applications, such as coherent optical communications, optical sensing, light detection and ranging (LIDAR) and spectroscopy [1]. In this work, we have demonstrated the hybrid integration of a low-loss, passive Si₃N₄ external cavity with a RSOA on silicon photonics platform to greatly reduce the laser linewidth and obtain the tunability. In addition to the quantum-well RSOA working around 1.55 μm , a GaAs RSOA at 1 μm with wider tunability can also be integrated in the hybrid platform due to the broad transparency window of the silicon nitride.



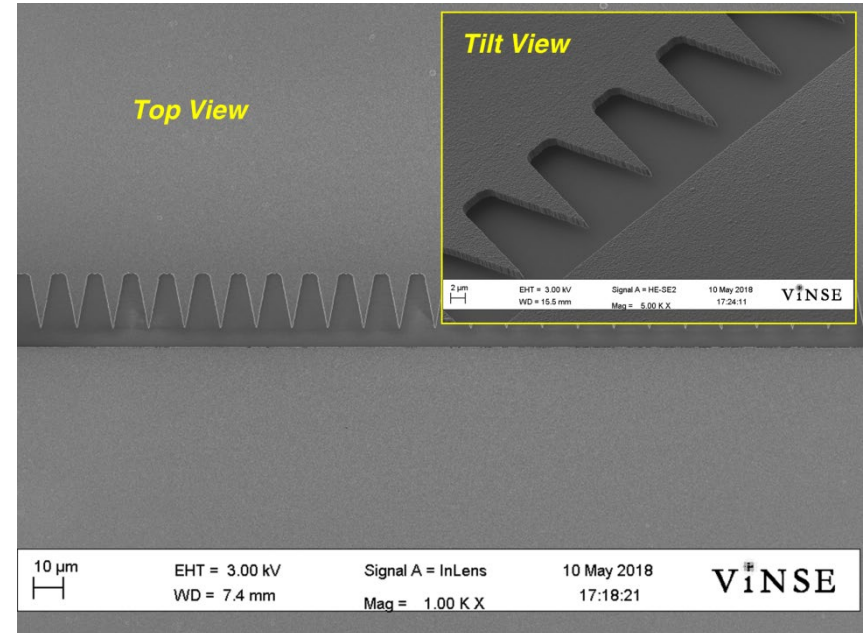
(a) Schematic plot of the hybridly integrated diode lasers;
(b) The SEM images of the fabricated double-ring filter and cleaved waveguide facet.

Yeyu Zhu, Siwei Zeng, Xiaolei Zhao, Yunsong Zhao, and Lin Zhu, Department of Electrical and Computer Engineering, Clemson University. Work performed at Georgia Tech's Institute for Electronics and Nanotechnology.

This work was supported by Army Research Office (W911NF-14-1-0640) and Office of Naval Research (N00014-17-1-2556). Zhu, Yeyu, et al., CLEO: Science and Innovations, Optical Society of America, 2018.

Radiation Hardened Electronics using Diamond Vacuum Field Emission Devices

Vacuum micro/nanoelectronics (cold cathode) is an emerging technology that will lead to the development of “extreme” electronic devices with greater performance and higher radiation operational limits than those found in solid-state devices. Despite the popularity and wide deployment of solid-state semiconductor technology, its performance is primarily dominated by electron scattering transport in which the electron transport is impeded by the crystal lattice. The operational characteristics of vacuum field emission devices, where electrons transport through vacuum environment, are essentially independent of the ambient temperature and are insensitive to radiation damage. The “junction-free” vacuum electronic devices possess a wide bandwidth, high-speed throughput, and long operational lifetime.



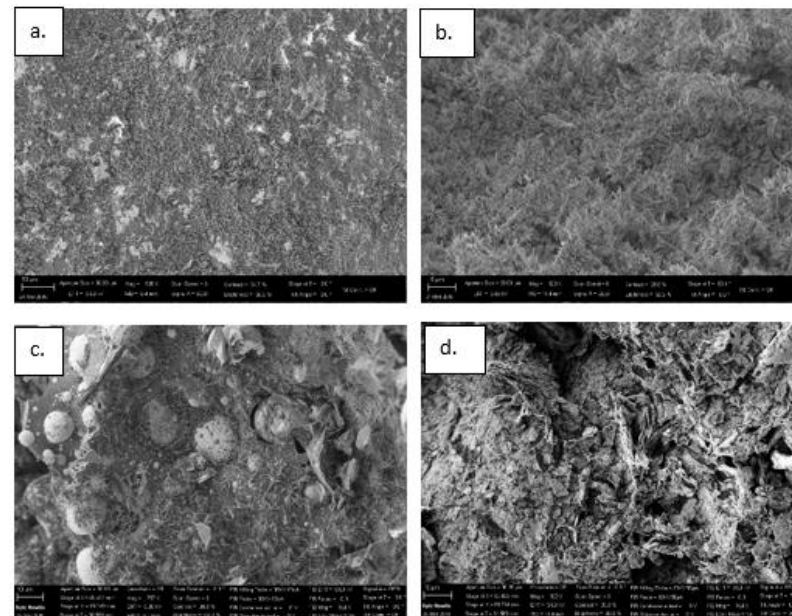
SEM micrograph of diamond based vacuum field emission diode in a lateral configuration for radiation hardened electronics.

Supil Raina, Mesut Yilmaz, Mick Howell, Weng P Kang, Department of Electrical Engineering and Computer Science, Vanderbilt University.

Work performed at Georgia Tech's Institute for Electronics and Nanotechnology.

Investigating Sintering Mechanisms for Additive Manufacturing of Conductive Traces

This research explores a hybrid additive manufacturing technology. A variety of conductive materials were deposited on both rigid (glass) and flexible (Kapton) substrates. The deposited traces were cured using two sintering mechanisms which include furnace heating and in situ laser irradiation. The effect of curing mechanism on the conductance of deposited traces was evaluated. An increase in the laser power resulted in lower resistivity of the traces. The lowest resistivity was achieved at 40W laser power with a single laser pass. Scanning electron microscopy and energy dispersive spectroscopy were used to characterize the trace morphology and elemental compositions. Higher power laser curing resulted in better bonding of the particles. Laser cured samples had minimal oxidation to the cross-section region of the traces as compared to furnace cured samples.



Cross-sectional SEM images of silver traces (a) furnace top view (b) furnace cross-sectional view (c) 40W laser top view (d) 40W cross-sectional view

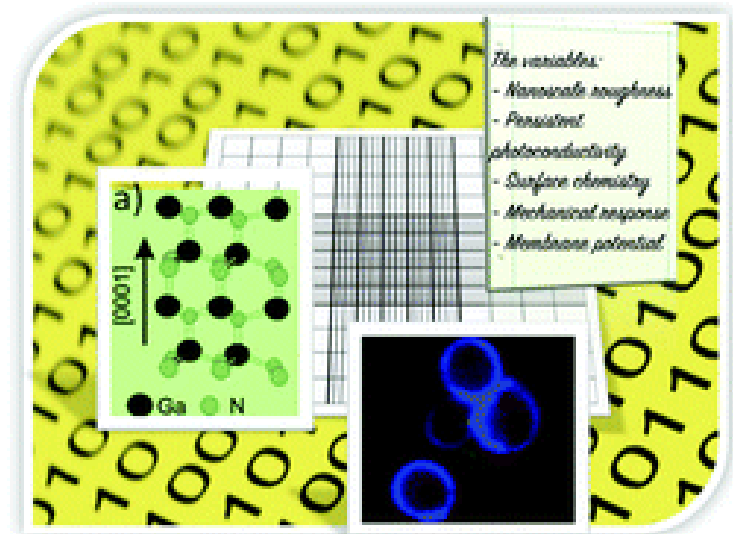
Salil Desai, Department of Industrial & Systems Engineering, North Carolina A&T State University. Work performed at Joint School of Nanoscience and Nanoengineering.

This work was supported by NSF CMMI: Award 1435649.

McKenzie, J., & Desai, S. (2018). *American J. of Engineering and Applied Sciences*, 11(2).

Bioelectronics Communication: Encoding Yeast Regulatory Responses using Nano GaN

Baker's yeast, *S. cerevisiae*, is a model organism that is used in synthetic biology. The work demonstrates how GaN nanostructured thin films can encode physiological responses in *S. cerevisiae* yeast. The Ga-polar, n-type, GaN thin films are characterized via Photocurrent Measurements, Atomic Force Microscopy and Kelvin Probe Force Microscopy. UV light is used to induce persistent photoconductivity that results in charge accumulation on the surface. The morphological, chemical and electronic properties of the nanostructured films are utilized to activate the cell wall integrity pathway and alter the amount of chitin produced by the yeast. The encoded cell responses are induced by the semiconductor interfacial properties associated with nanoscale topography and the accumulation of charge on the surface that promotes the build-up of oxygen species and in turn cause a hyperoxia related change in the yeast. The results thus define a strategy for bioelectronics communication.



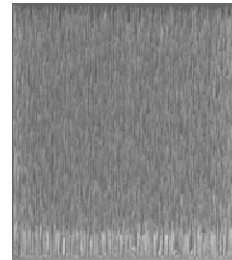
Yeast cell interaction with GaN semiconductor materials elicit special behavioral and physiological changes

Snyder, LaJeunesse, Reddy, Kirste, Collazo, Ivanisevic, Materials Science and Engineering, NC State University, Nanoscience, UNC Greensboro and Adroit Materials. Part of this work was performed at Joint School of Nanoscience and Nanoengineering.

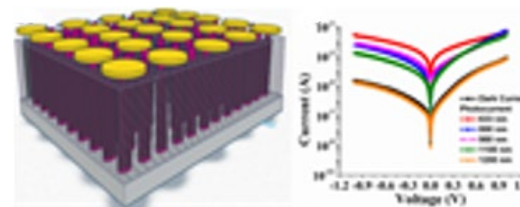
Partial financial support from NSF DMR-1312582, ECCS-1542174, ECCS-1653383 and NIH 1R15EB024921-01. Snyder et al., *Nanoscale*, 2018,10, 11506.

GaAsSb Nanowires for IR Photodetectors

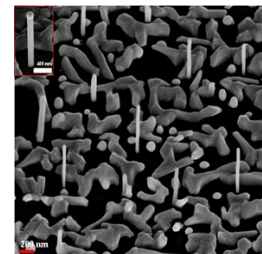
The focus of this work is on the Ga assisted molecular beam epitaxial growth of GaAsSb nanowires (NWs), characterization and demonstration of NW based photodetector in the near infrared region. High quality nanowires were grown as seen by the narrow full width half maxima of low temperature photoluminescence line-shape and lack of any defects in the transmission electron microscope images. In addition, site-specific growth of GaAsSb NWs with >90% hole occupancy and pitch induced band gap tuning were successfully shown. Next, GaAsSb NW photodetector device exhibited good spectral response up to 1.1 μm . Lastly, growth of GaAsSb NWs of high quality on monolayer graphene have also been demonstrated for the first time for flexible applications



SEM micrograph of GaAsSb patterned NW arrays by electron beam lithography.



Axial p-i GaAsSb/GaAlAs core-shell NW ensemble photodetector



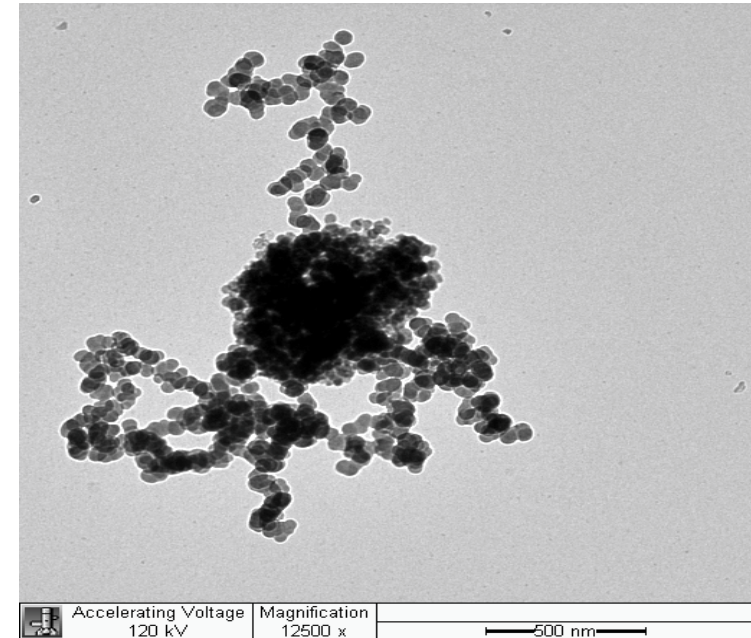
GaAsSb NWs on graphene

Shanthi Iyer, Nanoengineering/Electrical and Computer Engineering, North Carolina A&T State University. Work performed at Joint School of Nanoscience and Nanoengineering.

This work has been supported by ARO W911NF-15-1-0379, NSF HRD-1649517, ONR N00014-16-1-2720. P. Deshmukh et al. *Sem. Sci. Tech.* 33, 125007(2018), Estiak Ahmad et al. *Scientific Rep.* 7, 10111 (2017), M. Sharma et al. *Crystal Growth & Design*, 17, 307 (2017).

Modeling Refractive Indices of Biomass Burning Aerosols

Biomass burning emissions are a major source of fractal aggregates which are clusters of spherules forming aerosols of non-spherical shape. Both the developed and developing world are subject to biomass burning events through agricultural burning, wildfires, and domestic burning applications. Accurate quantification of their optical properties is important both for their measurement and for predicting their radiative effect. Raleigh-Debye -Gans (RDG) assumes that each monomer in the aggregate interacts independently with radiation, by neglecting multiple scattering and shadowing. Absorption is an incoherent process and as a result the absorption of the aggregate is equal to the number of monomers, N , times the absorption of a single monomer. TEM images are used to determine the size parameters of the fractal aggregates. We use T-Matrix and RDG theory to fit experimentally measured optical properties to extract the refractive indices of biomass burning aerosols.



	Accelerating Voltage 120 kV	Magnification 12500 x	 500 nm
---	--------------------------------	--------------------------	--

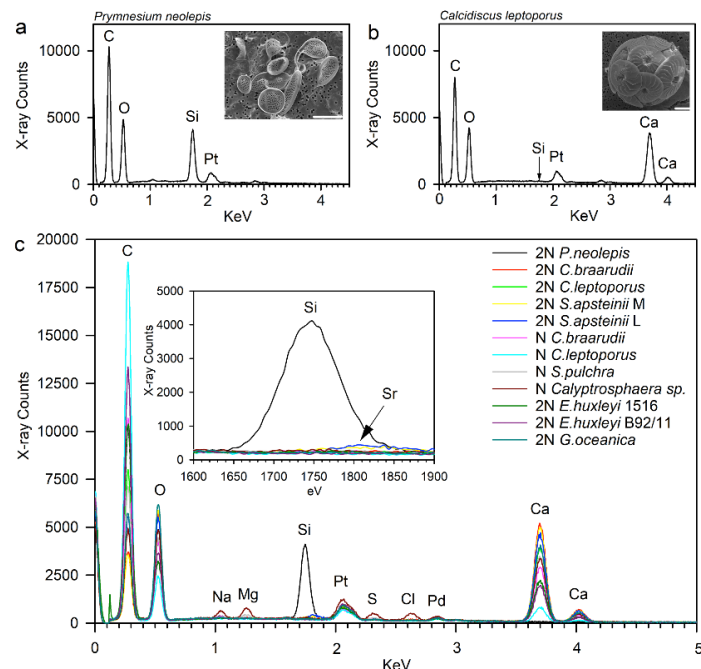
TEM images of biomass burning aerosols collected on filters

Solomon Bililign and Marc Fiddler, Department of Physics, North Carolina A&T State University. Work performed at Joint School of Nanoscience and Nanoengineering.

This work was supported by NSF Award AGS-1831013 and AGS-1555479. Poudel et al., *Atmosphere* 2017, 8, 228.

Biom mineralization Mechanisms in Marine Phytoplankton

Coccolithophores are calcifying marine algae which produce taxonomically distinct CaCO₃ (calcite) coccoliths to form an outer covering of the cell. Certain species form large blooms, which can account for nearly half of global annual CaCO₃ production. Despite their significant impact on biogeochemical cycles, the cellular mechanisms of calcification remain poorly understood. Coccoliths are produced in a highly regulated intracellular process that involves crystal nucleation on an organic baseplate, interactions with organic macromolecules, Ca²⁺, HCO₃⁻ and other cations. This work utilizes analytical SEM to understand the role of key elements such as Si and Sr in the precipitation and nanomorphology of the biom mineral structures in order to better understand the mechanisms of coccolith production by these globally important marine microbial organisms.



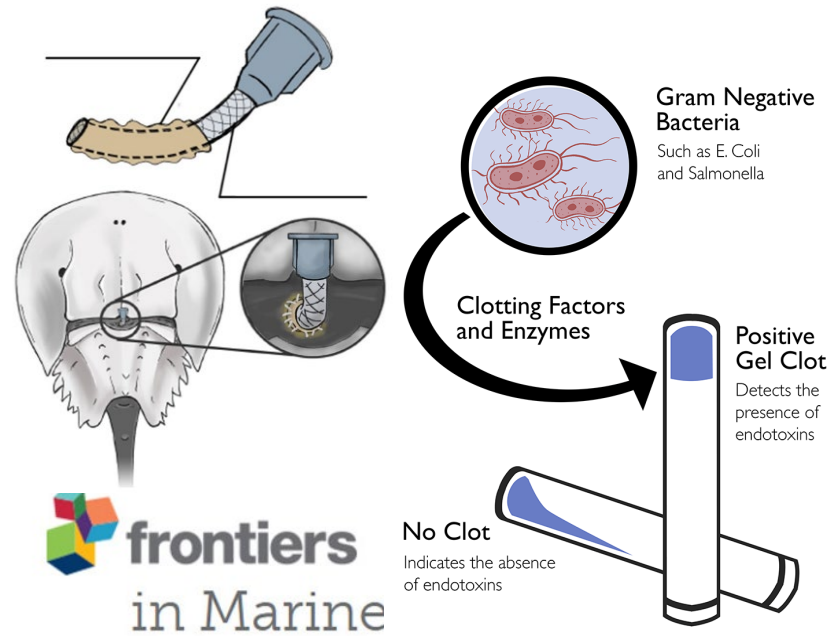
Elemental analysis of (a) a silicifying haptophyte (*Pymnesium neolepis*) and (b) calcifying *Calcidiscus leptoporus* using EDS. Note Si and Ca peaks respectively. (c) EDS analysis across multiple species. A small Sr peak was observed for *Scyphosphaera apsteinii* (arrow).

Erin Meyer and Alison Taylor, Biology and Marine Biology, University of North Carolina Wilmington.
Work performed at Joint School of Nanoscience and Nanoengineering.

This work was supported by NSF Award # OCE-1638838.
Walker C., Taylor A.R. et al., *New Phytologist*, 2018

Innovation for Horseshoe Crab Bleeding and Management

Kepley BioSystems Inc (KBI), a JSNN NIC member was recently awarded NSF Phase 1 SBIR grant to develop a novel surgical implant and management strategy to improve the harvest of amebocytes from horseshoe crabs. Amebocytes play a critical role in safeguarding modern medicine and serve as the back bone of the FDA mandated QC method for drug developers, however currently used methods are deleterious to the species viability and have been estimated to cause a 26% mortality rate, annually.



Surgical Implant to Improve Bleeding Horseshoe Crabs

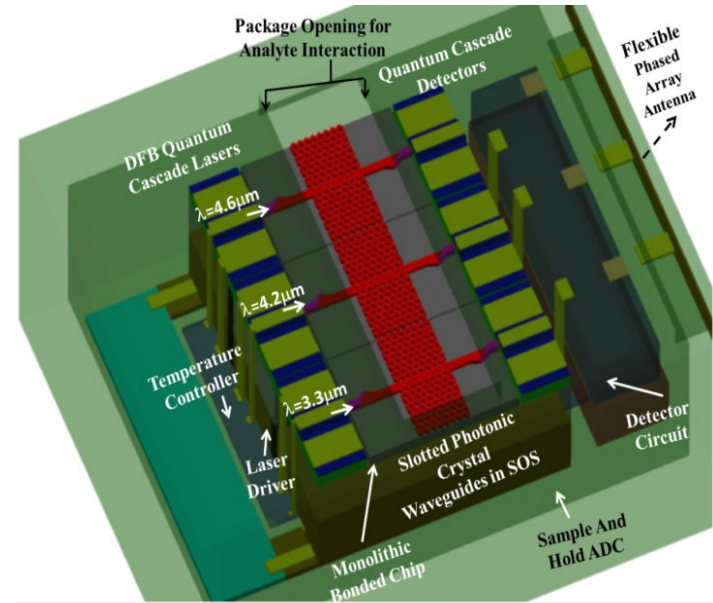
Kristen Dellinger, Chris Kepley, Anthony Dellinger, Kepley Biosystems, Greensboro, NC.
Work performed at Joint School of Nanoscience and Nanoengineering

This work was supported by NSF SBIR Phase II Award #1555752. Gannon et al., The Role of Horseshoe Crabs in the Biomedical Industry and Recent Trends Impacting Species Sustainability, *Front. Mar. Sci.*, 2018.

Texas Nanofabrication Facility (TNF)

PPB Carbon Monoxide Sensing in Silicon-on-Sapphire Mid-Infrared Photonic Crystal Waveguides

With recent advances in optoelectronics and photonics, optical sensors have flourished. Optical sensors are typically built of three parts: a light source and detector, a photonic crystal substrate, and an analyte flow mechanism made of microfluidic channels. Experimentally demonstrated mid-IR slotted photonic crystal waveguides at $\lambda=4.55$ micron in silicon-on-sapphire. Experimentally detected 3ppm CO with mid-IR absorbance signatures. Feasibility of parts per billion sensing was shown. Experiments in progress to validate ppb- sensitivity.

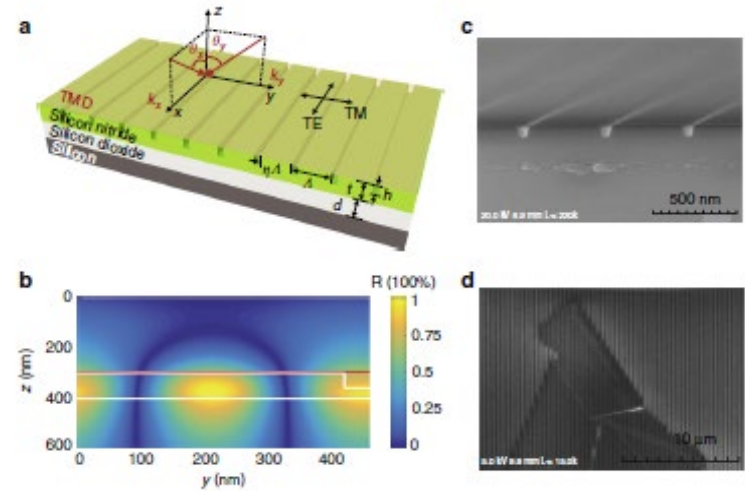


Swapnajit Chakravarty, Omega Optics. Work performed at Texas Nanofabrication Facility.

This work was supported by NASA SBIR Contract #: NNX17CA44P, NSF Grant #:1711824

Photonic-crystal exciton-polaritons in monolayer semiconductors

Semiconductor microcavity polaritons, formed via strong exciton-photon coupling, provide a quantum many-body system on a chip, featuring rich physics phenomena for better photonic technology. However, conventional polariton cavities are bulky, difficult to integrate, and inflexible for mode control, especially for room-temperature materials. Here we demonstrate sub-wavelength-thick, one-dimensional photonic crystals as a designable, compact, and practical platform for strong coupling with atomically thin van der Waals crystals. Polariton dispersions and mode anti-crossings are measured up to room temperature. Non-radiative decay to dark excitons is suppressed due to polariton enhancement of the radiative decay. Unusual features, including highly anisotropic dispersions and adjustable Fano resonances in reflectance, may facilitate high temperature polariton condensation in variable dimensions. Combining slab photonic crystals and van der Waals crystals in the strong coupling regime allows unprecedented engineering flexibility for exploring novel polariton phenomena and device concepts.

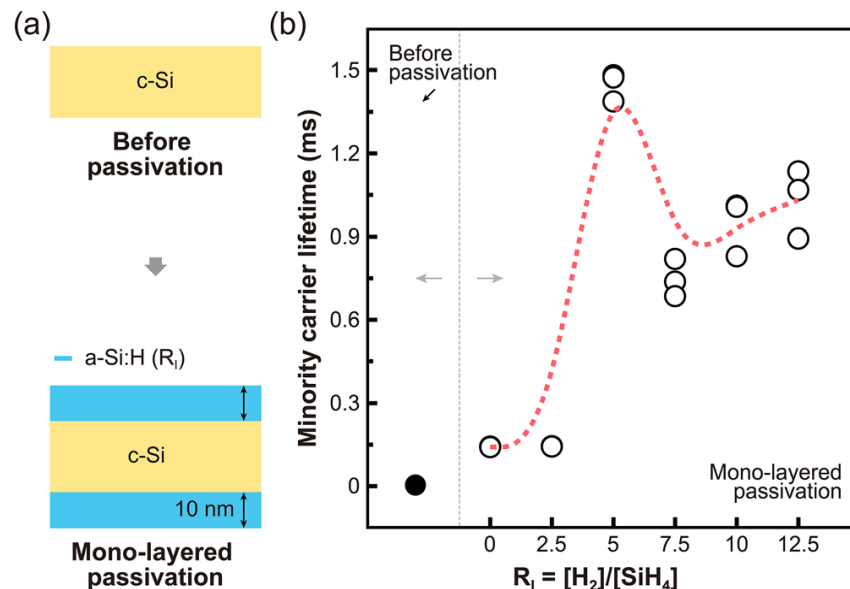


Long Zhang, Rahul Gogna, Will Burg, Emanuel Tutuc, Hui Deng, Univ. Texas and Univ. Michigan

This work was supported by Army Research Office Award W911NF-17-1-0312 .
Nature Communications, volume 9, Article number: 713 (2018).

Highly improved passivation of c-Si surfaces using a gradient i a-Si:H layer

Surface passivation using intrinsic a-Si:H (i a-Si:H) films plays a key role in high efficiency c-Si heterojunction solar cells. In this study, we demonstrate improved passivation quality using i a-Si:H films with a gradient-layered structure consisting of interfacial, transition, and capping layers deposited on c-Si surfaces. The H₂ dilution ratio (R) during deposition was optimized individually for the interfacial and capping layers, which were separated by a transition layer for which R changed gradually between its values for the interfacial and capping layers. This approach yielded a significant reduction in surface carrier recombination, resulting in improvement of the minority carrier lifetime from 1480 μs for mono-layered i a-Si:H passivation to 2550 μs for the gradient-layered passivation approach.



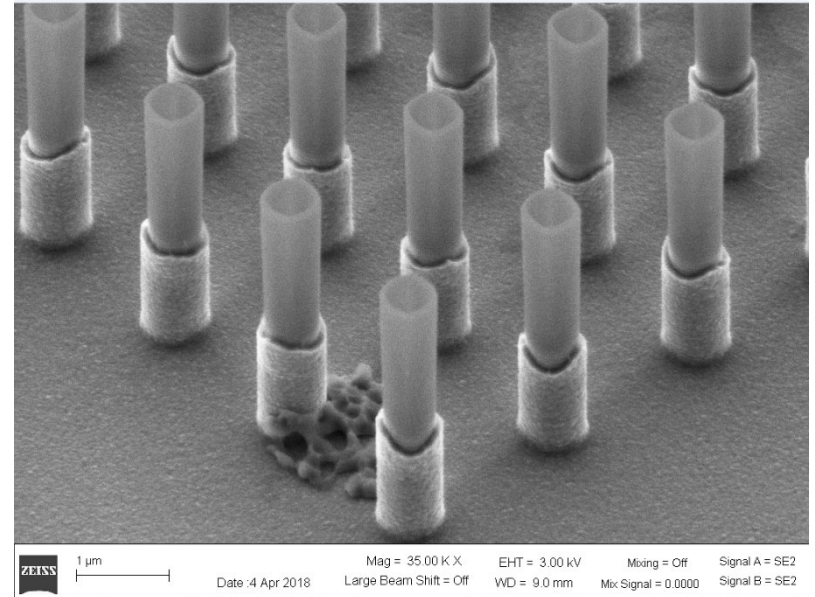
Soonil Lee, Jaehyun Ahn, Leo Mathew, Rajesh Rao, and Edward T. Yu, Univ. of Texas. Work done at Texas Nanofabrication Facility, Microelectronics Research Center.

Work supported by U.S. Army Research Laboratory.
Journal of Applied Physics 123, 163101 (2018)

Thin Crystalline Silicon Vertical Power Transistor- Fabricated without Grinding away the Substrate

AND Inc. has developed a thin crystalline technology that can peel off 20 - 50 μ m of silicon from semi-processed wafers and enable reuse of the parent wafer. Using this exfoliation technology, AND has recently demonstrated the world's first Thin Crystalline (~30 Microns) Silicon Vertical Power MOSFET fabricated without grinding away the substrate.

The industry standard process for vertical power MOSFET and IGBTs is to use a back grinding process. Several companies have used this back grinding process to demonstrate thin power MOSFET wafers for different applications. The standard toolset provided by Disco for this process was used, and compared with the wafers fabricated with back grinding against the thin crystalline wafers fabricated by AND. The thin crystalline process has been scaled to 12" semi standard wafers. AND has developed a unique self-aligned vertical power MOSFET architecture. This architecture brings in significant process simplification and device benefits. AND is combining this device architecture with thin crystalline Si technology to target record device performance of power MOSFETs.

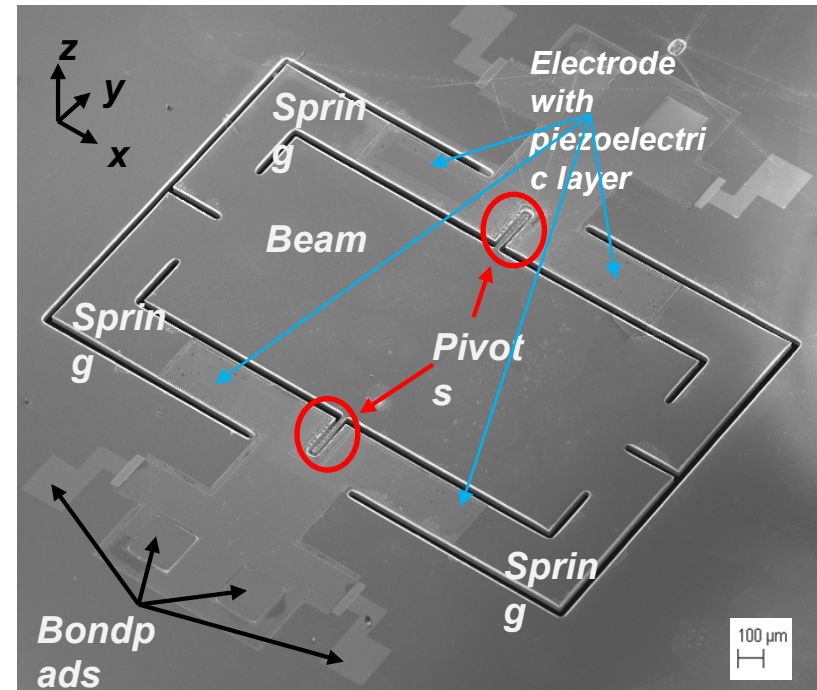


Leo Mathew and Rajesh Rao, Applied Novel Devices (AND). Work performed at Texas Nanofabrication Facility.

This work was supported by NSF SBIR grant.

New Acoustic MEMS Based on a Fly's Acute Hearing for Hearing Aids and Military

Silicon Audio has developed a tiny prototype device that mimics a parasitic fly's hearing mechanism, which may be useful for a new generation of hypersensitive hearing aids. The 2-millimeter-wide device uses piezoelectric materials, which turn mechanical strain into electric signals. The use of these materials means that the device requires very little power. Humans and other mammals have the ability to pinpoint sound sources because of the finite speed of sound combined with the separation between our ears. The fly has evolved an unusual physiological mechanism to make the most of that tiny difference in time. The fly's ear has a structure that resembles a tiny teeter-totter seesaw about 1.5 mm long. Teeter-totters, by their very nature, vibrate such that opposing ends have 180-degree phase difference, so even very small phase differences in incident pressure waves force a mechanical motion that is 180 degrees out of phase with the other end. This effectively amplifies the four-millionths of a second time delay.

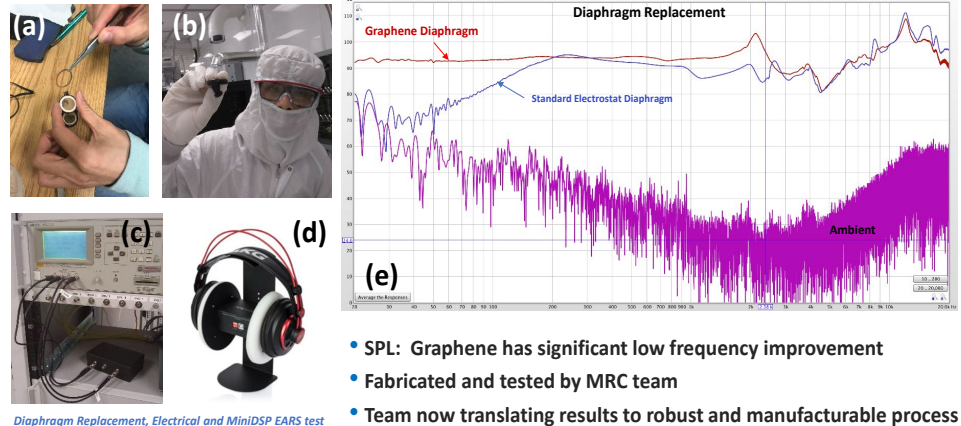


N Hall, Silicon Audio. Work performed at Texas Nanofabrication Facility, Microelectronics Research Center.

Funded by DARPA.

Graphene Enabled Acoustics

GraphAudio is developing a new generation of graphene based micro audio componentry that will outperform the current generation and open new realms of capabilities. Graphene enabled acoustic devices with no distortion are running on much lower power and having much better form factors than current technology. In production, GraphAudio graphene transducers can be economically produced in high volume utilizing high technology foundries for micro-speakers, mobile devices, earbuds and headphones in the next three to five years. GraphAudio's patent pending graphene based transducer delivers an electrostatic micro speaker and enhancements through digital manipulation that is the solution to unlock a revolution in micro audio componentry. UT MRC team are coordinating goals with researchers at UC Berkeley and UN Lincoln. Transducer design functions as speaker or microphone, or both. Graphene diaphragm is thinner, stronger and more responsive. Air dampening improves response and energy efficiency. New range of acoustic capabilities individually or in arrays.

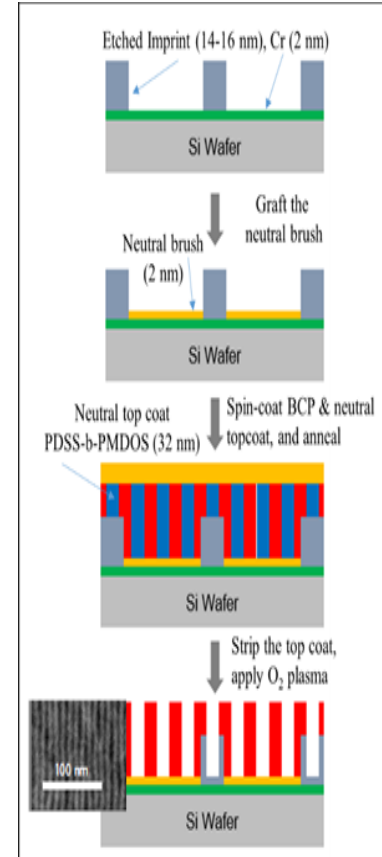
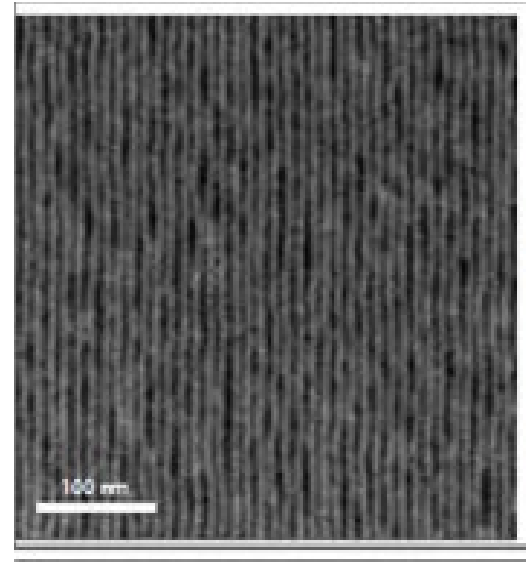


Burt Fowler, Harry Chou, Yuanjun Fan, Jeff Maag, Mike Olla, Mike Klasco and Lorance Wilson, GraphAudio. Synthesis, characterization, and fabrication performed at NNCI TNF.

Funded by Venture Capital.

Oriented lamellae of a Si-containing BCP after selectively removing one block with RIE

The directed self-assembly (DSA) of block copolymers (BCP) is a potentially lower cost lithography alternative to enable the continued scaling of devices to smaller dimensions. Organometallic block copolymers have been developed to form patterns down to 5 nm critical dimensions. Graphene nanoribbons have been fabricated using block copolymer lithography. Si-containing BCP material has been developed and incorporated into a process involving a nanoimprinted Cr layer to produce long-ranged parallel lines. Annealing, topcoat strip, and O₂ plasma etch has led to the demonstration of patterning with 5nm lines and spaces. DSA of BCP and our earlier results in nanoshape imprinting demonstrates unprecedented patterning capability that far exceeds the resolution of photo- and EUV lithography.

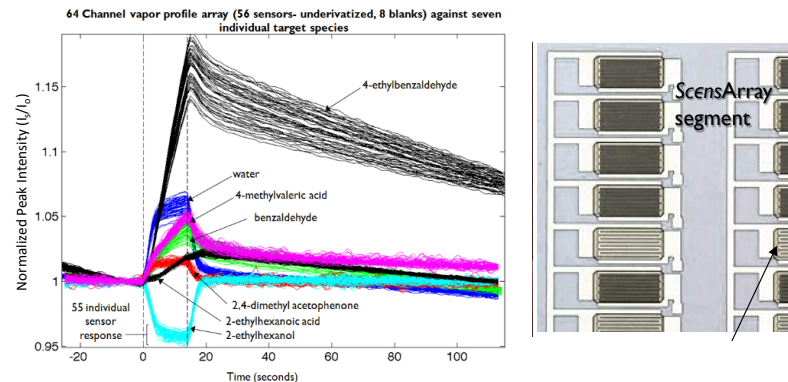


Steve Sirad, Lam. Work performed in part at Texas Nanofabrication Facility.

Funded by Lam Research Corporation.

Multiplexed Metal-Oxide Gas and Fluid Sensor Arrays

Bioassays employed to evaluate the diverse range of biomarkers associated with organ injury are time-consuming, costly and require multiple instruments/testing formats to reach a diagnosis (i.e. fluorescence-based capture, ELISAs, PCR, etc.). Individually, these platforms are incapable of predicting the onset of irreversible organ tissue injury (e.g. kidney, liver, heart and lung). One barrier to transitioning microarray technology into multiplex medicinal diagnostics has been the limitations imposed by fluorescence/optical-based labeling and endpoint detection. To overcome these limitations, Nanohmics Inc., developed the SnO₂ nanowire chemiresistive sensor array. The diverse surface derivitizations across array elements allows for incident gas/ion species identification. The platforms are room temperature operable and provide fast response in gas applications.

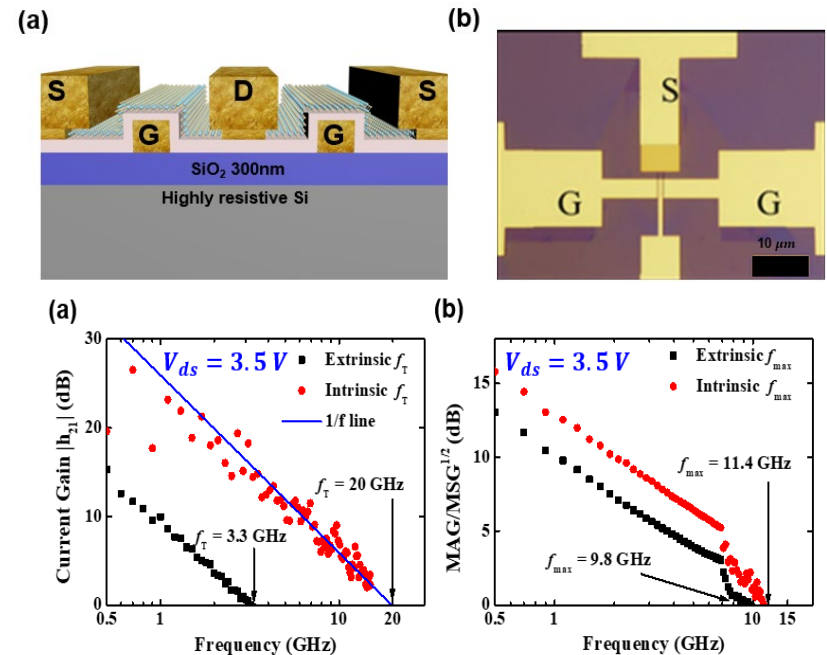


Steve Savoy, Nanohmics. Work performed in part at Texas Nanofabrication Facility Microelectronics Research Center.

Funded by DHP Phase II SBIR Program and NIH Phase I SBIR Program.

CVD-grown MoS₂ High Frequency FETs

State-of-the-art large area CVD monolayer MoS₂-based RF transistors and RF switches were fabricated. An embedded gate structure was used to fabricate short channel CVD MoS₂ RF FETs with an intrinsic f_T of 20 GHz, intrinsic f_{max} of 11.4 GHz, and the high-field saturation velocity v_{sat} of 1.88×10^6 cm/s. The gate-first process allows for enhancement mode operation, I_{ON}/I_{OFF} ratio of 10^8 , and a transconductance (g_m) of $70 \mu\text{S}/\mu\text{m}$. Also, we use a vertical MIM structure for a RF switch based on CVD MoS₂. The device was programmed with a voltage as low as 1 V, and achieves an ON-state resistance of $\sim 5 \Omega$ and an OFF-state capacitance of ~ 6 fF. We measured and simulated the RF performance of the device up to 67 GHz and report 0.5 dB insertion loss, 15 dB isolation (both at 50 GHz), and 5 THz cutoff frequency. Short circuit current gain, $|h_{21}|$, versus frequency shows an extrinsic f_T of 3.3 GHz and an intrinsic f_T of 20 GHz at a V_{ds} of 3.5 V with a 150 nm gate length. **(b)** Maximum available power gain, $\text{MAG}^{1/2}$, versus frequency shows an extrinsic f_{max} of 9.8 GHz and an intrinsic f_{max} of 11.4 GHz.



A.Rai, A.Sanne, Deji Akinwande and Sanjay Banerjee, Univ. of Texas at Austin. Work is performed in part at Texas Nanofabrication Facility Microelectronics Research Center.

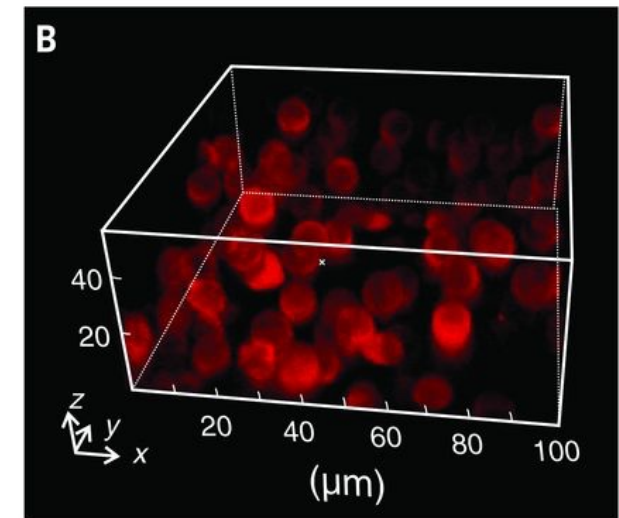
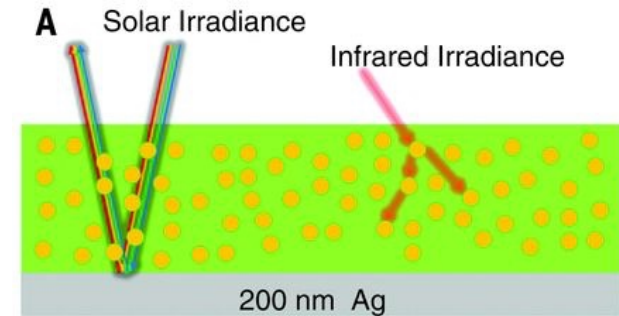
Funded by Army STTR grant.

Crystals, Vol. 8, Iss. 8, Article Number 316, 2018.

Fabrication of metamaterials for efficient passive cooling

Spectroscopic response of the hybrid metamaterial. **(A)** Schematic of the hybrid metamaterial backed with a thin silver film. The silver film diffusively reflects most of the incident solar irradiance, whereas the hybrid material absorbs all incident infrared irradiance and is highly infrared emissive. **(B)** Three-dimensional confocal microscope image of the hybrid metamaterial. The microspheres are visible because of the autofluorescence of SiO_2 .

We embedded resonant polar dielectric microspheres randomly in a polymeric matrix, resulting in a metamaterial that is fully transparent to the solar spectrum while having an infrared emissivity greater than 0.93 across the atmospheric window. When backed with a silver coating, the metamaterial shows a noontime radiative cooling power of 93 watts per square meter under direct sunshine. More critically, we demonstrated high-throughput, economical roll-to-roll manufacturing of the metamaterial, which is vital for promoting radiative cooling as a viable energy technology.

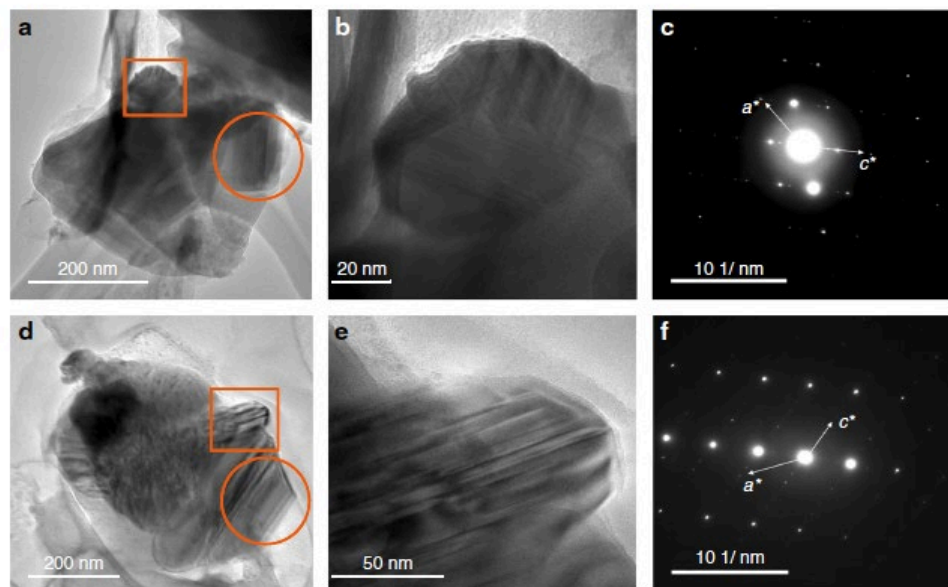


A Heltzel, PC Krause and Associates. Work performed at Texas Nanofabrication Facility, Texas Materials Institute.

***Virginia Tech National Center for Earth and
Environmental Nanotechnology
Infrastructure (NanoEarth)***

Discovery of a new pathogen from coal burning

Burning coal produces more global warming CO₂ relative to all other fossil fuels. In addition, dealing with the downsides of burning coal on massive, protracted scales includes severe human health impacts. The most important short-term consequence is that coal-burning is a major contributor to atmospheric particulate matter with aerodynamic diameter smaller than 2.5 μm (so-called PM2.5). We have discovered that burning coal produces large quantities of otherwise rare Magnéli phases (Ti_xO_{2x-1} with 4 ≤ x ≤ 9) which are derived from TiO₂ minerals naturally present in coal. This provides a new tracer for tracking solid-state emissions worldwide from industrial coal-burning. In its first toxicity testing in zebrafish and mice, we have also shown that nanoscale Magnéli phases, likely, have toxicity pathways human lungs. In the future, these phases should be thoroughly tested for their toxicity in humans. This work was reported in many dozens of new outlets internationally.



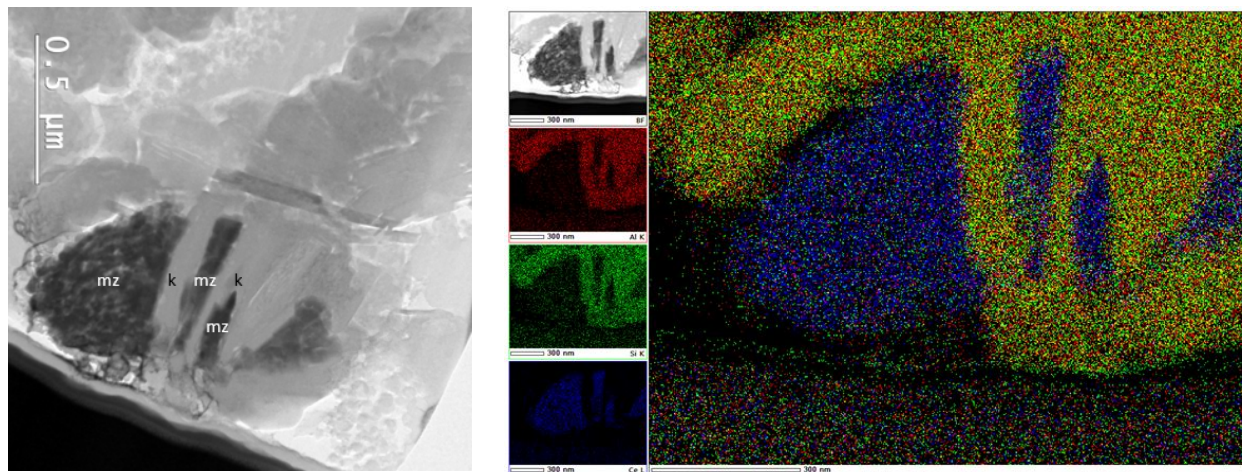
TEM image of a Magnéli phase (Ti_xO_{2x-1}) in a typical coal ash. (b) A magnified TEM image of the square selected area in a. (c) Selected area electron diffraction (SAED) pattern of the circular selected area in a. (d) TEM image of Ti_xO_{2x-1} in another coal ash. (e) A magnified TEM image of the square selected area in d. (f) SAED pattern of the circular area in d.

Yang Y., Chen B., Hower J., Schindler M., Winkler C., Brandt J., Di Giulio R., Liu M., Fu Y., Zhang L., Priya S., Hochella M.F. Jr. East China Univ., U. Kentucky, Laurentian U. (Canada), Duke U., and Virginia Tech.
Work performed at NanoEarth.

This work was supported by NSF Award # ECCS 1542100. Published in *Nature Communications* (2017)

Rare Earth Elements from Coal and Coal Ash

Rare earth elements (REE) are vital in many modern electronics and optics. Coal and coal-combustion products have attracted attention as sources of the entire REE suite. The Fire Clay coal in eastern Kentucky is the premier coal-based REE resource in the eastern US, if not in the entire country. Studies of the Fire Clay coal (figure below) and of fly ash from the combustion of the coal have been vital in both confirming assumptions about the element associations and in discovering additional associations among the sub-micron minerals. REE-bearing minerals are not always evident in fly ash because of the comminution of the minerals at combustion temperatures. When minerals are not visible in the fly ash, REE concentrations can be detected within the Al-Si glass and diffuse, non-determinate crystallinity can be observed, indicating that the elements are not necessarily dissolved in the glass, but are, instead, present as nano-size grains dispersed in the fly ash glass.



TEM image of a mixed monazite (mz)/kaolinite (k) grain in the Fire Clay coal (left) with the Al, Si, and Ce element overlay map of the same grain (right). Ce is the most abundant of the REE's and is one of the REE in monazite, therefore, it is used as a proxy for the presence of REE in coal or fly ash.

Hood, M.M. et al., Univ. of Kentucky, East China Univ., and Virginia Tech.

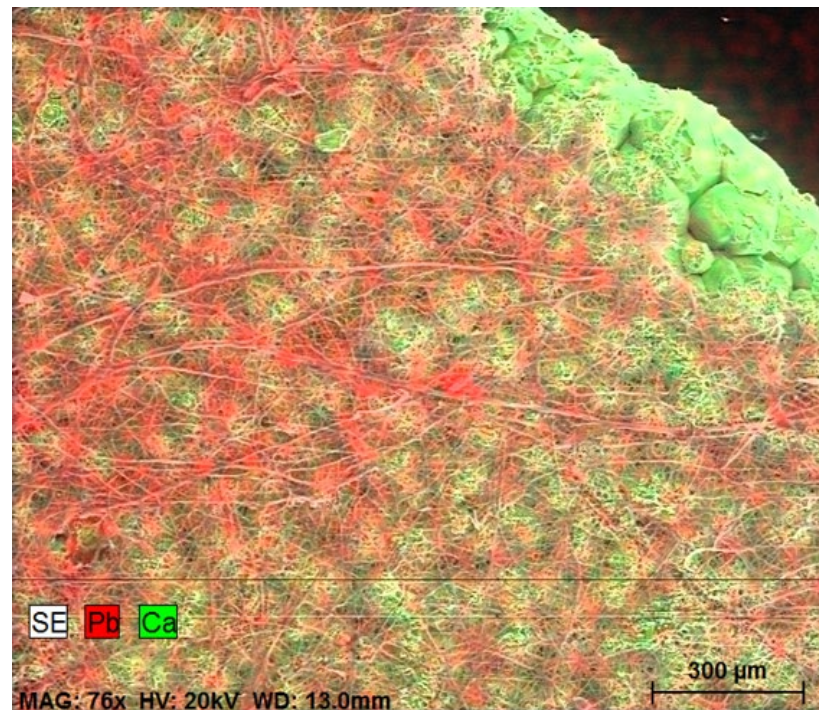
This work was supported by NSF Award # ECCS 1542100., and the Department of Energy.

Hood, M.M. et al. (2017) *Coal Combustion & Gasification Products*, 9, 22-33. Hower, J.C., et al. (2018) *International Journal of Coal Geology*, 193, 73-86.

PoSH™ Waste Materials as Low-Cost Sorbents for Water- and Air- Pollutants

With the mission to reduce the size of landfills, the PoSH™ (Porous Shells and Husks) project utilizes agricultural waste and industrial by-products as potential sorbents for water- and air-pollutants. To-date, the PoSH™ project has screened and tested many waste materials, disposed from households, restaurants, farms and various industries, for sorption of several heavy metal pollutants, viz. lead (Pb), zinc (Zn), copper (Cu) and nickel (Ni) from contaminated water.

Low-cost PoSH™ materials showed a great potential in adsorbing the studied heavy metals from contaminated water. More specifically, egg shells, coffee grinds, corn husks, peanut hulls and other waste materials removed 70-90 % of the heavy metals present in water within 1 hr of contact time. Studies to determine the optimum contact time (sorbent/contaminated medium) are underway along with studies on the effects of other parameters (pH, temperature, PoSH™ material particle size, PoSH™ sorbent/contaminated water weight ratio) on the sorption of heavy metals and other types of pollutants by PoSH™ materials. Moreover, assessment of real-life air- and water-samples taken from different locations and subjected to decontamination by PoSH™ sorbents is envisioned.



SEM micrograph with EDS analysis of egg shell used in decontamination study of Pb-contaminated water.

Anna Maria Petkoska (Yahya Kemal High School, Skopje, Macedonia), Jack Dawson (Virginia Tech, Blacksburg, VA) and Joshua Dicken, Landon Ferrell, Remington Conner, Elizabeth Duncan and Abbie Richardson (ABCA, Riner, VA). Work performed at Virginia Tech, VT NCFL and VTSuN.

This work was supported by NSF Award # ECCS 1542100.

Scalable Purification of Nanoparticle-Containing Liquid Waste Streams

This work targets the removal of nanoparticle contaminants from aqueous waste streams. A filter-free industrial-scale water purification technology effectively separated a nanomaterial-containing liquid waste stream into two components – 1) a clear product fraction and 2) a concentrated brine/waste fraction. Visual data are supported by physicochemical analyses, which indicate a >90% decrease in total dissolved solids (TDS) from the source water relative to the product fraction. Most importantly, gold, titanium, and silver, all of which were present in the mixed nanoparticle waste stream, were reduced by more than 99.8%. Collectively, these results demonstrate a filter-free, scalable approach to removing nanoparticle contaminants from aqueous waste streams.

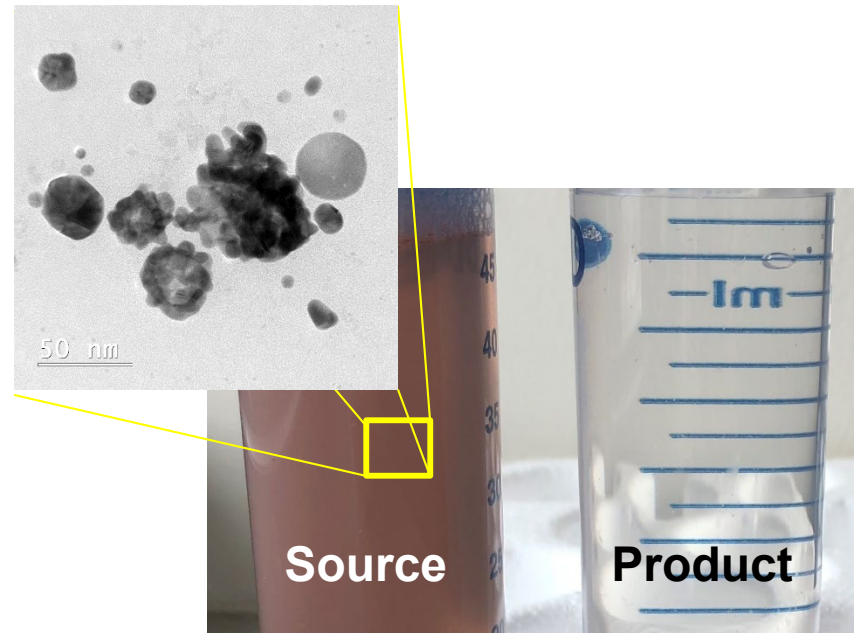


Photo of mixed nanoparticle waste (left) and purified product water (right). Gold nanoparticles (inset TEM image) are responsible for the reddish color of the source water. >99% of the nanoparticles are removed in the product water.

External users from industry, not named due to proprietary considerations. Internal users: Hull, M., Leng, W., Berti, D. (Institute for Critical Technology and Applied Science, Virginia Tech). Work performed at Virginia Tech's National Center for Earth and Environmental Nanotechnology Infrastructure (NanoEarth).

This work was supported by NSF Award # ECCS 1542100.

Nano-enabled Approaches to Protect Endangered Freshwater Mussels of Appalachia

A cross-sector, interdisciplinary research team is working to better understand the nanoscale components of Total Dissolved and Suspended Solids (TDS and TSS) and how these components may potentially impact freshwater mussel fauna in select reaches of the Clinch River and similar watersheds. The project is leveraging advanced nanoscale characterization tools that are not used routinely to study aquatic ecosystems, and aims to contribute fundamental, new science and understanding regarding particulate matter in surface waters and their potential impacts on aquatic biota. Ultimately, these results may help improve the success of efforts aimed at restoring sensitive species to ecosystems degraded by anthropogenic activities.

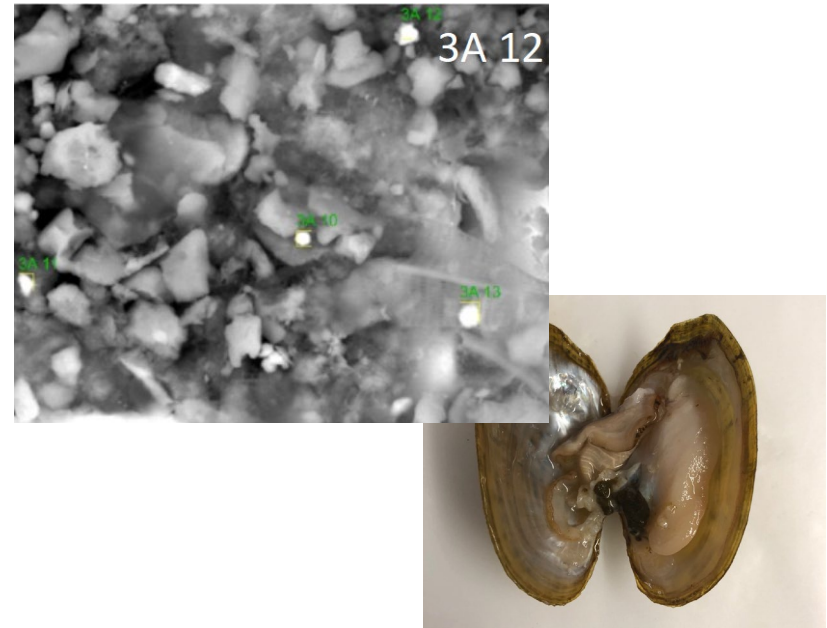


Photo of freshwater mussel undergoing dissection to remove the digestive gland for examination by electron microscopy. Inset shows an electron micrograph of harvested gut contents.

Hull, M., Yu, Y.P., Stewart, R. Zipper, C., Jones, J., Beatty, B., Riecks-Soucek, D., Timpano, T. Insitute for Critical Technology and Applied Science (ICTAS), Virginia Tech. Work performed at Virginia Tech's National Center for Earth and Environmental Nanotechnology Infrastructure (NanoEarth).

This work was supported by NSF Award # ECCS 1542100.

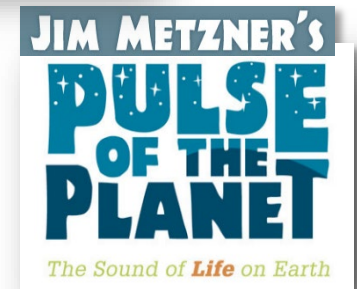
Education and Outreach

High Impact Educational Engagements

Greater than 271,000 people chose to directly interact with NanoEarth's educational initiatives in 2017/2018 (the two most popular programs are shown below)

Pulse of the Planet

Jim Metzner's *Pulse of the Planet* has been a radio program on NPR and several high-end commercial radio stations for over 30 years. It is heard by more than a million people weekly. NanoEarth produced 10 two-minute "Pulse" programs relevant to Earth and environmental nano topics in 2017-18. Besides the radio listening audience, podcasts of NanoEarth shows had 270,000 listens during our 2017-18 season.



USA Science and Engineering Festival

NanoEarth lead a team of undergraduate and graduate students to the USA Science and Engineering Festival in Washington DC. Over three days, the team engaged >1,000 individuals with demos showing the ubiquitous nature of the nanoscale sciences, and gave hints of fundamental scientific theory underlying nanoscience in an approachable manner.



Educational engagement activities supported by NSF Award # ECCS 1542100. Additional support provided by the Virginia Tech Graduate School via the Sustainable Nanotechnology Interdisciplinary Graduate Education Program.

High Impact Diversity Initiatives

Historically Black Colleges and University Research Summit

NanoEarth served as an organizer for the 2019 HBCU Research Summit organized by Virginia Tech's Office of Recruitment and Diversity Initiatives. NanoEarth recruited, and paid all expenses for 10 attendees for meetings, instrument demonstrations, networking, and travel/food/lodging.

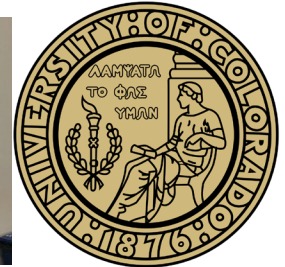


MUNI User: Dr. Cynthia Hall, West Chester University

Dr. Cynthia Hall utilized the NanoEarth Multicultural and Underrepresented Nanoscience Initiative (MUNI) grant and conducted SEM and Raman analysis on lead contaminated soil samples collected in the Philadelphia area. Dr. Hall also gave a seminar to NanoEarth faculty and students. MUNI cover all expenses for Dr. Hall, including travel/food/lodging.

MUNI User: Dr. Marina Vance, University of Colorado

Dr. Marina Vance utilized the NanoEarth MUNI grant and conducted XPS and Raman analysis to characterize nano-enabled film coatings for glass surfaces that confers “anti-reflective”, “anti-fouling”, and “hydrophobic” properties. Dr. Vance also gave a seminar to NanoEarth faculty and students. MUNI cover all expenses for Dr. Hall, including travel/food/lodging.



Diversity initiative-related activity was supported by NSF Award # ECCS 1542100. Additional support provided by the Virginia Tech Graduate School via the Sustainable Nanotechnology Interdisciplinary Graduate Education Program, the Virginia Tech Office for Inclusion and Diversity, and the Virginia Tech Institute for Critical Technology and Applied Science.

NNI: Regional Hub for Nano-Education

Hands-on nanotechnology activities for over 15,000 residents of the Pacific Northwest.

- ◆ Assessing and shaping the public perception of nanotechnology

Partnering with regional tribal schools to host Native American student visits and cleanroom internships

22 Cleanroom Interns, including 7 women, 4 URM



NNI hosted the Pacific Northwest's first National Nanotechnology Day attended by over 2,000 members of the public

Nanotechnology, A Maker's Course

Massive Open Online Course on Coursera platform, providing education in nano-fabrication and -characterization

Lectures and in-lab demonstrations of equipment in RTNN labs

Launched September 2017

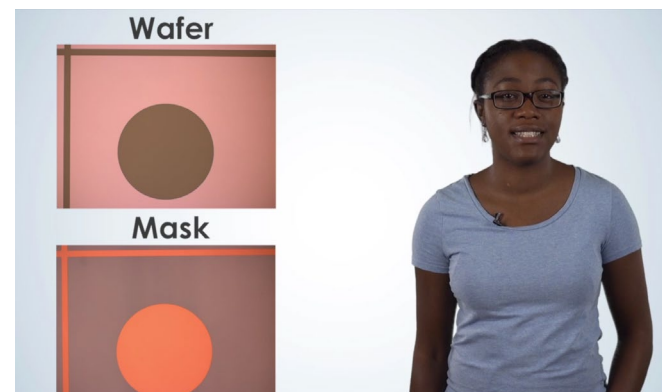
>22,000 visitors

>9,000 enrolled

Learners from >130 countries

High satisfaction, e.g. course instruction rated 6.5 on a scale with 7 being the highest

93% of respondents “likely” or “very likely” to recommend course



Course lecture on photolithography

*“I like the speaker very much, I hope I can be a scientist like her.”
– anonymous, from evaluation*

Faculty and staff at NC State, UNC-Chapel Hill, and Duke

Work performed at Duke's Shared Materials Instrumentation Facility, NC State's Analytical Instrumentation Facility, NC State's Nanofabrication Facility, and UNC's Chapel Hill Analytical and Nanofabrication Laboratory

Work supported by NSF Award # ECCS-1542015

Girls STEM Day @ Duke

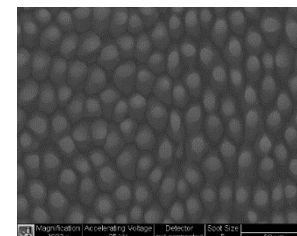
Goals:

1. Encourage girls toward STEM careers
2. Earn Girl Scout badges in forensics (spectroscopy) and digital photography (SEM)

>100 North Carolina girls and Girl Scouts and their families

>100 volunteers from 30+ organizations, companies, and institutions

RTNN (all 3 institutions) developed technical content, trained volunteers, and staffed event



Faculty and staff at NC State, UNC-Chapel Hill, and Duke

Work performed at Duke's Shared Materials Instrumentation Facility

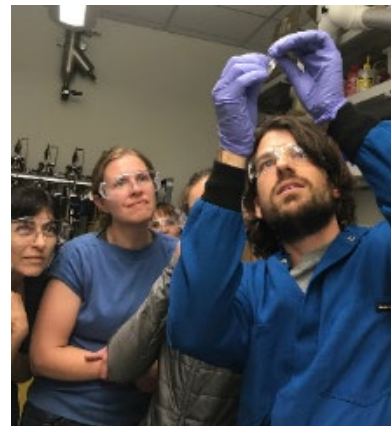
Work supported by NSF Award # ECCS-1542015, IBM, Triangle Women in STEM, Credit Suisse, and Duke's Pratt School of Engineering and Trinity College of Arts and Sciences



Nanoscience Summer Institute for Middle School Teachers (NanoSIMST)

The NNCI Site at Stanford hosted the 2nd NanoSIMST in June 2018. 15 local Bay Area middle school teachers participate in a 4-day, summer workshop to learn more about nanoscience and how to implement it into their classroom. The curriculum includes hands-on experiments teachers can bring back to their classroom; lesson plan development that aligns with their specific curriculum; and interactive components through lectures and lab & facility visits.

After the program, teachers showed a large shift in their confidence in understanding and teaching nanoscience, as well as an increase in excitement for teaching nanoscience curriculum.



Partnership with California State University, East Bay

The NNCI Site at Stanford formed a partnership with California State University, East Bay during the first year of NNCI. Since then, CSUEB faculty and students visited the NNCI Site @ Stanford University several times to participate in lab tours and use of the facilities for fabrication and characterization.

In 2018, a team of CSUEB and Stanford published an article in the American Journal of Physics, describing an upper-division undergraduate physics laboratory experiment that integrates the fabrication and characterization of a p-n junction in silicon. This low-cost, engaging, and effective lab can be adapted to undergraduate physics courses at various institutes.

Work performed at the NNCI Site @ Stanford.

American Journal of Physics 86, 740 (2018)

 American Journal of Physics

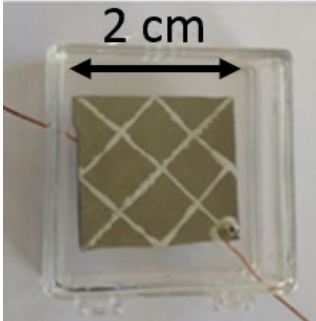
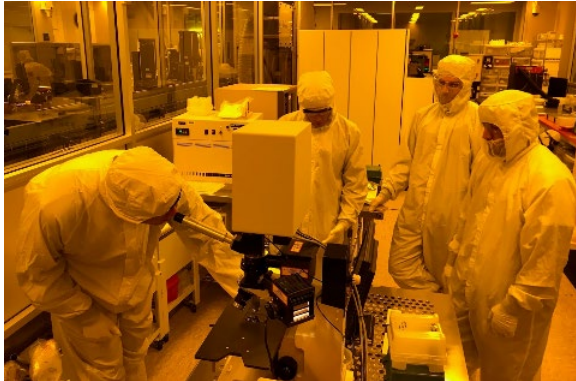
HOME BROWSE INFO FOR AUTHORS COLLECTIONS

Home > American Journal of Physics > Volume 86, Issue 10 > 10.1119/1.5046424
Open - Published Online: 19 September 2018 Accepted: June 2018

Introduction to semiconductor processing: Fabrication and characterization of p-n junction silicon solar cells

American Journal of Physics 86, 740 (2018); <https://doi.org/10.1119/1.5046424>

Ryan P. Smith
• Department of Physics, California State University - East Bay, Hayward, California 94542
Angela An-Chi Hwang and Tobias Beetz
• Stanford Nano Shared Facilities, Stanford, California 94305
Erik Helgren
• Department of Physics, California State University - East Bay, Hayward, California 94542
less



Solar cell shows the silver paint front contact pattern and is housed in a transparent sample box